

ABSTRACT

LEE, CHUL-HO. Design and Analysis of Opportunistic Forwarding in Challenged Networks. (Under the direction of Dr. Do Young Eun.)

Challenged networks are those networks, e.g., mobile opportunistic networks (MONs), a.k.a., delay/disruption tolerant networks, and power-constrained or duty-cycled wireless sensor networks (WSNs), where traditional Internet architectures fail to ensure end-to-end communication due to the lack of ‘always-on’ well-connected infrastructures and its resulting intermittent connectivity. Opportunistic forwarding has emerged as a new communication principle relying on node mobility (or relaying information upon contacts between mobile nodes by chance) for effective communication in MONs, while a different form of opportunistic forwarding, or randomized routing, has been also popular for many applications in WSNs due to their desirable properties. In this dissertation, we study the design and analysis of opportunistic forwarding in such challenged networks. Since the challenged networks are highly heterogeneous and dynamic in many aspects, in our study, we carefully take into account, through systematic stochastic analysis, the random, dynamic underlying heterogeneity so as to correctly understand the system behaviors and design new algorithms/procedures to adapt to and exploit the heterogeneity.

In the first part of this dissertation, we present our study on analyzing and improving forwarding performance under heterogeneous contact dynamics in MONs. We first discuss how the heterogeneity in mobile nodes’ contact dynamics impacts the forwarding performance in MONs. In particular, we show, through formal stochastic comparisons, that different heterogeneous structures lead to an entirely opposite delay performance, cautioning that one should carefully evaluate the performance of forwarding algorithms under a properly chosen heterogeneous network setting. We next undertake to develop an analytical framework in order to quantify the performance gain achievable by exploiting the heterogeneous contact dynamics to our advantage. The framework enables us to obtain a heterogeneity-aware forwarding policy with its guaranteed delay bound and thus provides quantitative results on the benefit of leveraging underlying heterogeneity structure in the design of forwarding algorithms.

In the second part of this dissertation, we study the design of smart/distributed duty-cycling for opportunistic forwarding in heterogeneous and dynamic WSNs toward faster information delivery and longer network lifetime. We first propose and analyze a simple yet effective modification of random duty cycling, named Smart Sleep, for opportunistic forwarding in duty-cycled WSNs. By judiciously exploiting temporal dynamics or intentionally correlating duty-cycling with packet transmission activity, our proposed Smart Sleep breaks the typical delay-power tradeoff and achieves smaller delay as well as more power-saving at each sensor leading to longer network life. We next introduce a distributed wake-up rate control scheme taking advantage of

local heterogeneity structure, which is complementary to Smart Sleep, and demonstrate that it also improves both delay and network lifetime for opportunistic forwarding in duty-cycled WSNs.

Copyright 2012 by Chul-Ho Lee

All Rights Reserved

Design and Analysis of Opportunistic Forwarding in Challenged Networks

by
Chul-Ho Lee

A dissertation submitted to the Graduate Faculty of
North Carolina State University
in partial fulfillment of the
requirements for the Degree of
Doctor of Philosophy

Computer Engineering

Raleigh, North Carolina

2012

APPROVED BY:

Dr. Wenye Wang

Dr. Mihail Sichitiu

Dr. Harry Perros

Dr. Do Young Eun
Chair of Advisory Committee

DEDICATION

To my family

BIOGRAPHY

Chul-Ho Lee received his B.E. degree with high honors in Information and Telecommunication Engineering from Korea Aerospace University, Goyang, Korea, in 2003 and his M.S. degree in Information and Communications from Gwangju Institute of Science and Technology (GIST), Gwangju, Korea, in 2005. Since August 2006, he has been a Ph.D. student in the Department of Electrical and Computer Engineering at North Carolina State University, Raleigh, NC. His research interests include performance modeling and analysis, wireless and mobile networks, and mobility modeling.

ACKNOWLEDGEMENTS

First and foremost, I would like to express my deep and sincere gratitude to my advisor, Dr. Do Young Eun, for his greatest guidance and generous support throughout my Ph.D. study at North Carolina State University. His invaluable comments, constructive criticism, and consistent encouragement have been most helpful to me during the course of my Ph.D. study, especially when I faced difficulties while doing research. Without him, this dissertation could not have been completed. I will always feel fortunate to have been his student.

I would like to thank Dr. Wenye Wang, Dr. Mihail Sichitiu, and Dr. Harry Perros for serving on my advisory committee and providing me with many useful comments and suggestions on my research. I am also grateful to Dr. Min Kang. She was always willing to spend time to kindly answer every single question while I took her classes on probability theory and stochastic processes, and also gave me a chance to be a grader for her class.

It was my great pleasure to have met my friends and colleagues, Dr. Yuh-Ming Chiu, Dr. Han Cai, Dr. Sungwon Kim, Jaewook Kwak, Xin Xu, and Xin Chen. I learned so much from stimulating technical discussions with them. I greatly appreciate their friendship.

Last but not least, I would like to thank my family for their constant unconditional love, support, and encouragement. I also owe an enormous debt of gratitude to my sweetheart, Jiyeon Jinny Kim, for everything she has done for me. Words cannot express my heartfelt gratitude and appreciation for them. Without them, it would have been impossible for me to finish this work.

TABLE OF CONTENTS

List of Figures	vii
Chapter 1 Introduction	1
1.1 Analyzing and Improving Forwarding Performance under Heterogeneous Contact Dynamics in MONs	2
1.2 Smart/Distributed Duty-Cycling for Faster Information Delivery and Longer Network Lifetime in WSNs	6
1.3 Organization	10
Chapter 2 Heterogeneous Contact Dynamics in MONs	11
2.1 Individually Heterogeneous Network Model	11
2.2 Spatially Heterogeneous Network Model	13
Chapter 3 Impact of Heterogeneity in Mobile Nodes' Contact Dynamics on Forwarding Performance	15
3.1 Inter-contact Time under Heterogeneous Network Models	15
3.2 Delay Performance of Direct Forwarding	17
3.3 Delay Performance of Multicopy Two-hop Relay Protocol	21
3.4 Simulation Results	27
Chapter 4 Exploiting Heterogeneity in Mobile Nodes' Contact Dynamics to Improving Forwarding Performance	32
4.1 Problem Formulation	32
4.2 Delay Analysis	36
4.2.1 An Upper Bound of Message Delivery Delay	36
4.2.2 A Special Case: Multicopy Two-hop Relay Protocol	37
4.3 Main Results	39
4.3.1 A Sub-Optimal Forwarding Policy	40
4.3.2 Performance Gain of Exploiting Heterogeneity	43
Chapter 5 Opportunistic Forwarding in Duty-Cycled WSNs	48
5.1 Network Model	48
5.2 Random Duty Cycling and Opportunistic Forwarding	49
5.3 Simple Random Walk Model For Opportunistic Forwarding	50
Chapter 6 <i>Smart Sleep</i>: Sleep More to Reduce Delay in Duty-Cycled WSNs	52
6.1 Smart Sleep: How To Sleep More and Better	52
6.2 p -Backtracking Random Walk and Its Connection to Smart Sleep	55
6.2.1 p -Backtracking Random Walk	56
6.2.2 Properties of p -BRW	57
6.2.3 How To Choose Each Backtracking Probability p_i ?	61
6.2.4 From p -Backtracking Random Walk To Smart Sleep	62

6.3	Simulation Results	65
Chapter 7 Exploiting Heterogeneity for Delay and Power Efficient WSNs –		
	A Delay Perspective	69
7.1	Opportunistic Forwarding under An Asynchronous, Heterogeneous Random Duty Cycling	69
7.2	Performance Modeling and Analysis	71
	7.2.1 Continuous-Time Random Walk on A Graph	71
	7.2.2 Performance Metric and Analysis	72
7.3	A Distributed Wake-up Rate Control Based on Local Degree Information	73
7.4	Numerical Evaluations and Simulation Results	78
Chapter 8 Exploiting Heterogeneity for Delay and Power Efficient WSNs –		
	A Network Lifetime Perspective	81
8.1	Background	81
	8.1.1 A Generalized Random Graph Model	81
	8.1.2 Definitions	82
8.2	A Critical Point of Site Percolation	82
8.3	From Site Percolation To Network Lifetime	85
	8.3.1 Degree-independent Node Lifetime	86
	8.3.2 Degree-dependent Node Lifetime	87
Chapter 9 Conclusion 91		
References 93		
Appendix 100		
	Appendix A	101

LIST OF FIGURES

Figure 2.1	An example for spatial and social (individual) heterogeneity in an opportunistic campus mobile network.	12
Figure 2.2	Examples of the individual and spatial models.	13
Figure 3.1	Three different settings of n two-hop relay paths with varying degrees of heterogeneity: (a) a fully heterogeneous setting, (b) a partially homogeneous setting where each relay path is homogeneous. (i.e., two-hop components in each relay path have the same average inter-contact time as $1/\mu_i = \frac{1}{2}[1/\lambda_{sr_i} + 1/\lambda_{r_i d}]$), and (c) a fully homogeneous setting where the average inter-contact time for any node pair is $\tau = \frac{1}{2n} \sum_{i=1}^n [1/\lambda_{sr_i} + 1/\lambda_{r_i d}]$	24
Figure 3.2	Pairwise inter-contact time distribution under the two-states spatial model with varying q_{12} ($= q_{21}$). $\tau=8000$ for both cases.	28
Figure 3.3	The average delay of multicopy two-hop relay protocol under the spatial, individual, and homogeneous models, all of which have the same average aggregate inter-contact time.	29
Figure 3.4	The average delay of epidemic protocol under the spatial, individual, and homogeneous models, all of which remain the same in the average inter-contact time of a random pair of nodes.	30
Figure 4.1	A class of probabilistic two-hop forwarding policies. Source S forwards a message copy to relay node r_i with probability p_i	33
Figure 4.2	Decomposition of a heterogeneous network into n partially homogeneous networks \mathfrak{N}_i ($i = 1, \dots, n$). K two-hop relay paths in \mathfrak{N}_i are <i>i.i.d.</i> copies of the two-hop relay path via relay node r_i in the original heterogeneous network.	38
Figure 4.3	Average delay achieved via the sub-optimal two-hop forwarding policy per each given number of message copies under heterogeneous and corresponding homogeneous network settings. The horizontal thick line indicates the optimal delay that any two-hop forwarding policy cannot exceed under the homogeneous settings.	45
Figure 4.4	Average delay achieved via the sub-optimal two-hop forwarding policy per each given number of message copies under a heterogeneous network setting (<i>Infocom</i> trace) and its homogeneous counterpart. The horizontal thick line indicates the optimal delay that any two-hop forwarding policy cannot exceed under the homogeneous setting.	46
Figure 4.5	Histogram of average <i>pairwise</i> inter-contact times over all node pairs in <i>Infocom</i> trace.	46
Figure 5.1	The operation of data transmission via the opportunistic forwarding under the random duty cycling. Here, nodes B and C are the neighbors of node A , and a (data) packet is transmitted from node A to node B	50

Figure 6.1	A series of four nodes in 1-D ring	53
Figure 6.2	Illustration of transitions of p -BRW. (a) A p -BRW is located at node i at time $t-1$ and is going to move to node j . (b) At time t , the p -BRW chooses one of the neighbors of node j according to the transition probability in (6.3) as the next node that it will move to.	57
Figure 6.3	Effect of different backtracking probabilities p on the second moment of return time to a given node and the mean first hitting time to that node under a 2-D torus with $n=11 \times 11$	62
Figure 6.4	A snapshot of a part of 2-D grid topology when a packet of interest reaches node l via path $i \rightarrow j \rightarrow k \rightarrow l$. If T is very large, nodes i, j, k can be still in a sleep mode by the time the packet reaches l	63
Figure 6.5	A relationship between the sleep duration T and the interval τ between two consecutive packets arriving to sensor i	64
Figure 6.6	Performance comparison on the packet delivery for the farthest s-d pair while varying T under 1-D ring with $n=20$	66
Figure 6.7	Performance comparison on the packet delivery for the farthest s-d pair while varying T under 2-D grid with $n=100$	66
Figure 6.8	Performance comparison on the packet delivery for the farthest s-d pair while varying T under a sample graph of $RGG(200, 0.13)$	67
Figure 6.9	(a) A sample topology of $RGG(200, 0.13)$; (b) Measured wake-up frequency for a sensor under various topologies as T varies.	68
Figure 7.1	The operation of data transmission via an opportunistic forwarding under an asynchronous, heterogeneous random duty cycling	70
Figure 7.2	\bar{H}_{max} under 50 different sample topologies of $RGG(50, 0.3)$	79
Figure 7.3	Statistics of node degrees of 50 different sample topologies of $RGG(50, 0.3)$ used in Figure 7.2.	79
Figure 7.4	Average performance improvement in \bar{H}_{max} over 500 different sample topologies of $RGG(50, 0.3)$ while varying β in (7.13).	79
Figure 8.1	The comparison between the network lifetime induced from the degree-dependent node lifetime with different β and its corresponding network lifetime under the degree-independent node lifetime.	90

Chapter 1

Introduction

Challenged networks are those networks where traditional TCP/IP-based Internet protocol architectures fail to ensure efficient and effective end-to-end communication. While the conventional networks operate assuming the presence of a stable end-to-end path and its easy maintenance against infrequent failures, challenged networks violate such assumptions and arises primarily as a result of intermittent link/network connectivity – driven by node mobility, nodal churn, power limitation/management, scarce computing resources, dynamic network conditions (e.g., interference), among others. Common examples of challenged networks include:

- **Delay/disruption tolerant networks (DTNs):** These networks range from inter-planetary networks [17] to mobile opportunistic networks (MONs) – an extension of mobile ad-hoc networks (MANETs), toward several applications such as pocket switched networks [21] or UMass dieselnet [8]. In these networks, especially MONs, link or network connectivity is changing over time and frequently disrupted due to random node mobility, power limitation, etc. In particular, the random mobility pattern of mobile nodes in these networks has been considered as the main source of uncertainty and disruption of communication links among nodes, but also the mobility can enable us to achieve reliable and predictable performance, if it is properly and actively exploited. In this regard, MONs employ a *‘store-carry-and-forward’* principle leveraging node mobility to overcome the intermittent connectivity nature, in which mobile nodes can carry messages and copy and/or relay them to other nodes upon encounter, which in turn ensures that the messages eventually reach their destinations. Most of research works regarding MONs/DTNs has been centered, among others, around how to utilize nodes’ mobility for effective and efficient communication and better network performance.

- **Power-constrained wireless sensor networks (WSNs):** These networks have found various applications ranging from event detection/monitoring, surveillance, information delivery and dissemination in a sensor field, data gathering/ harvesting, to more recent urban/participatory sensing with hand-held mobile devices [1]. Such WSNs typically consist of a

large number of sensor nodes that are often unreliable, faulty, and equipped with only limited amount of battery and computing power, yet still are expected to self-organize/configure and perform tasks in a fully distributed and autonomous manner. Research works on WSNs have been largely centered around delay-efficient routing or information delivery, and power/energy-efficient protocol and management to get the most out of scarce power resource and increase the network lifetime without compromising other requirements.

On the other hand, these challenged networks are highly heterogeneous and dynamic in diverse attributes of nodes and links composing the networks, and other dimensions. In particular, various heterogeneity structures present, ranging from node- and link-level heterogeneity such as different computing and communication capabilities at nodes and various link qualities to global network-level heterogeneity in network connectivity or topological structure. It is thus evident that the underlying heterogeneous and dynamic structures govern the performance of information delay or other relevant system performance, but the underlying structures can be also even leveraged as an asset to improve the performance.

However, due to intrinsic *random* nature in heterogeneous and dynamic environments, it is challenging to correctly measure the impact of the random, dynamic underlying heterogeneous structures on the system performance, and is non-trivial to devise efficient networked systems or algorithms/protocols to properly exploit and adapt to the underlying structures. In particular, it is often problematical to reach such goals through simplified *deterministic* and/or *homogeneous* frameworks, as they only provide limited and inaccurate view of system behaviors and in turn lead to poor design guidelines. Thus, a common theme in this dissertation is, through systematic stochastic analysis, not only to address the impact of the random, dynamic underlying heterogeneity on the performance of challenged networks, but also to design efficient algorithms/protocols taking advantage of such heterogeneity to enhance the performance. This dissertation is divided into two parts: **(I)** analyzing and improving forwarding performance under heterogeneous contact dynamics in MONs and **(II)** the design of smart/distributed duty-cycling for opportunistic forwarding in heterogeneous and dynamic WSNs to achieve faster information delivery and longer network lifetime.

1.1 Analyzing and Improving Forwarding Performance under Heterogeneous Contact Dynamics in MONs

Motivation

There has been a great deal of work in the literature as to how to utilize nodes' mobility or how to relay/copy messages to mobile nodes upon encounter for better performance of information or message delivery in MONs. Many forwarding/routing algorithms such as epidemic routing [88],

two-hop relay [40, 39], spray and wait [81], to name a few, have been proposed and commonly analyzed based upon an over-simplifying assumption, or a ‘homogeneous’ network model, in which contacts between every pair of nodes is making contacts with each other according to a given Poisson process. [81, 39, 48, 96, 83]. This homogeneous model is typically supported by observing that the inter-contact time* between two successive contacts for *any* node pair follows an exponential distribution via numerical simulations under synthetic mobility models [39, 96]. Other analytical works also fully resort to the homogeneous model for their investigation on the capacity-delay tradeoff [40, 78], the cost-delay tradeoff [80, 64], the design of forwarding policy [4], and content distribution [42].

However, many measurement studies [43, 75, 25, 44, 10, 70] point out the existence of heterogeneity in a wide range of mobile networking scenarios, while recent empirical and/or analytical observations [50, 19] show that the inter-contact time distribution is no longer pure exponential; rather, it is a mixture of power-law and exponential distributions. In particular, from real mobility traces and survey data, [25, 44] observe the characteristics of heterogeneity in mobile nodes’ contact dynamics, and [43, 75, 44, 10, 70] uncover spatially and/or socially formatted community structures in nodes’ mobility, which all make contact dynamics deviate from a pure Poisson process. The observed heterogeneity structures have been actively used for the development of new mobility models [43, 63, 70] and empirically exploited to design new forwarding algorithms [75, 82, 28, 44].

While the underlying heterogeneity structure in mobile nodes’ contact dynamics has been empirically investigated and exploited in the design of new forwarding algorithms, it has been typically ignored or marginalized when it comes to rigorous performance analysis of such algorithms. The current literature still lacks analytical studies on (i) the impact of heterogeneity in mobile nodes’ contact dynamics on the performance of forwarding/routing algorithms, and (ii) exploiting the heterogeneity structure to correctly understand the resulting performance gain, which we address in the first part of this dissertation.

Impact of Heterogeneity in Mobile Nodes’ Contact Dynamics on Forwarding Performance

In this research thrust, we examine how the forwarding/routing performance under two representative heterogeneous network models widely used in the current literature [25, 45, 47, 37, 84, 10, 22], each of which captures the empirically observed *individual (social)* or *spatial* heterogeneity structure, deviates from that under the aforementioned homogeneous model. In the individually heterogeneous network model [25, 47, 26, 37, 84], the heterogeneity is character-

*The inter-contact time of two mobile nodes is defined as the time interval from when their communication becomes unavailable to the time when the communication resumes. See [50, 18] for its formal definition.

ized by allowing different contact rates for different node pairs, while the inter-contact time distribution of each pair is still exponential (but with different rates). On the other hand, in the spatially heterogeneous network model [10, 22], the heterogeneity arises on each spatial cluster (site) in which mobile nodes reside, while they can move to the other spatial clusters. However, none of these works analytically investigates how the heterogeneity structure impacts the performance of forwarding algorithms, not to mention whether the considered heterogeneity improves or deteriorates the performance.

We first show that *each* of the heterogeneous models correctly captures the non-Poisson contact dynamics (i.e., non-exponential inter-contact time distribution of a random pair of nodes) as observed in real traces. Then, we rigorously establish stochastic/convex ordering relationships among the delay performance of direct forwarding and multicopy two-hop relay protocol [39, 96, 41, 45] under the two heterogeneous models and the corresponding homogeneous model, all of which are *indistinguishable* from the viewpoint of the average inter-contact time of a random node pair.

Specifically, we prove that the message delivery delays of direct forwarding and multicopy two-hop relay protocol under the spatially heterogeneous model are *stochastically larger* than those under the corresponding homogeneous model, respectively. We also prove that the delay of direct forwarding under the individually heterogeneous model is *larger* than that under the corresponding homogeneous model *in convex ordering*, while the average delay of multicopy two-hop relay protocol under the individually heterogeneous model is *smaller* than that under the corresponding homogeneous model. As a special case of the above results, we show that the heterogeneity structure in the spatially heterogeneous model *deteriorates* the average delay performance of multicopy two-hop relay protocol, whereas the other heterogeneity structure in the individually heterogeneous model *improves* its average delay performance when compared with that under the corresponding homogeneous model. This implies that each of the two heterogeneous models predicts an entirely opposite average delay performance. We also observe this opposite performance result for epidemic routing protocol[†] [88, 39, 48, 96, 45, 47] via numerical simulations.

We further demonstrate that the delay performance of direct forwarding and multicopy two-hop relay protocol under the spatially heterogeneous model is *worse* than that under the individually heterogeneous model, even when the *entire distributions* of inter-contact time of a random node pair under both heterogeneous models are precisely matched. Our results collectively suggest that merely capturing non-Poisson contact dynamics from the viewpoint of a random node pair is not enough and that one should carefully evaluate the performance of

[†]The forwarding algorithms considered in this research thrust are ‘oblivious’ to the underlying network structures, which enables an unbiased evaluation on the forwarding performance under heterogeneous contact behaviors of mobile nodes.

forwarding algorithms under a properly chosen heterogeneous network setting. Our results will also be useful in correctly exploiting the underlying heterogeneity structure so as to achieve better forwarding performance.

Exploiting Heterogeneity in Mobile Nodes' Contact Dynamics to Improving Forwarding Performance

In this research thrust, we analytically investigate how much benefit the heterogeneity in mobile nodes' contact dynamics can bring in the forwarding performance. To this end, we employ the individually heterogeneous network model used in the previous research thrust as well as in the literature [25, 45, 47, 37, 84] in which the pairwise inter-contact time of a given node pair is exponentially distributed but with *different* rates over different pairs. Under this heterogeneous setting, we then consider a class of probabilistic two-hop forwarding policies in which a source node forwards a message with probability p_i to each relay node i upon encounter. Since message delivery delay and the number of (used) message copies are both mainly functions of p_i and the heterogeneity of contact rates over different node pairs, we are led to find an optimal forwarding policy $\{p_i^*\}$, maximally exploiting the heterogeneity structure, to minimize the message delivery delay under a given constraint on the number of message copies.

Rather than directly solving the optimization problem, as a viable alternative, we derive a delay upper bound of any two-hop forwarding policy and find an optimal forwarding policy that minimizes the delay bound while satisfying the given constraint on the number of message copies. Although this solution is sub-optimal to the original problem, we are able to derive a *closed-form* expression of its guaranteed delay bound, which in turn enables to quantify the performance gain achievable by exploiting the heterogeneity structure in contact dynamics. In particular, when obtaining the closed-form expression of the delay bound, we provide an idea to *decompose* an original heterogeneous network into a set of several (partially) homogeneous networks, which makes the delay analysis more tractable.

We then analytically show that *less than 20%* of unlimited message copies is only enough under various heterogeneous network settings to achieve the same delay as the optimal delay (obtained at the expense of unlimited message copies by multicopy two-hop relay protocol) that any two-hop forwarding policy cannot exceed when the networks become homogeneous. Moreover, since the considerable performance improvement is still demonstrated through the delay upper bound of the sub-optimal two-hop forwarding policy, the maximally achievable performance gain by exploiting the heterogeneity in mobile nodes' contact dynamics will be much higher than expected. We also provide independent simulation results including real trace-driven evaluation to support our analytical results and to show the usefulness of the derived delay bound. Although there have been several empirical works [75, 82, 28, 44] that propose

heuristic forwarding/routing algorithms utilizing the underlying heterogeneity structure, in this research thrust, we take the first step toward analytically quantifying the attainable performance gain by exploiting the underlying heterogeneity structure.

1.2 Smart/Distributed Duty-Cycling for Faster Information Delivery and Longer Network Lifetime in WSNs

Motivation

- *Power consumption and the need for duty cycling:* Power consumption is one of the most critical resource constraints in WSNs, as it is often difficult and requires high cost to replace or recharge the exhausted batteries of sensor nodes in a deployed network. Understanding the power consumption characteristics of a sensor node and how to prolong the network-wide longevity or lifetime have been recognized as critical research issues for WSNs [73, 1]. Many measurement-based studies [79, 69, 71] have, thus, uncovered the detailed characteristics of the power consumption of widely used sensor devices. A common observation is that the RF component of a sensor just for idle listening (turning ‘on’ the RF radio) consumes about the same order of power as that for transmitting packets. In addition, when it’s turned off, it consumes 1000 times less power than ‘on’ RF radio. Therefore, duty cycling (or periodically turning off the RF radio of each sensor node – being in a “sleep” mode) has been considered as a necessary and viable approach for energy conservation, which in turn prolongs the lifetime of individual sensor node as well as the network lifetime.

- *Opportunistic forwarding or randomized routing (random walk based):* The delay performance of routing or information delivery in WSNs can be made close to optimal by using topology-driven algorithms such as the shortest-path, cluster-head based algorithms, or geographical routing. These methods, however, tend to incur critical points of failure and non-uniform energy depletion caused by hot spots or congested areas [6, 72, 55, 61, 30], and mostly suitable for static environment while consuming significant computational overheads. In contrast, random walk based algorithms – a form of opportunistic forwarding or randomized routing, have been preferred mainly because of their inherent distributed/autonomous nature, simple implementation with virtually no computational overhead, scalability, load balancing, and robustness/resilience to topological changes, and no need for coordination, although their delay performance is less than ideal due to their lack of ‘directionality’ and the absence of topological information. Indeed, random walk based algorithms find various applications, thanks to their desirable properties, as a method of message-passing over the nodes in WSNs. They have been popular for information querying and/or delivery for generic sensor networking applications [14, 6, 7, 77, 58, 57, 35]. They are also used for distributed networked storage

applications [56, 52, 91, 90] and security problems [68, 49, 95]. In most of these related works, a simple random walk (SRW), among many other variants in the literature, has been used as a means of probabilistic packet forwarding, where each packet is forwarded from a node to one of its neighbors chosen uniformly at random (in a SRW fashion). We note that the power consumption is not a primary concern, or rather, ignored/marginalized in the related works.

- *Going beyond the delay-power tradeoff*: Only very recently, [11, 24] have begun to consider a SRW as a method of packet forwarding under the presence of random duty cycling. Specifically, under synchronous, homogeneous random duty cycling, an opportunistic forwarding, in which each node having a packet forwards it to the first awake neighboring node (the node who turns on its RF transceiver for the first time among the neighbors), can be translated into the resulting packet trajectory done in a SRW fashion with heterogeneous sojourn time at each sensor. While a SRW or its variant has been the integral component of many applications in WSNs, it has one unavoidable downside – slow diffusion or exploration over the space, which in turn leads to longer delay to reach the destination. Thus, it is very important and highly desirable to speed up such a walk (leading to faster information delivery) without requiring more power consumption or compromising the network lifetime, while maintaining the aforementioned benefits of random walk based approaches. This is our objective in the second part of this dissertation. We demonstrate two different designs of smart/distributed random duty cycling exploiting temporal dynamics and local heterogeneity structure, which breaks the delay-power tradeoff and achieves the best of both worlds in terms of *smaller delay* and *longer network lifetime* in a completely distributed and autonomous manner.

Smart Sleep: Sleep More to Reduce Delay in Duty-Cycled WSNs

In this research thrust, we propose a simple yet effective modification, named *Smart Sleep*, on the random duty cycling, in order to overcome the slow diffusion of SRW-based forwarding (or opportunistic forwarding) while saving more power at every sensor thus leading longer network life. Smart Sleep operates as follows: whenever each sensor node successfully forwards a packet to one of its neighbor, it goes to sleep for T seconds, making itself unavailable in the network. This temporary ‘forced’ sleep right after forwarding a packet reduces the chance of the same packet coming back to the same sensor (backtracking) for a while, thereby facilitating faster exploration for other sensor nodes and ‘speeding up’ the packet for faster delivery. After this sleep period of T seconds, the sensor resumes its normal random duty cycling, preparing itself for forwarding/receiving other packets. Too large value of T will put many sensors into sleep for a long time and outweigh the benefit of faster diffusion of the packet that leaves such a long ‘trail’, thus slowing down the delivery of other packets in the network overall.

To set the stage for analytical treatment of Smart Sleep protocol, we introduce a class of

p-backtracking random walks (*p*-BRW) on a general graph, which captures such dynamics of packet transitions – less backtracking to the previously visited node. Contrary to SRW in which the walker moves to one of its neighbors uniformly at random, in *p*-BRW, the random walker (currently at node *i*) remembers the previous position and goes back to this previously visited node with probability p_i ; otherwise, it moves to any one of other neighbors equally likely. We prove that the stationary distribution of the *p*-BRW is invariant with respect to the choice of p_i . This immediately implies that the average return time of *p*-BRW to a given node is also invariant. We then illustrate how the packet trajectory under our Smart Sleep can be best described by *p*-BRW with some backtracking probabilities $\{p_i\}$, which is generally a function of *T* and underlying network topology. By exploiting the close relationship among p_i , *T*, and other network characteristics and at the same time by leveraging the invariance property of the stationary distribution of the packet position, we study how to choose the sleep duration *T* toward better shaping of the distribution of the return time to our advantage, leading to better delay performance as well as transmission cost, while power saving due to additional sleep is self-evident. We then derive a necessary condition for the optimal sleep duration T^* in minimizing the packet delay, and demonstrate the significant performance improvement through independent numerical simulations over various network topologies. Therefore, in our Smart Sleep, the delay and power becomes *no longer a typical tradeoff* and both can be improved together, while retaining all the aforementioned desirable properties of random walks-based algorithms for dynamic networks.

Exploiting Heterogeneity for Delay and Power Efficient WSNs

In this research thrust, we design a distributed wake-up rate control scheme leveraging local heterogeneity structure for the opportunistic forwarding so as to achieve both smaller delay and longer network lifetime, which is also complementary to Smart Sleep presented in the previous research thrust. To this end, we consider an *asynchronous, heterogeneous* random duty cycling where each sensor node *i* wakes up according to a Poisson process with rate λ_i . The asynchronous duty cycling does not entail any synchronization overhead and complexity, which is necessary for any typical synchronous network operation. We first show that the opportunistic forwarding under the asynchronous and heterogeneous duty cycling can be translated into a continuous-time random walk on a graph, or equivalently, a discrete-time random walk with heterogeneous sojourn time in each vertex of the graph. This construction is rather similar to the one in [11, 24] but our case covers much wider class of random walks with different λ_i , while only homogeneous duty-cycling with $\lambda_i = \lambda$ for all *i* was considered there.

In this setup, we provide an analytical formula for the average delay performance of the opportunistic forwarding with the duty cycling, and then address how to control the wake-up

rate λ_i for each node i in a *distributed* manner so as to improve the delay performance. Since extremely large end-to-end delay is prohibitive even for most delay-tolerant applications, we propose a distributed wake-up control scheme with heterogeneous duty cycling in which each node i autonomously adjusts its wake-up rate λ_i based only on its own degree information to improve the worst-case average end-to-end delay for any given network. By extending a recent result in [46], we prove that our proposed algorithm brings out performance improvement from $O(n^3)$ (guaranteed under pure homogeneous duty cycling) to $O(\sqrt{d_{max}}n^2)$ in the asymptotic upper bound of the worst-case average delay for *any* graph, where n is the total number of nodes and d_{max} is the maximum degree over the network. In particular, we also compare the exact performance of worst-case average delay of our proposed algorithm with that of pure homogeneous duty cycling through numerical evaluations and independent simulation results. We then show that our algorithm leads to more than 35% performance improvement on average under various network topologies.

We next evaluate the network lifetime induced from the proposed distributed wake-up rate control scheme. The network lifetime has been typically defined as the time until any first sensor node dies or runs out of its battery power [23, 92, 59, 51, 93, 29]. Or, it can be the time after which isolated sensor nodes (a blind spot) appear [54, 34]. However, these definitions are too stringent or conservative to declare that the network no longer functions. Even if a single node runs out of its battery power or isolated nodes appear, other sensor nodes can ensure the network connectivity, still enabling timely information delivery over the network. Since WSNs are typically composed of low-cost, low-power sensor devices, it is mostly likely that a few sensor nodes stop functioning right after network deployment. To be fault-tolerant, sensor devices are densely deployed and node redundancy is normally granted [29], which relaxes the requirement of full connectivity.

In this research thrust, we focus on the network lifetime defined as the time before a giant component, in which a majority of functional nodes are connected with each other, remains to form in the network or after which the network becomes fully fragmented. The presence of a giant component can ensure the network to properly operate, even if it loses a connection with a static base station, through leveraging multiple and/or mobile sinks (e.g., data mules). This version of network lifetime was studied via a percolation theory in [94] where the lifetime of every node is *i.i.d.*. The percolation theory has been also used in [54, 34] to analyze the related devolution process of a large-scale WSN with *i.i.d.* node lifetime.

While we also consult the percolation theory, in contrast, our focus is to examine the network lifetime in the presence of *degree-dependent* node lifetime or how the underlying heterogeneity over the node degrees can be exploited to prolong the network lifetime. This is because our proposed distributed wake-up rate control scheme requires only local degree information at each sensor. Specifically, we provide an analytical framework to evaluate the network lifetime

induced from degree-dependent node lifetime (including the degree-independent or *i.i.d.* node lifetime as a special case) by extending the theory of site percolation on a random graph model with an arbitrarily given degree distribution, which has been popular in statistical physics literature [20, 67, 66]. We then recover the main results obtained in [94] on the network lifetime, determined by a priori given degree-independent node lifetime distributions, as an evidence to demonstrate the effectiveness of our framework. We finally show that if the lifetime of each sensor node can be properly controlled based on its own degree, then its resulting network lifetime can be longer than that under its comparable degree-independence node lifetime. That is, our proposed distributed wake-up rate control scheme leads to longer network lifetime.

1.3 Organization

The rest of this dissertation is organized as follows. We discuss the first part of this dissertation – analyzing and improving forwarding performance under heterogeneous contact dynamics in MONs in Chapters 2–4. Chapter 2 presents the formal description of two representative (individually and spatially) heterogeneous network models to be used in Chapters 3–4. In Chapter 3, we study the impact of heterogeneity in mobile node’s contact dynamics on the forwarding performance. Chapter 4 provides our analysis on exploiting the heterogeneity over different node pairs to improving the forwarding performance.

We next discuss, as the second part of this dissertation, the design of smart/distributed duty-cycling for opportunistic forwarding in heterogeneous and dynamic WSNs to achieve faster information delivery and longer network lifetime in Chapters 5–8. Chapter 5 presents preliminaries on network model and base setup for networking operations including opportunistic forwarding and duty cycling to be used in Chapters 6–8. In Chapter 6, we present a design of smart/distributed random duty cycling leveraging temporal dynamics, Smart Sleep, and demonstrate its remarkable performance improvement for both delay and power. We then provide another design of random duty cycling exploiting local heterogeneity structure and study its delay and network lifetime perspectives in Chapters 7–8. We finally conclude in Chapter 9.

Chapter 2

Heterogeneous Contact Dynamics in MONs

In this chapter, we present the details of two heterogeneous network models to be used in Chapters 3 and 4. In general, mobile nodes typically belong to different societal groups, with different preferred sites following different mobility patterns. For example, in Figure 2.1, there exist several popular places (e.g., library, dormitory, or dining hall) in a campus and students may form spatially separate clusters around the popular places, while occasionally move to other clusters according to their own daily schedules. Further, in each spatial cluster, students from different groups (e.g., ECE/CS departments or undergraduate/graduate) typically mix together, but making more frequent contacts with others from the same group than from different groups. These social (or individual) and spatial heterogeneity structures can be captured under the following two heterogeneous network models [25, 47, 26, 37, 84, 10, 22], each of which directly characterizes the heterogeneity in mobile nodes' contact dynamics in a different manner, rather than defining detailed mobile trajectories inside a small domain or group (or social 'clique').

2.1 Individually Heterogeneous Network Model

An individually heterogeneous network model (simply, an individual model) was introduced in [25] and described as follows. This individual model has been also used in [26, 47, 37, 84].

Consider a set of mobile nodes \mathcal{N} in the network. The pairwise inter-contact time between nodes i and j follows an independent exponential distribution with rate λ_{ij} , i.e., contacts between nodes i and j occur according to a Poisson process with rate parameter λ_{ij} , where $i, j \in N$ and $i \neq j$ and $\lambda_{ji} = \lambda_{ij}$. The pairwise inter-contact times between any two node pairs are also mutually independent. In this model, the heterogeneity in mobile nodes' contact dynamics is captured by different contact rates λ_{ij} .

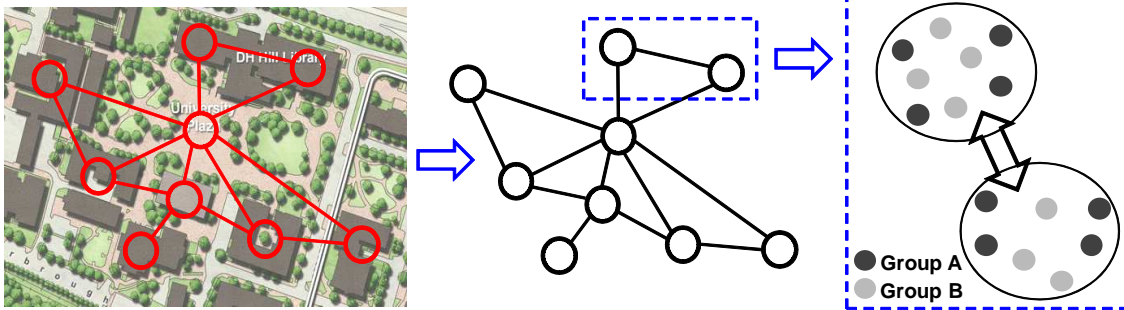


Figure 2.1: An example for spatial and social (individual) heterogeneity in an opportunistic campus mobile network.

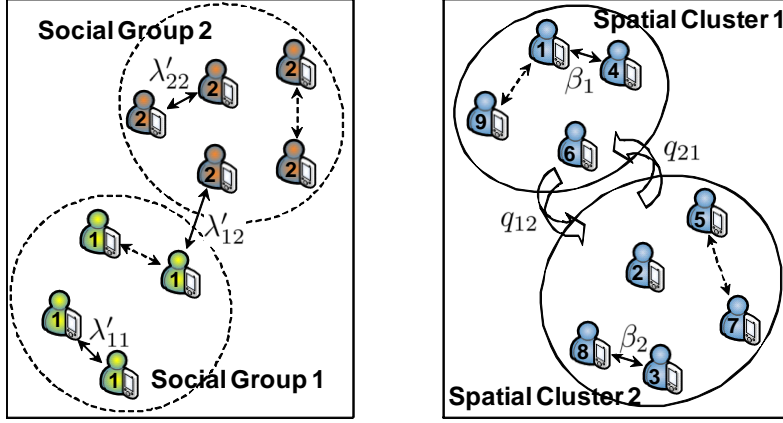
If $\lambda_{ij} = \lambda$ for all i, j ($i \neq j$), then the individual model reduces to the homogeneous network model (a.k.a. Poisson contact model) in which contacts between *any pair* of mobile nodes occur according to a Poisson process with same rate parameter λ . This heterogeneous model also captures a social community structure [37] as a special case. Suppose that there are K different social groups G_i ($i = 1, 2, \dots, L$) forming a partition of \mathcal{N} , i.e., $\mathcal{N} = \bigcup_{i=1}^L G_i$. Let λ'_{lk} be common contact rate between any member of G_l and another member of G_k for $l, k = 1, 2, \dots, L$. That is, $\lambda_{ij} = \lambda'_{lk}$ for all $i \in G_l$ and $j \in G_k$. Figure 2.2(a) shows an example with $K = 2$.

The individual model has been validated in [25, 37]. They independently show through statistical methods that empirical pairwise inter-contact time distributions, obtained in real mobility traces, for a large portion of node pairs can be well fitted by exponential distributions but with different rates. In particular, it was shown in [37] that over 85% of node pairs in *Infocom* and *MIT Reality** can be well approximated by exponential distributions with different rates.

A spatially heterogeneous network model (simply, a spatial model) is introduced in [10] and described formally as follows. This spatial model is also similarly used in [22]. Consider a set of mobile nodes \mathcal{N} in the whole network domain. There are M different spatial clusters (or preferred sites). Let S_i be a spatial cluster (site) i , where $i \in \{1, \dots, M\}$. Then, each mobile node moves and encounters with others independently between sites and within each site as follows:

- (i) Each mobile node in site S_i moves to site S_j with rate q_{ij} at any time t .
- (ii) Any pair of mobile nodes in site S_i has independent Poisson contacts with rate β_i , i.e. the inter-contact time distribution for a node pair in site S_i is independently and exponentially

*These are Bluetooth contact traces and we refer to [37] for details.



(a) A case of two social groups

(b) A case of two spatial clusters

Figure 2.2: Examples of the individual and spatial models.

distributed with mean $1/\beta_i$.

2.2 Spatially Heterogeneous Network Model

A spatially heterogeneous network model (simply, a spatial model) was introduced in [10] and also similarly used in [22]. This spatial model is formally described below.

Consider a set of mobile nodes \mathcal{N} in the network. There are M different spatial clusters (or preferred sites). Let S_i be a spatial cluster (site) i , where $i = 1, 2, \dots, M$. Then, each mobile node independently moves between sites and encounters with others within each site as follows:

- (i) Each mobile node in site S_i moves to site S_j with rate q_{ij} at any time t .
- (ii) Any pair of mobile nodes in site S_i has Poisson contacts with rate β_i , i.e. the inter-contact time distribution for a node pair in site S_i is independently and exponentially distributed with mean $1/\beta_i$. The pairwise inter-contact times between any two node pairs in site S_i are also mutually independent.

If there is only one spatial cluster, i.e., $M = 1$, then the spatial model reduces to the homogeneous model in which contacts between *any pair* of mobile nodes occur according to a Poisson process with same rate parameter $\lambda = \beta_1$. Figure 2.2(b) depicts an example with $M = 2$.

Let $X(t) \in \{S_1, \dots, S_M\} \triangleq \Omega$ be the site that a mobile node belongs to at time t . From the condition (i), $\{X(t)\}_{t \geq 0}$ is a continuous time Markov chain with transition rate matrix (or infinitesimal generator) $\mathbf{Q} = \{q_{ij}\}$. We assume $\{X(t)\}$ is irreducible, i.e., any mobile node

can reach everywhere in finite time with positive probability. For analytical simplicity, we also assume that $q_{ij} = q_{ji}$, i.e., the transition rates of mobile nodes between sites S_i and S_j are the same.

The spatial model was justified in [10]. In particular, the condition (ii) is supported in [10] by empirically observing that 90% of all the inter-contacts gathered in a confined area, a subset of whole network domain, approximately follows an exponential distribution but with different rates over different subsets. The Poisson contacts over a small confined area has been also theoretically justified in [18], regardless of the mobility pattern of each mobile node inside that small confined area. In this spatial model, the heterogeneity arises by allowing different contact rates β_i over different sites.

Chapter 3

Impact of Heterogeneity in Mobile Nodes' Contact Dynamics on Forwarding Performance

In this chapter, we study how each heterogeneity structure in the aforementioned two representative heterogeneous network models (individual and spatial models defined in Chapter 2) impacts the forwarding/routing performance. In Section 3.1, we first presents the characteristics of inter-contact time under each of the two heterogeneous models. In Sections 3.2 and 3.3, we then provide our theoretical results on the stochastic comparison of message delivery delays for direct forwarding and multicopy two-hop relay protocol between each of the heterogeneous models and its corresponding homogeneous model, respectively. We also provide simulation results in Section 3.4.

3.1 Inter-contact Time under Heterogeneous Network Models

In this section, we show that each heterogeneous network model can capture non-Poisson contact dynamics as observed in real traces. For notational simplicity, we enumerate each of node pairs and define an index set for the node pair as $\mathcal{I} = \{1, 2, \dots, |\mathcal{N}|(|\mathcal{N}| - 1)/2\}$. We also define by I a random variable to indicate a random node pair, which is uniformly distributed over \mathcal{I} . Further, we define by T_I and T_i the *aggregate* inter-contact time over all node pairs and *pairwise* inter-contact time for a given node pair $i \in \mathcal{I}$, respectively. Here, the aggregate inter-contact time distribution can be obtained by randomizing the pairwise inter-contact time distributions

over all node pairs, i.e.,

$$\mathbb{P}\{T_I > t\} = \mathbb{E}\{\mathbb{P}\{T_I > t|I\}\} = \sum_{i \in \mathcal{I}} \mathbb{P}\{T_i > t\} \frac{1}{|\mathcal{I}|}.$$

We will use different superscripts ‘IN’, ‘SP’, and ‘HO’ to distinguish T_I and T_i for the individual, spatial, and homogeneous models, respectively.

From the definition of the individual model, it follows that

$$\mathbb{P}\{T_i^{\text{IN}} > t\} = e^{-\lambda_i t}, \text{ and } \mathbb{P}\{T_I^{\text{IN}} > t\} = \sum_{i \in \mathcal{I}} e^{-\lambda_i t} \frac{1}{|\mathcal{I}|},$$

where λ_i is the contact rate of a given node pair $i \in \mathcal{I}$. We can rewrite this as

$$\mathbb{P}\{T_I^{\text{IN}} > t\} = \mathbb{E}\{e^{-t/X_{\text{IN}}}\}, \tag{3.1}$$

where X_{IN} is a discrete random variable taking values $\frac{1}{\lambda_i}$ with probability $\frac{1}{|\mathcal{I}|}$. Note that the actual distribution of X_{IN} can be quite general by suitably setting λ_i .*

For the spatial model, we have the following results:

Proposition 1. *For the spatial heterogeneous model as defined earlier, we have for any $i \in \mathcal{I}$,*

$$\mathbb{P}\{T_i^{\text{SP}} > t\} = \mathbb{P}\{T_I^{\text{SP}} > t\} = \mathbb{E}\{e^{-t/X_{\text{SP}}}\}, \tag{3.2}$$

for some positive random variable X_{SP} . □

Proof. See Appendix A.1. ■

Proposition 1 says that the inter-contact time for spatial model follows a hyper-exponential distribution. Here, the random variable X_{SP} depends on \mathbf{Q} and β_i . We refer to the proof of Proposition 1 for more details. From (3.1)–(3.2) and by noting that $\mathbb{E}\{T\} = \int_0^\infty \mathbb{P}\{T > t\} dt$, we have

$$\mathbb{E}\{T_I^{\text{IN}}\} = \mathbb{E}\{X_{\text{IN}}\} = \sum_{i \in \mathcal{I}} \frac{1}{\lambda_i} \frac{1}{|\mathcal{I}|}, \text{ and } \mathbb{E}\{T_I^{\text{SP}}\} = \mathbb{E}\{X_{\text{SP}}\}.$$

It was addressed in [31] how to approximate a power-law (heavy-tail) distribution in the regions of *primary interest* by a mixture of exponentials while the approximated distribution still has an exponential tail. This implies that the observed ‘dichotomic’ inter-contact time distribution with power-law and exponential mixture [50] can be approximated by hyper-exponential

*For example, setting $\lambda_1 = \lambda_2 \neq \lambda_i$ for $i \geq 3$ will give non-uniform distribution while setting $\lambda_i = \lambda$ for all i makes $X_{\text{IN}} = 1/\lambda$, for which the aggregate inter-contact time follows a pure exponential distribution.

distributions within any desired degree of accuracy. Note that the ‘dichotomic’ inter-contact time distribution is mainly obtained from aggregate inter-contact time samples. Since the aggregate inter-contact time distribution under both the individual and spatial models is a form of hyper-exponential distributions as shown in (3.1)–(3.2), both models can capture this non-exponential inter-contact time behavior.

Throughout the rest of this chapter, we focus on the stochastic comparison of message delivery delays for direct forwarding and multicopy two-hop relay protocol under the individual, spatial, and corresponding homogeneous models. By the homogeneous model, we hereafter mean that for all $i \in \mathcal{I}$,

$$\mathbb{P}\{T_i^{\text{HO}} > t\} = \mathbb{P}\{T_I^{\text{HO}} > t\} = e^{-t/\tau}, \quad (3.3)$$

where $\tau = \mathbb{E}\{X_{\text{IN}}\} = \mathbb{E}\{X_{\text{SP}}\}$, unless otherwise specified. Thus, under the constructed homogeneous model, the inter-contact time of any pair of nodes is exponentially distributed (thus giving Poisson contacts) with the same *average* aggregate inter-contact time as the other heterogeneous models.

In the following stochastic comparisons in Sections 3.2 and 3.3, we assume the followings as in other analytical works [39, 96, 41, 45, 26, 10]. First, the network is sparse and network traffic is light. We also assume that each node has no resource constraint, i.e., it has infinite bandwidth and buffer. Hence, the interference and contention incurred during message transfer are not primary factors that govern the forwarding performance. In addition, we assume that message transfer between any two nodes at their contact instant takes a negligible time with respect to their inter-contact time. Finally, we consider the delay performance of a source and destination pair which is uniformly chosen over \mathcal{I} unless specified.

3.2 Delay Performance of Direct Forwarding

In this section, we first stochastically compare the delay performance of direct forwarding (i.e., a source node waits until it meets a destination node to deliver a message) under the three models. Although the direct forwarding is very simple and there certainly exist other algorithms with better performance, its performance can serve as a basis for performance evaluation or prediction of two-hop or multi-hop forwarding algorithms. Let $D_{\text{IN}}^{[1]}$, $D_{\text{SP}}^{[1]}$, and $D_{\text{HO}}^{[1]}$ be the message delivery delay of direct forwarding under the individual, spatial, and homogeneous models, respectively.

To proceed, we need the following definitions for the stochastic and convex orderings between two random variables Y and Z , denoted by $Y \geq_{(\cdot)} Z$, if $\mathbb{E}\{\phi(Y)\} \geq \mathbb{E}\{\phi(Z)\}$ for a class of functions ϕ for which the expectation exists.

Definition 1. [76] Y is said to be larger than Z in the usual stochastic order (denoted by $Y \geq_{st} Z$) if $\mathbb{E}\{\phi(Y)\} \geq \mathbb{E}\{\phi(Z)\}$ holds for any increasing function ϕ , or equivalently if $\mathbb{P}\{Y > u\} \geq \mathbb{P}\{Z > u\}$ for all $u \in \mathbb{R}$. \square

Definition 2. [76] We define a convex (resp. concave) order, written $Y \geq_{cx} Z$ (resp. $Y \geq_{cv} Z$), if $\mathbb{E}\{\phi(Y)\} \geq \mathbb{E}\{\phi(Z)\}$ holds for any convex (resp. concave) function ϕ . Similarly, we also define an increasing convex (resp. increasing concave) order, written $Y \geq_{icx} Z$ (resp. $Y \geq_{icv} Z$), if $\mathbb{E}\{\phi(Y)\} \geq \mathbb{E}\{\phi(Z)\}$ holds for any increasing[†] convex (resp. increasing concave) function ϕ . \square

From Definitions 1–2, one can easily establish the following implications. If $Y \geq_{st} Z$, then $Y \geq_{icx} Z$ and $Y \geq_{icv} Z$. Similarly, if $Y \geq_{cx} Z$ (resp. $Y \geq_{cv} Z$), then $Y \geq_{icx} Z$ (resp. $Y \geq_{icv} Z$). Also, by noting that ϕ is concave if $-\phi$ is convex, from Definition 2, $Y \geq_{cx} Z$ implies $Y \leq_{cv} Z$. Moreover, by Definition 1, if $Y \geq_{st} Z$, then $\mathbb{E}\{Y\} \geq \mathbb{E}\{Z\}$, while from Definition 2, if $Y \geq_{cx} Z$, then $\mathbb{E}\{Y\} = \mathbb{E}\{Z\}$ and $\text{Var}\{Y\} \geq \text{Var}\{Z\}$ by taking $\phi(\cdot) = (\cdot)^2$.

The message delivery delay for a given source and destination pair is nothing but their residual (or remaining) inter-contact time after the message is generated at the source node. First, for the homogeneous model, we have

$$\mathbb{P}\{D_{\text{HO}}^{[1]} > t\} = \mathbb{P}\{T_I^{\text{HO}} > t\} = e^{-t/\tau}$$

due to the memoryless property of the exponential inter-contact time distribution with mean τ for any pair of nodes. Similarly, for the individual model,

$$\mathbb{P}\{D_{\text{IN}}^{[1]} > t | I = i\} = \mathbb{P}\{T_I^{\text{IN}} > t | I = i\} = e^{-\lambda_i t}$$

for a given pair $i \in \mathcal{I}$, thus from (3.1), we have

$$\mathbb{P}\{D_{\text{IN}}^{[1]} > t\} = \mathbb{E}\{\mathbb{P}\{D_{\text{IN}}^{[1]} > t | I\}\} = \mathbb{P}\{T_I^{\text{IN}} > t\} = \mathbb{E}\{e^{-t/X_{\text{IN}}}\}.$$

However, for the spatial model, the inter-contact time of a given pair $i \in \mathcal{I}$ is no longer memoryless but of hyper-exponential form as in (3.2). Under stationary regime, note that the residual inter-contact time R_i of a pair $i \in \mathcal{I}$ follows the equilibrium distribution of T_i [21, 41,

[†]Here, ‘increasing’ means non-decreasing.

19], i.e., $\mathbb{P}\{R_i > t\} = \frac{1}{\mathbb{E}\{T_i\}} \int_t^\infty \mathbb{P}\{T_i > u\} du$. Then, from (3.2), we can write for any $i \in \mathcal{I}$,

$$\begin{aligned} \mathbb{P}\{R_i > t\} &= \frac{1}{\mathbb{E}\{T_i\}} \int_t^\infty \mathbb{E}\{e^{-u/X}\} du = \frac{1}{\mathbb{E}\{T_i\}} \mathbb{E}\left\{\int_t^\infty e^{-u/X} du\right\} \\ &= \frac{1}{\mathbb{E}\{X\}} \mathbb{E}\{Xe^{-t/X}\}, \end{aligned} \quad (3.4)$$

where T_i and X here represent T_i^{SP} and X_{SP} for the spatial model, respectively. Since (3.4) holds for any $i \in \mathcal{I}$, we have

$$\mathbb{P}\{D_{\text{SP}}^{[1]} > t\} = \mathbb{P}\{R_i > t\} = \frac{1}{\mathbb{E}\{X_{\text{SP}}\}} \mathbb{E}\{X_{\text{SP}} \cdot e^{-t/X_{\text{SP}}}\}.$$

Now, we present our results for stochastic comparison on the delay performance of direct forwarding under the individual, spatial, and homogeneous models.

Proposition 2. *Let X_{IN1} , X_{IN2} be random variables in (3.1) for two different scenarios under the individual model, and $D_{\text{IN1}}^{[1]}$, $D_{\text{IN2}}^{[1]}$ be the corresponding message delivery delays of direct forwarding. Then, if $X_{\text{IN1}} \geq_{cx} X_{\text{IN2}}$, we have $D_{\text{IN1}}^{[1]} \geq_{cx} D_{\text{IN2}}^{[1]}$. \square*

Proof. By noting that $\mathbb{P}\{D_{\text{IN}}^{[1]} > t\} = \mathbb{E}\{e^{-t/X_{\text{IN}}}\}$ and $\mathbb{E}\{X_{\text{IN1}}\} = \mathbb{E}\{X_{\text{IN2}}\}$, we have $\mathbb{E}\{D_{\text{IN1}}^{[1]}\} = \mathbb{E}\{D_{\text{IN2}}^{[1]}\}$. Thus, in order to prove $D_{\text{IN1}}^{[1]} \geq_{cx} D_{\text{IN2}}^{[1]}$, it is enough to show that $\int_a^\infty \mathbb{P}\{D_{\text{IN1}}^{[1]} > t\} dt \geq \int_a^\infty \mathbb{P}\{D_{\text{IN2}}^{[1]} > t\} dt$ for all $a > 0$ [76]. It is equivalent to showing that

$$\mathbb{E}\{X_{\text{IN1}} \cdot e^{-a/X_{\text{IN1}}}\} \geq \mathbb{E}\{X_{\text{IN2}} \cdot e^{-a/X_{\text{IN2}}}\}, \quad (3.5)$$

for all $a > 0$.

Let $g(x) \triangleq xe^{-a/x}$. It is easy to see that $g(x)$ is a convex function of $x > 0$ for all $a > 0$. Thus, from $X_{\text{IN1}} \geq_{cx} X_{\text{IN2}}$ and Definition 2, the above inequality (3.5) holds by taking $\phi(x) = xe^{-a/x}$. This completes the proof. \blacksquare

Proposition 2 says the message delivery delay gets larger in the sense of convex order, as the underlying individual model becomes ‘more heterogeneous’ (in larger convex ordering of X). In particular, if $\mathbb{E}\{T_I^{\text{IN}}\} = \mathbb{E}\{T_I^{\text{HO}}\} = \tau$ (the same average aggregated inter-contact time under the individual and homogeneous models), we have

$$D_{\text{IN}}^{[1]} \geq_{cx} D_{\text{HO}}^{[1]},$$

since $X_{\text{IN}} \geq_{cx} \mathbb{E}\{X_{\text{IN}}\} = \mathbb{E}\{T_I^{\text{IN}}\} = \tau$. This means that the message delivery delay of direct forwarding under the individual model is *more variable* than that under the homogeneous

model, while the average delays under both models are the same.

Proposition 3. *If $\mathbb{E}\{T_I^{SP}\} = \mathbb{E}\{T_I^{HO}\}$, then $D_{SP}^{[1]} \geq_{st} D_{HO}^{[1]}$.* □

Proof. Recall that $\mathbb{P}\{D_{HO}^{[1]} > t\} = e^{-t/\tau}$ and

$$\mathbb{P}\{D_{SP}^{[1]} > t\} = \frac{1}{\mathbb{E}\{X_{SP}\}} \mathbb{E}\{X_{SP} \cdot e^{-t/X_{SP}}\}.$$

Note also that $X_{SP} \geq_{cx} \mathbb{E}\{X_{SP}\} = \mathbb{E}\{T_I^{SP}\} = \tau$. Let X_{HO} be a random variable that takes the value $\tau = \mathbb{E}\{X_{SP}\}$ with probability 1. Then, we can write

$$\mathbb{P}\{D_{HO}^{[1]} > t\} = \frac{1}{\mathbb{E}\{X_{HO}\}} \mathbb{E}\{X_{HO} \cdot e^{-t/X_{HO}}\}.$$

Hence, since $X_{SP} \geq_{cx} X_{HO}$ and $xe^{-t/x}$ is a convex function of $x > 0$ for all $t > 0$, from Definition 2, we have

$$\mathbb{E}\{X_{SP} \cdot e^{-t/X_{SP}}\} \geq \mathbb{E}\{X_{HO} \cdot e^{-t/X_{HO}}\}$$

for all $t > 0$. Then, by noting that $\mathbb{E}\{X_{SP}\} = \mathbb{E}\{X_{HO}\}$, it follows that $\mathbb{P}\{D_{SP}^{[1]} > t\} \geq \mathbb{P}\{D_{HO}^{[1]} > t\}$ for all $t > 0$. From Definition 1, the result follows. ■

Proposition 3 says that the message delivery delay of direct forwarding under the spatial model is stochastically larger than that under the homogeneous model, when the average inter-contact time under both models are matched. From Propositions 2 and 3, we see that the delay performance of direct forwarding under each heterogeneous model deviates from that under the homogeneous model in a different manner, though three models are the same in the average aggregate inter-contact time point of view.

Next, we compare the delay performance of direct forwarding under the spatial and individual models, when their *entire distributions* of the aggregate inter-contact time remain identical. This can be achieved by setting $X_{SP} \stackrel{d}{=} X_{IN}$ in (3.1)–(3.2). Still, our next result tells us that the delay of direct forwarding under the spatial model is always stochastically larger than that under the individual model.

Proposition 4. *If $T_I^{SP} \stackrel{d}{=} T_I^{IN}$, then $D_{SP}^{[1]} \geq_{st} D_{IN}^{[1]}$.* □

Proof. Recall that $\mathbb{P}\{D_{IN}^{[1]} > t\} = \mathbb{E}\{e^{-t/X_{IN}}\}$ and

$$\mathbb{P}\{D_{SP}^{[1]} > t\} = \frac{1}{\mathbb{E}\{X_{SP}\}} \mathbb{E}\{X_{SP} \cdot e^{-t/X_{SP}}\}.$$

Since $e^{-t/x}$ is increasing in $x > 0$ for any given $t > 0$, we have

$$\mathbb{E}\{X_{\text{SP}} \cdot e^{-t/X_{\text{SP}}}\} \geq \mathbb{E}\{X_{\text{SP}}\} \cdot \mathbb{E}\{e^{-t/X_{\text{SP}}}\}. \quad (3.6)$$

Then, from the assumption that

$$\mathbb{P}\{T_I^{\text{SP}} > t\} = \mathbb{E}\{e^{-t/X_{\text{SP}}}\} = \mathbb{E}\{e^{-t/X_{\text{IN}}}\} = \mathbb{P}\{T_I^{\text{IN}} > t\}$$

for any given $t > 0$, and from (3.6) we have

$$\mathbb{P}\{D_{\text{SP}}^{[1]} > t\} = \frac{1}{\mathbb{E}\{X_{\text{SP}}\}} \mathbb{E}\{X_{\text{SP}} \cdot e^{-t/X_{\text{SP}}}\} \geq \mathbb{E}\{e^{-t/X_{\text{SP}}}\} = \mathbb{E}\{e^{-t/X_{\text{IN}}}\} = \mathbb{P}\{D_{\text{IN}}^{[1]} > t\},$$

for all $t > 0$. From Definition 1, the result follows. \blacksquare

To sum up, from Propositions 2–4, we observe that the performance of direct forwarding varies depending on which of the two heterogeneous models is chosen, i.e., how the non-Poisson contact dynamics observed in the real traces are modeled. In addition, the aggregated inter-contact time statistics (the whole distribution) are still insufficient to correctly predict the forwarding performance, even though many existing works [21, 50, 10] have relied on the aggregated inter-contact time samples to uncover the characteristics of mobile nodes' contact patterns and justify their modeling choices.

3.3 Delay Performance of Multicopy Two-hop Relay Protocol

We now turn our attention to multicopy two-hop relay protocol [39, 96, 41, 45] as a test case for a further investigation of the impact of the heterogeneity structure on the forwarding performance. In this protocol, only source node can replicate a message and forward its copy to any relay node that does not have the message copy upon encounter.

Consider the delivery of a single message in the network with $|\mathcal{N}| = n + 2$. Given a pair of source s and destination d which is uniformly chosen over \mathcal{I} , there are n possible relay nodes (r_1, r_2, \dots, r_n) . We hereafter use T_{ij} , instead of T_l ($l \in \mathcal{I}$), to represent the pairwise inter-contact time of nodes i and j if needed to specify nodes (i, j) of each node pair, where $i, j \in \{s, r_1, \dots, r_n, d\}$ and $i \neq j$. Similarly, R_{ij} stands for the residual inter-contact time of nodes i and j . Then, as shown in [41, 45], the message delivery delay of the multicopy two-hop relay protocol (denoted by D) – the time interval from the time when the message is generated at a source node to the time when any copy of the message first reaches its destination, is given by

$$D \stackrel{d}{=} \min\{R_{sd}, R_{sr_1} + R_{r_1d}, \dots, R_{sr_n} + R_{r_nd}\}. \quad (3.7)$$

As before, $D_{\text{IN}}^{[2]}$, $D_{\text{SP}}^{[2]}$, and $D_{\text{HO}}^{[2]}$ denote the message delivery delay of multicopy two-hop relay protocol under individual, spatial, and homogeneous models, respectively. Here, we use superscript $D^{[2]}$ to indicate the multicopy two-hop relay protocol, whereby $D^{[1]}$ was used for the direct forwarding (single-hop) protocol in Section 3.2.

We first show that the stochastic ordering relationship in Proposition 3 still holds for the message delay delays of multicopy two-hop relay protocol under the spatial and homogeneous models.

Proposition 5. *If $\mathbb{E}\{T_I^{\text{SP}}\} = \mathbb{E}\{T_I^{\text{HO}}\}$, then $D_{\text{SP}}^{[2]} \geq_{st} D_{\text{HO}}^{[2]}$.* □

Proof. Let R_{ij}^{SP} and R_{ij}^{HO} be the residual inter-contact time of a given node pair (i, j) under the spatial and homogeneous models, respectively. From Proposition 3, we have $R_{ij}^{\text{SP}} \geq_{st} R_{ij}^{\text{HO}}$. From the independence of R_{ij}^{SP} and R_{ij}^{HO} over different node (i, j) pairs, the stochastic order is also closed under convolutions [76]. Thus, $R_{sd}^{\text{SP}} \geq_{st} R_{sd}^{\text{HO}}$ and $R_{sr_i}^{\text{SP}} + R_{r_i d}^{\text{SP}} \geq_{st} R_{sr_i}^{\text{HO}} + R_{r_i d}^{\text{HO}}$ ($i = 1, 2, \dots, n$). Then, it easily follows that these stochastic ordering relationships still hold for their first order statistic, i.e.,

$$\min\{R_{sd}^{\text{SP}}, R_{sr_1}^{\text{SP}} + R_{r_1 d}^{\text{SP}}, \dots, R_{sr_n}^{\text{SP}} + R_{r_n d}^{\text{SP}}\} \geq_{st} \min\{R_{sd}^{\text{HO}}, R_{sr_1}^{\text{HO}} + R_{r_1 d}^{\text{HO}}, \dots, R_{sr_n}^{\text{HO}} + R_{r_n d}^{\text{HO}}\}.$$

That is, $D_{\text{SP}}^{[2]} \geq_{st} D_{\text{HO}}^{[2]}$, which completes the proof. ■

Proposition 5 also implies that the hyper-exponential inter-contact time yields stochastically larger delay than the exponential inter-contact time for the multicopy two-hop relay protocol when their average inter-contact times are matched.

Next, we show the stochastic comparison for the delays of multicopy two-hop relay protocol under the individual and homogeneous models. Specifically, we first compare the delay performance for *a given source and destination pair* under the individual and homogeneous models, as the pairwise inter-contact times are statistically different for different node pairs under the individual model unlike to the spatial and homogeneous models. Later on, we will continue our stochastic comparison on the delay performance for *a uniformly and randomly chosen source and destination pair* under both models. In this stochastic comparison, we assume that each message reaches its destination via relay nodes only and the direct path from source to destination is not considered. This may be the case with a moderate to large number of mobile nodes (e.g., campus-wide MONs), i.e., the ‘best’ of n relay nodes is likely to reach the destination earlier than the source node does.

Let $D_{\text{IN}(s,d)}^{[2]}$ be the message delivery delay for a given source and destination (s, d) pair under the individual model. Here, for a proper comparison between $D_{\text{IN}(s,d)}^{[2]}$ and $D_{\text{HO}}^{[2]}$, we set

the average inter-contact time for the corresponding homogeneous model as

$$\tau = \frac{1}{2n} \sum_{i=1}^n \left[\frac{1}{\lambda_{sr_i}} + \frac{1}{\lambda_{r_id}} \right]. \quad (3.8)$$

That is, the average inter-contact time for any node pair under the constructed homogeneous model is simply the arithmetic mean of the average inter-contact times over all node pairs in n two-hop relay paths under the individual model. Let T_{ij}^{IN} and T_{ij}^{HO} be the inter-contact time of each node pair (i, j) under the individual and homogeneous models, respectively. Then, due to the memoryless property of exponential pairwise inter-contact time distributions under the individual and homogeneous models, $D_{\text{IN}(s,d)}^{[2]}$ and $D_{\text{HO}}^{[2]}$ are given by

$$D_{\text{IN}(s,d)}^{[2]} = \min\{T_{sr_1}^{\text{IN}} + T_{r_1d}^{\text{IN}}, \dots, T_{sr_n}^{\text{IN}} + T_{r_nd}^{\text{IN}}\}, \quad (3.9)$$

$$D_{\text{HO}}^{[2]} = \min\{T_{sr_1}^{\text{HO}} + T_{r_1d}^{\text{HO}}, \dots, T_{sr_n}^{\text{HO}} + T_{r_nd}^{\text{HO}}\}. \quad (3.10)$$

Instead of directly comparing $D_{\text{IN}(s,d)}^{[2]}$ with $D_{\text{HO}}^{[2]}$, we compare *each* of these message delivery delays with that under a *partially homogeneous* setting (a special case of the individual model). Figure 3.1(b) shows this partially homogeneous setting in which the delay over each relay path is now a sum of two *i.i.d.* exponential random variables with mean $\frac{1}{2}[1/\lambda_{sr_i} + 1/\lambda_{r_id}]$ (homogeneous for a given path, but heterogeneous over different paths). Let S_{sr_i} and S_{r_id} be *i.i.d.* exponential random variables with mean

$$\frac{1}{\mu_i} \triangleq \frac{1}{2} \left[\frac{1}{\lambda_{sr_i}} + \frac{1}{\lambda_{r_id}} \right], \quad (3.11)$$

where $i = 1, \dots, n$. Then, the message delivery delay in this partially homogeneous model, $\tilde{D}_{\text{IN}(s,d)}^{[2]}$, is given by

$$\tilde{D}_{\text{IN}(s,d)}^{[2]} = \min\{S_{sr_1} + S_{r_1d}, \dots, S_{sr_n} + S_{r_nd}\}. \quad (3.12)$$

Figure 3.1 depicts the aforementioned three different settings of n two-hop relay paths with varying degrees of heterogeneity over the average inter-contact times in the network.

To proceed, we collect several definitions on majorization [60] ordering. This is a partial order over vectors of real numbers and is useful in capturing the degree of heterogeneity in vector components.

Definition 3. [60] For $\vec{y}, \vec{z} \in \mathbb{R}^n$, \vec{y} is said to be majorized by \vec{z} , or \vec{z} majorizes \vec{y} , (written $\vec{y} \prec \vec{z}$), if $\sum_{i=1}^m y_{[i]} \leq \sum_{i=1}^m z_{[i]}$, ($m = 1, 2, \dots, n-1$), and $\sum_{i=1}^n y_{[i]} = \sum_{i=1}^n z_{[i]}$, where $y_{[1]} \geq y_{[2]} \geq \dots \geq y_{[n]}$ ($z_{[1]} \geq z_{[2]} \geq \dots \geq z_{[n]}$) denote the components of \vec{y} (resp. \vec{z}) in decreasing order. \square

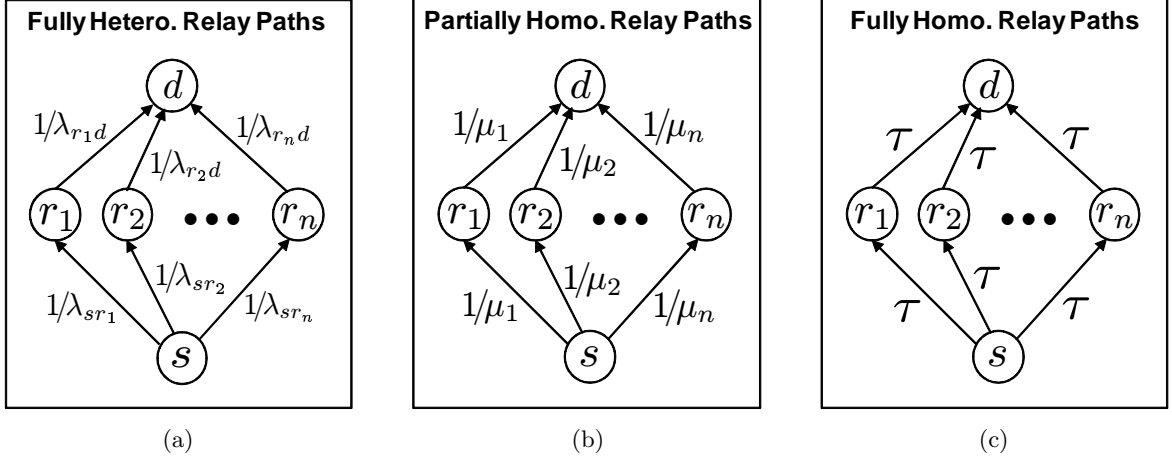


Figure 3.1: Three different settings of n two-hop relay paths with varying degrees of heterogeneity: (a) a fully heterogeneous setting, (b) a partially homogeneous setting where each relay path is homogeneous. (i.e., two-hop components in each relay path have the same average inter-contact time as $1/\mu_i = \frac{1}{2}[1/\lambda_{sr_i} + 1/\lambda_{r_i,d}]$), and (c) a fully homogeneous setting where the average inter-contact time for any node pair is $\tau = \frac{1}{2n} \sum_{i=1}^n [1/\lambda_{sr_i} + 1/\lambda_{r_i,d}]$.

From (3.11) and Definition 3, we have

$$\left(\frac{1}{\lambda_{sr_i}}, \frac{1}{\lambda_{r_i,d}} \right) \succ \left(\frac{1}{\mu_i}, \frac{1}{\mu_i} \right) \quad (3.13)$$

for any $\lambda_{sr_i}, \lambda_{r_i,d} > 0$, and $(1/\mu_i, 1/\mu_i)$ is the smallest in the sense of majorization ordering. Further, note that from (3.8) and (3.11),

$$\tau = \frac{1}{2n} \sum_{i=1}^n \left[\frac{1}{\lambda_{sr_i}} + \frac{1}{\lambda_{r_i,d}} \right] = \frac{1}{n} \sum_{i=1}^n \frac{1}{\mu_i}.$$

This implies that

$$\left(\frac{1}{\mu_1}, \dots, \frac{1}{\mu_n} \right) \succ (\tau, \dots, \tau) \quad (3.14)$$

for any $\mu_i > 0$.

Definition 4. [60] For $\vec{y}, \vec{z} \in \mathbb{R}^n$, a real-valued function ψ defined on \mathbb{R}^n is said to be Schur-convex, if $\vec{y} \prec \vec{z}$ implies $\psi(\vec{y}) \leq \psi(\vec{z})$. Similarly, ψ is said to be Schur-concave, if $\vec{y} \prec \vec{z}$ implies $\psi(\vec{y}) \geq \psi(\vec{z})$. \square

We also need the following result on the preservation of the increasing concave ordering.

Proposition 6. [74, Proposition 9.5.4] If Y_1, \dots, Y_n are independent random variables and

Z_1, \dots, Z_n are independent random variables, and $Y_i \geq_{icv} Z_i$ for each $i = 1, \dots, n$, then $f(Y_1, \dots, Y_n) \geq_{icv} f(Z_1, \dots, Z_n)$ for all increasing and componentwise concave function f . \square

Now we present our main result on the stochastic comparison among $D_{\text{IN}(s,d)}^{[2]}$, $\tilde{D}_{\text{IN}(s,d)}^{[2]}$, $D_{\text{HO}}^{[2]}$ – the message delivery delay of multicopy two-hop relay protocol over the network setting in Figure 3.1(a), (b), (c), respectively.

Theorem 1. *If $\mathbb{E}\{T_I^{\text{HO}}\} = \tau = \frac{1}{2n} \sum_{i=1}^n \left[\frac{1}{\lambda_{sr_i}} + \frac{1}{\lambda_{r_id}} \right]$, then $D_{\text{IN}(s,d)}^{[2]} \leq_{icv} \tilde{D}_{\text{IN}(s,d)}^{[2]} \leq_{st} D_{\text{HO}}^{[2]}$. \square*

Proof. (A) Proof of $D_{\text{IN}(s,d)}^{[2]} \leq_{icv} \tilde{D}_{\text{IN}(s,d)}^{[2]}$: Let U_1 and U_2 be *i.i.d.* exponential random variables with rate one. Then, observe that

$$T_{sr_i}^{\text{IN}} \stackrel{d}{=} \frac{1}{\lambda_{sr_i}} U_1, \text{ and } T_{r_id}^{\text{IN}} \stackrel{d}{=} \frac{1}{\lambda_{r_id}} U_2.$$

Similarly, we have

$$S_{sr_i} \stackrel{d}{=} \frac{1}{\mu_i} U_1, \text{ and } S_{r_id} \stackrel{d}{=} \frac{1}{\mu_i} U_2.$$

Thus, from the independence of $T_{sr_i}^{\text{IN}}$ and $T_{r_id}^{\text{IN}}$ and the independence of S_{sr_i} and S_{r_id} , we have

$$\begin{aligned} T_{sr_i}^{\text{IN}} + T_{r_id}^{\text{IN}} &\stackrel{d}{=} \frac{1}{\lambda_{sr_i}} U_1 + \frac{1}{\lambda_{r_id}} U_2, \\ S_{sr_i} + S_{r_id} &\stackrel{d}{=} \frac{1}{\mu_i} U_1 + \frac{1}{\mu_i} U_2. \end{aligned} \tag{3.15}$$

Note that if Y_1, \dots, Y_n are exchangeable random variables, then $\psi(\vec{a}) = \mathbb{E}\{f(\sum a_i Y_i)\}$ is Schur-convex on \mathbb{R}^n for any convex function f [60, p.287, Proposition B.2]. Thus, from (3.13), (3.15), and Definition 4, we have,

$$\begin{aligned} \mathbb{E}\{f(T_{sr_i}^{\text{IN}} + T_{r_id}^{\text{IN}})\} &= \mathbb{E}\left\{f\left(\frac{1}{\lambda_{sr_i}} U_1 + \frac{1}{\lambda_{r_id}} U_2\right)\right\} \\ &\geq \mathbb{E}\left\{f\left(\frac{1}{\mu_i} U_1 + \frac{1}{\mu_i} U_2\right)\right\} = \mathbb{E}\{f(S_{sr_i} + S_{r_id})\}, \end{aligned}$$

for any convex function f . Equivalently, from Definition 2, we have $T_{sr_i}^{\text{IN}} + T_{r_id}^{\text{IN}} \geq_{cx} S_{sr_i} + S_{r_id}$ for each $i = 1, \dots, n$. As mentioned in Section 3.2, it follows that

$$T_{sr_i}^{\text{IN}} + T_{r_id}^{\text{IN}} \geq_{cx} S_{sr_i} + S_{r_id} \Rightarrow T_{sr_i}^{\text{IN}} + T_{r_id}^{\text{IN}} \leq_{cv} S_{sr_i} + S_{r_id} \Rightarrow T_{sr_i}^{\text{IN}} + T_{r_id}^{\text{IN}} \leq_{icv} S_{sr_i} + S_{r_id},$$

for any i . Then, since $\min\{x_1, \dots, x_n\}$ is increasing on \mathbb{R}^n and concave in each argument x_i ,

from (3.9), (3.12), and Proposition 6, we have

$$D_{\text{IN}(s,d)}^{[2]} \leq_{icv} \tilde{D}_{\text{IN}(s,d)}^{[2]}. \quad (3.16)$$

(B) Proof of $\tilde{D}_{\text{IN}(s,d)}^{[2]} \leq_{st} D_{\text{HO}}^{[2]}$: Let $\nu_i \triangleq \frac{1}{\mu_i}$ and

$$g(\nu_i) \triangleq \mathbb{P}\{S_{sr_i} + S_{r_i d} > t\} = \left(1 + \frac{t}{\nu_i}\right) e^{-t/\nu_i}$$

for any given $t > 0$. We also define another function by

$$h(\vec{\nu}) \triangleq \mathbb{P}\left\{\tilde{D}_{\text{IN}(s,d)}^{[2]} > t\right\} = \prod_{i=1}^n g(\nu_i),$$

where $\vec{\nu} \triangleq (\nu_1, \nu_2, \dots, \nu_n)$. It is straightforward to check $\log g(\nu_i)$ is concave in $\nu_i > 0$ for all $t > 0$. Then, since $g(\nu_i)$ is log-concave, $h(\vec{\nu}) = \prod g(\nu_i)$ is Schur-concave on $(0, \infty)^n$ [60, p.73, Proposition E.1]. Thus, from (3.10), (3.12), (3.14) and Definition 4, we have for any $\vec{\nu} \in (0, \infty)^n$,

$$\mathbb{P}\left\{\tilde{D}_{\text{IN}(s,d)}^{[2]} > t\right\} = h(\nu_1, \dots, \nu_n) \leq h(\tau, \dots, \tau) = \mathbb{P}\left\{D_{\text{HO}}^{[2]} > t\right\},$$

for any given $t > 0$. In other words, by Definition 1,

$$\tilde{D}_{\text{IN}(s,d)}^{[2]} \leq_{st} D_{\text{HO}}^{[2]}. \quad (3.17)$$

From (3.16) and (3.17), we are done. ■

By noting that $\leq_{st} \Rightarrow \leq_{icv}$, Theorem 1 implies that if $\mathbb{E}\{T_I^{\text{HO}}\} = \frac{1}{2n} \sum_{i=1}^n [1/\lambda_{sr_i} + 1/\lambda_{r_i d}]$, then

$$D_{\text{IN}(s,d)}^{[2]} \leq_{icv} D_{\text{HO}}^{[2]}.$$

Since $\phi(x) = x$ is increasing and concave, from Definition 2, it further implies

$$\mathbb{E}\{D_{\text{IN}(s,d)}^{[2]}\} \leq \mathbb{E}\{D_{\text{HO}}^{[2]}\}. \quad (3.18)$$

We now move on to the stochastic comparison on message delivery delays for a *uniform* source and destination pair. Note that the average message delivery delay of a uniform pair is nothing but the arithmetic mean of the average message delivery delays over all possible $|\mathcal{N}|(|\mathcal{N}| - 1)/2$ source and destination (s, d) pairs. Also, as in (3.18), for each (s, d) pair, if $\mathbb{E}\{T_I^{\text{HO}}\} = \frac{1}{2n} \sum_{i=1}^n [1/\lambda_{sr_i} + 1/\lambda_{r_i d}]$, then $\mathbb{E}\{D_{\text{HO}}^{[2]}\}$ becomes an upper bound of $\mathbb{E}\{D_{\text{IN}(s,d)}^{[2]}\}$.

Hence, after computing the arithmetic mean of the upper bounds of $\mathbb{E}\{D_{\text{IN}(s,d)}^{[2]}\}$ over all (s, d) pairs, we obtain the following corollary.

Corollary 1. *If $\mathbb{E}\{T_I^{\text{HO}}\} = \mathbb{E}\{T_I^{\text{IN}}\} = \sum_{i \in \mathcal{I}} \frac{1}{\lambda_i} \frac{1}{|\mathcal{I}|}$, then $\mathbb{E}\{D_{\text{IN}}^{[2]}\} \leq \mathbb{E}\{D_{\text{HO}}^{[2]}\}$.* \square

Proof. See Appendix A.2. ■

As shown in Theorem 1 and Corollary 1, the path diversity (heterogeneity) over n relay paths under the individual model results in better delay performance of multicopy two-hop relay protocol. It also turns out that Proposition 5 still holds under the same scenario (i.e., no direct path is used) considered in Corollary 1. Thus, under this scenario, if $\mathbb{E}\{T_I^{\text{SP}}\} = \mathbb{E}\{T_I^{\text{IN}}\} = \mathbb{E}\{T_I^{\text{HO}}\}$, we have

$$\mathbb{E}\{D_{\text{IN}}^{[2]}\} \leq \mathbb{E}\{D_{\text{HO}}^{[2]}\} \leq \mathbb{E}\{D_{\text{SP}}^{[2]}\}. \quad (3.19)$$

This means that the heterogeneity structure in the spatial model makes the average delay performance of multicopy two-hop relay protocol worse, whereas the other heterogeneity structure in the individual model is beneficial to its average delay performance when compared with that under the corresponding homogeneous model. In addition, even if the whole aggregate inter-contact time distribution under both the spatial and individual models remains the same, i.e., $T_I^{\text{SP}} \stackrel{d}{=} T_I^{\text{IN}}$, since $\mathbb{E}\{T_I^{\text{SP}}\} = \mathbb{E}\{T_I^{\text{IN}}\}$, it follows from (3.19) that

$$\mathbb{E}\{D_{\text{IN}}^{[2]}\} \leq \mathbb{E}\{D_{\text{SP}}^{[2]}\}.$$

Along with Proposition 4, it clearly shows that the aggregate inter-contact time statistics are still not sufficient in accurately estimating the forwarding performance.

From our theoretical results, we expect that the delay performance of other two-hop or multi-hop forwarding protocols under each heterogeneous model differs considerably from that under the homogeneous model and there exists a significant performance gap between the two heterogeneous models as we observed, even when the entire aggregate inter-contact time distributions are precisely matched.

3.4 Simulation Results

In this section, we present simulation results on the average delay performance of multicopy two-hop relay protocol and epidemic routing protocol for a uniform source and destination pair under the individual, spatial, and homogeneous models, all of which are the same in the average inter-contact time of a random pair of nodes (the same average aggregate inter-contact time) to support our analytical findings. In the epidemic routing protocol [88, 39, 48, 96, 45, 47],

a commonly used reference forwarding algorithm for MONs, every node can copy a message and forward its copy (‘infect’) to any other node that does not have the message already upon encounter. We use a custom event-driven simulator implemented using C++ to conduct numerical simulations.

Specifically, for the spatial model, we consider a two-states spatial model (a special case) where random contact events of each node pair occur according to a Poisson process with rate β_i only when two nodes of the pair reside in the same state (site) $i \in \{1, 2\}$, while every node can move between two states with transition rates q_{12}, q_{21} . In addition, we consider the following scenario for the individual model: all node pairs (total $|\mathcal{N}|(|\mathcal{N}| - 1)/2$ pairs) are equally divided into 5 groups, in which the contact rate of any node pair in each group is the same, but different from that of the other group, though the inter-contact time distribution of each pair is still exponential. For the homogeneous model, by its definition, contact events of *any* node pair happen according to a Poisson process with same rate parameter. We below explain parameter settings which ensure the same average aggregate inter-contact time for all the three models.

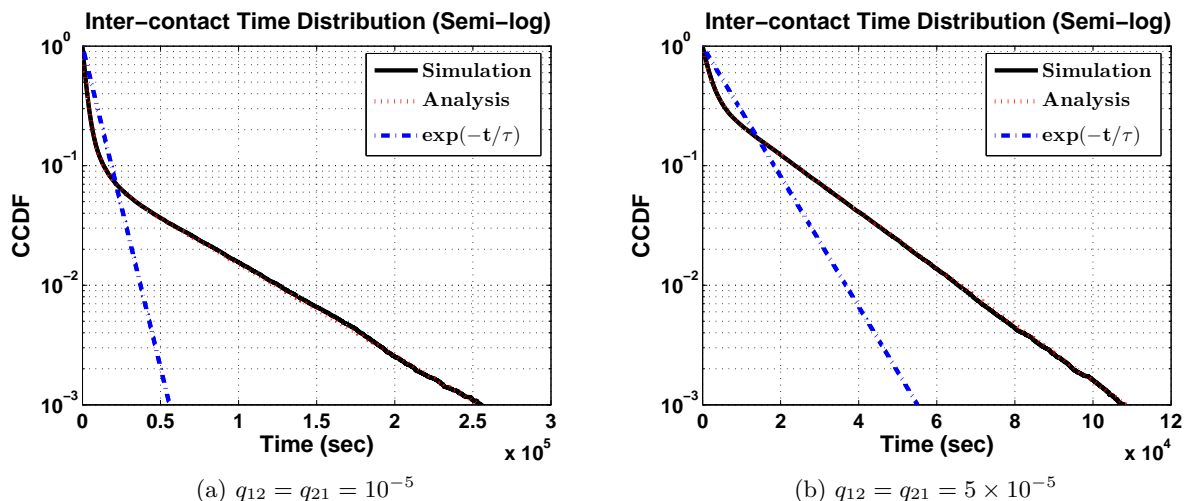


Figure 3.2: Pairwise inter-contact time distribution under the two-states spatial model with varying q_{12} ($= q_{21}$). $\tau = 8000$ for both cases.

In the simulations of the two-states spatial model, we use $\beta_1 = 10^{-4}$ and $\beta_2 = 4 \times 10^{-4}$ for the contact rates associated with states S_1 and S_2 , respectively, and consider two different cases of the transition rates q_{12} and q_{21} , i.e., $q_{12} = q_{21} = 10^{-5}$ and $q_{12} = q_{21} = 5 \times 10^{-5}$. We here present the complementary cumulative distribution function (CCDF) of the inter-contact time of a node pair on semi-log scale under the above parameter settings in Figure 3.2. The

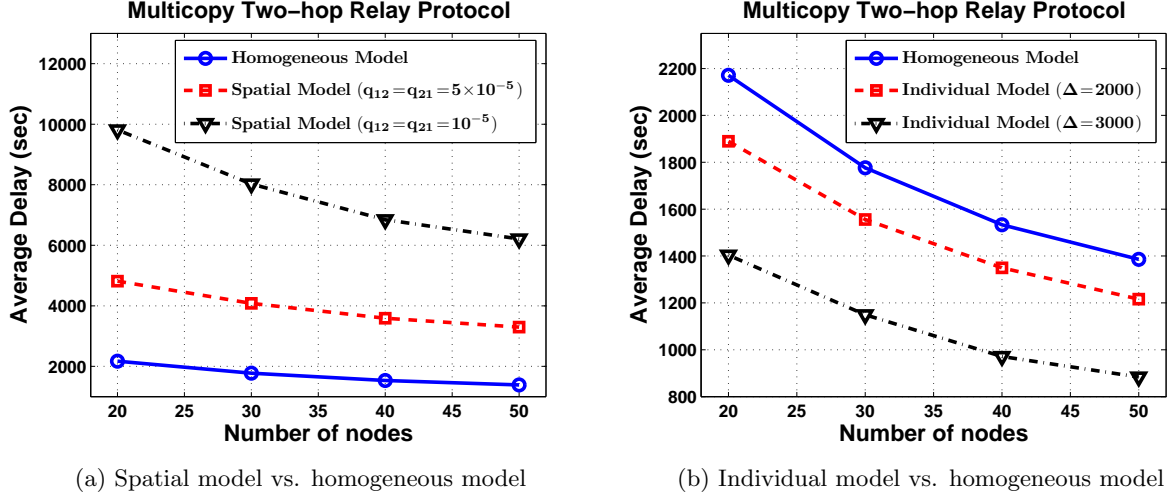


Figure 3.3: The average delay of multicopy two-hop relay protocol under the spatial, individual, and homogeneous models, all of which have the same average aggregate inter-contact time.

graphs labeled ‘simulation’ are plotted based on inter-contact time samples of a node pair from numerical simulations, while the other graphs labeled ‘analysis’ are obtained from the derivation of pairwise inter-contact time distribution shown in the proof of Proposition 1 (i.e., numerical computation of the equation (A.3) in Appendix A.1). From Figure 3.2, we can identify that the simulation results show a good agreement with the analysis of the pairwise inter-contact time distribution. In Figure 3.2, an exponential distribution with mean τ , which is set to be the same average inter-contact time observed in each simulation, is also drawn to explicitly show that the pairwise inter-contact time distribution under the two-states spatial model deviates much from that under the homogeneous model, an pure exponential distribution. Note the average inter-contact time observed under each of both simulations is almost the same as 8000 seconds (i.e., $\tau = 8000$). This value of τ is also used for the average inter-contact time of any node pair under the homogeneous model in the subsequent simulations. In addition, for the simulations of the individual model, the average inter-contact time for each of 5 groups of node pairs is given by $\tau - 2\Delta, \tau - \Delta, \tau, \tau + \Delta, \tau + 2\Delta$, respectively, where $\tau = 8000$ and $\Delta = 2000, 3000$. In this way, the average inter-contact time of a randomly chosen pair of nodes remains the same for the three models.

We then conduct numerical simulations to measure the average delay performance of multicopy two-hop relay protocol and epidemic routing protocol under each of the three models with the above parameter settings. In each simulation, a message is independently generated at a random time for a uniformly and randomly chosen source and destination pair and total 10^5 messages are generated during the simulation. All simulation results are obtained based upon

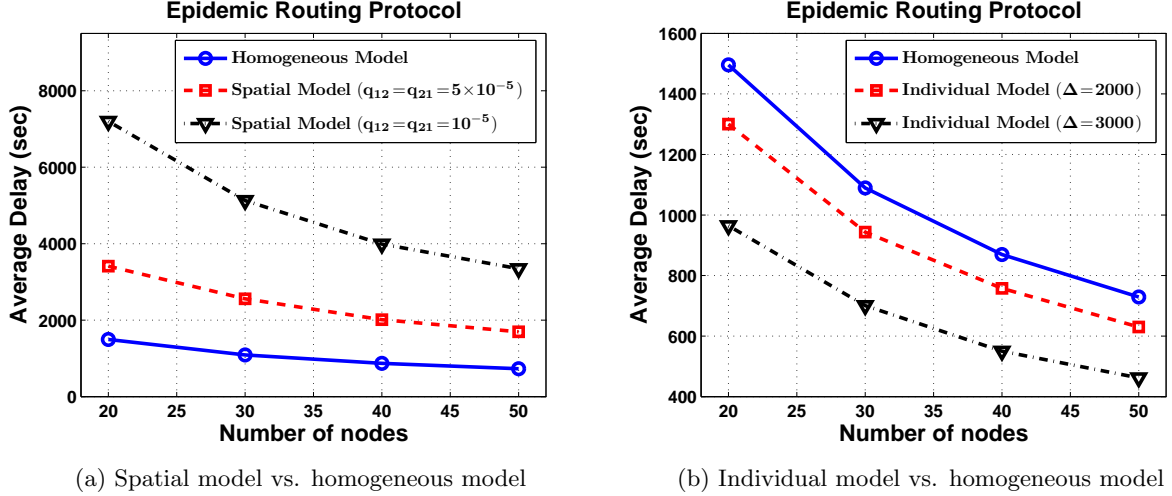


Figure 3.4: The average delay of epidemic protocol under the spatial, individual, and homogeneous models, all of which remain the same in the average inter-contact time of a random pair of nodes.

the message delivery of 10^5 messages. We also change the number of nodes $|\mathcal{N}|$ from 20 to 50 in the simulations.

Figure 3.3 shows the average delays of multicopy two-hop relay protocol under the spatial, individual, and homogeneous models. First, as shown in Figure 3.3(a), the spatial model with a different set of transition rates yields worse performance than the homogeneous model in terms of the average delay, which is in good agreement with our analytical findings in Section 3.3 (see Proposition 5 and (3.19)). This performance declination results from that pairwise inter-contact time under the spatial model is no longer memoryless and more variable, which tends to have longer inter-contact time sample with higher probability, as seen from Figure 3.2. We can further observe that for the spatial model, the average delay performance under the case of $q_{12} = q_{21} = 10^{-5}$ is worse than the other. This is also due to higher variability of inter-contact time under the former case.

In addition, as can be seen from Figure 3.3(b), the individual model (with $\Delta = 2000, 3000$) results in better average delay performance than the homogeneous model. This also confirms our findings in Theorem 1 and Corollary 1. As mentioned in Section 3.3, the main reason of the performance improvement is the *path diversity* in the individual model. In other words, since the message delivery delay is the *minimum* path delay over direct and two-hop relay paths, the diversity in path delays under the individual model can improve the delay performance. We also observe that the more variable scenario of the individual model in terms of the average inter-contact time for each node pair ($\Delta = 3000$), the smaller average delay of the multicopy

two-hop relay protocol. This improvement comes from higher path diversity for the case of $\Delta = 3000$.

We also present the average delays of epidemic routing protocol under the spatial, individual, and homogeneous models in Figure 3.4. We can see the same trend in the average delay performance of epidemic routing protocol as observed above for the multicopy two-hop relay protocol. Hence, all the simulation results collectively exhibit an opposite prediction on the forwarding performance from each of the two heterogeneous models and also show the presence of a performance gap between the performance predictions, which confirms our analytical results.

Chapter 4

Exploiting Heterogeneity in Mobile Nodes' Contact Dynamics to Improving Forwarding Performance

In Chapter 3, we have studied how two different sources of heterogeneity in mobile nodes' contact dynamics (individual and spatial heterogeneities) on the forwarding performance. In this chapter, we extend our investigation to *quantifying* the benefit of leveraging the underlying heterogeneity structure in the design of forwarding algorithms. Specifically, we analytically investigate how much benefit the heterogeneity in mobile nodes' contact dynamics can bring in the forwarding performance. We first present a class of probabilistic twohop forwarding policies and an optimization problem to find an optimal forwarding policy among the probabilistic forwarding policies in Section 4.1. Rather than directly solving the optimization problem, we instead derive a delay upper bound of any two-hop forwarding policy and obtain its closed-form expression in Section 4.2, and then find a sub-optimal forwarding policy which minimizes the derived delay upper bound while satisfying a given constraint in Section 4.3.1. In Section 4.3.2, we finally provide numerical evaluations of the forwarding performance via the sub-optimal policy as well as its simulation results to show the attainable performance gain through exploiting the heterogeneity in contact dynamics under various heterogeneous network settings.

4.1 Problem Formulation

In this section, we first explain a class of probabilistic two-hop forwarding policies with a given constraint on the number of message copies under the individually heterogeneous network model (individual model) defined in Chapter 2 in which the pairwise inter-contact time between mobile nodes i and j , denoted by T_{ij} , is independently drawn from an exponential distribution with

rate $\lambda_{ij} > 0$, where $i, j \in \mathcal{N}$ and $i \neq j$. We then formulate an optimization problem to find an optimal forwarding policy to minimize the message delivery delay while satisfying the constraint.

In the class of probabilistic two-hop forwarding policies, a source node forwards a message copy to each relay node r_i with probability $p_i \in [0, 1]$ upon encounter. Note that the source node has no benefit of forwarding a copy to each relay node upon the second or later encounter after skipping the first forwarding opportunity. Thus, the forwarding decision for each relay node is done only once upon the first encounter. Then, the forwarded message copies or an original message can be delivered to their destinations via relay nodes chosen in the forwarding decision or directly by the source, respectively. Figure 4.1 depicts this operation under the probabilistic two-hop forwarding policies.

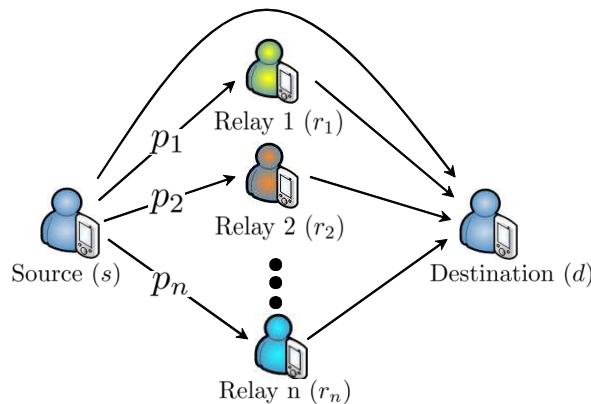


Figure 4.1: A class of probabilistic two-hop forwarding policies. Source S forwards a message copy to relay node r_i with probability p_i .

Our focus in this chapter is not to propose yet another forwarding algorithm but to analytically quantify the achievable performance gain by exploiting the heterogeneity in mobile nodes' contact dynamics. For tractable analysis (but still non-trivial), we do not consider two-hop forwarding policies which change relay paths or choose relay nodes on-the-fly upon encounter, i.e., the forwarding probability p_i for each relay node i is not changing over time but predetermined. As we shall show in Section 4.3, a two-hop forwarding policy obtained from a class of policies considered, which is below explained, still demonstrates its significant performance improvement by exploiting the underlying heterogeneity structure. We also discuss a further benefit possible by changing relay paths on-the-fly upon encounter in Section 4.3.

Each forwarding probability p_i should be chosen to satisfy a constraint on the number of message copies, which in turn controls network cost or the amount of resource consumption in-

curred by additional message transfers.* At the same time, the message delivery delay critically depends on how we choose p_i for each relay node r_i . Thus, we can formulate the problem of finding an optimal forwarding policy \vec{p}^* under the constraint on the number of message copies in the individual model as an optimization problem. In what follows, we describe this formulation step by step.

Throughout the formulation and subsequent delay analysis, we assume the followings as in other analytical works [81, 39, 96, 4, 42]. The network is sparse and network traffic is light such that interference and contention [48] are not important factors. In other words, we assume that each node has infinite bandwidth and buffer. In fact, as will be shown in Section 4.3, exploiting the heterogeneity in mobile nodes' contact dynamics is helpful in significantly reducing the number of message copies, which in turn keeps the network traffic low and thus decreases the effect of interference/contention. In addition, we assume that a message transfer between any two nodes at their contact instant takes a negligible time with respect to their inter-contact time.

Let $\mathcal{N} = \{s, r_1, \dots, r_n, d\}$ with source s and destination d , and n possible relay nodes r_1, r_2, \dots, r_n . Let $\{Y_i\}_{1 \leq i \leq n}$ be the set of independent Bernoulli random variables with

$$\mathbb{P}\{Y_i = 1\} = p_i \quad \text{and} \quad \mathbb{P}\{Y_i = 0\} = 1 - p_i,$$

to represent the forwarding decision to relay node r_i . For each i , we define a function I_{p_i} as

$$I_{p_i} = \begin{cases} 1 & \text{if } Y_i = 1, \\ \infty & \text{otherwise.} \end{cases} \quad (4.1)$$

Let $M = \sum_{i=1}^n Y_i$ denote the random variable to represent the number of message copies except the original message at the source node in the whole network. We also define $\vec{Y} \triangleq [Y_1, \dots, Y_n]$ and $\vec{p} \triangleq [p_1, \dots, p_n]$.

The message delivery delay D under a probabilistic two-hop forwarding policy with \vec{p} can then be written as

$$D = \min\{T_{sd}, (T_{sr_1} + T_{r_1d})I_{p_1}, \dots, (T_{sr_n} + T_{r_nd})I_{p_n}\}. \quad (4.2)$$

We want to compute $\mathbb{E}\{D\}$ in terms of forwarding policy $\{p_i\}$ and the network parameter λ_{ij} . Since all the random variables inside the minimum operator in (4.2) are independent of each

*As a special case, if $p_i = 1$ for all relay nodes (no resource constraint), then the probabilistic two-hop forwarding policy reduces to the multicopy two-hop relay protocol [39, 96, 41].

others, we have

$$\mathbb{P}\{D > t\} = \mathbb{P}\{T_{sd} > t\} \prod_{i=1}^n \mathbb{P}\{(T_{sr_i} + T_{r_i d})I_{p_i} > t\}. \quad (4.3)$$

By conditioning on I_{p_i} , we have

$$\begin{aligned} \mathbb{P}\{(T_{sr_i} + T_{r_i d})I_{p_i} > t\} &= \mathbb{E}\{\mathbb{P}\{(T_{sr_i} + T_{r_i d})I_{p_i} > t | I_{p_i}\}\} \\ &= \mathbb{P}\{T_{sr_i} + T_{r_i d} > t\} \mathbb{P}\{I_{p_i} = 1\} + \mathbb{P}\{t < \infty\} \mathbb{P}\{I_{p_i} = \infty\} \\ &= \mathbb{P}\{T_{sr_i} + T_{r_i d} > t\} p_i + (1 - p_i), \end{aligned} \quad (4.4)$$

where the last equality is from the definition of I_{p_i} in (4.1).

For notational simplicity, we define $f_0(t) \triangleq \mathbb{P}\{T_{sd} > t\}$ and $f_i(t) \triangleq \mathbb{P}\{T_{sr_i} + T_{r_i d} > t\}$, where T_{sd} , T_{sr_i} , and $T_{r_i d}$ are independent exponential random variables with rate λ_{sd} , λ_{sr_i} , and $\lambda_{r_i d}$, respectively. Then, from (4.4), (4.3) can be rewritten as

$$\mathbb{P}\{D > t\} = f_0(t) \prod_{i=1}^n [p_i f_i(t) + (1 - p_i)], \quad (4.5)$$

and thus, by noting that $\mathbb{E}\{D\} = \int_0^\infty \mathbb{P}\{D > t\} dt$, we have

$$\mathbb{E}\{D\}_{\vec{p}} = \int_0^\infty f_0(t) \prod_{i=1}^n [p_i f_i(t) + (1 - p_i)] dt, \quad (4.6)$$

where we use the subscript in $\mathbb{E}\{D\}_{\vec{p}}$ to clearly indicate that the average delay is a function of the forwarding policy $\vec{p} = [p_1, \dots, p_n]$.

Now, we formally state our problem to find an optimal forwarding policy \vec{p}^* under the constraint on the average number of message copies, i.e., $\mathbb{E}\{M\} = \mathbb{E}\{\sum_{i=1}^n Y_i\} = \sum_{i=1}^n p_i$, as the following optimization problem: For $\mathbb{E}\{D\}_{\vec{p}} : [0, 1]^n \rightarrow \mathbb{R}_+$,

$$\begin{aligned} &\mathbf{minimize} \quad \mathbb{E}\{D\}_{\vec{p}} \\ \text{(P1)} \quad &\mathbf{subject\ to} \quad \sum_{i=1}^n p_i \leq K, \end{aligned}$$

where \vec{p} denotes a forwarding policy and K is a positive integer ($1 \leq K \leq n$). As explicitly shown in (P1), the average number of copies (except the original message at the source node) allowed in the network is limited up to K -copies.

4.2 Delay Analysis

In this section, we derive an achievable upper bound on the delay in a tractable form, which leads us to find a sub-optimal solution to (P1). We also explain an intuition behind the delay upper bound by considering multicopy two-hop relay protocol [39, 96, 41] as an importance special case.

4.2.1 An Upper Bound of Message Delivery Delay

A difficulty in solving the optimization problem (P1) arises, since it is not a convex optimization problem, which can be checked by showing that the Hessian matrix of $\mathbb{E}\{D\}_{\vec{p}}$ with respect to \vec{p} is neither positive semidefinite nor negative semidefinite. Thus, we cannot resort to the standard convex optimization techniques [13] to find the optimal solution of (P1). Instead, we below derive an upper bound of $\mathbb{E}\{D\}_{\vec{p}}$ from (4.6), which becomes mathematically more tractable.

First, by noting that T_{sd} is an exponential random variable with rate λ_{sd} , we rewrite (4.6) as

$$\begin{aligned} \mathbb{E}\{D\}_{\vec{p}} &= \int_0^\infty e^{-\lambda_{sd}t} \prod_{i=1}^n [p_i f_i(t) + (1 - p_i)] dt \\ &= \frac{1}{\lambda_{sd}} \int_0^\infty \left(\prod_{i=1}^n [p_i f_i(t) + (1 - p_i)] \right) \lambda_{sd} e^{-\lambda_{sd}t} dt \\ &= \frac{1}{\lambda_{sd}} \mathbb{E} \left\{ \prod_{i=1}^n [p_i f_i(T_{sd}) + (1 - p_i)] \right\}, \end{aligned} \quad (4.7)$$

where the expectation is with respect to T_{sd} .

We denote $\|X\|_q$ to be the L_q norm of a (real-valued) random variable X , i.e., $\|X\|_q \triangleq [\mathbb{E}\{|X|^q\}]^{1/q}$ for $0 < q < \infty$, and $\|X\|_\infty \triangleq \inf\{c \in \mathbb{R} : \mathbb{P}\{|X| > c\} = 0\}$. We also define by \mathcal{L}^q a set of all random variables X for which $\|X\|_q < \infty$.

To proceed, we need the following two inequalities that will be used to derive the upper bound of $\mathbb{E}\{D\}_{\vec{p}}$ from (4.7).

Theorem 2. [33, 87] (Generalized Hölder's Inequality) *Let $1 \leq q_i \leq \infty$ with $\sum_{i=1}^n 1/q_i = 1$. If $X_i \in \mathcal{L}^{q_i}$ for $1 \leq i \leq n$, then $\prod_{i=1}^n X_i \in \mathcal{L}^1$ and*

$$\left\| \prod_{i=1}^n X_i \right\|_1 \leq \prod_{i=1}^n \|X_i\|_{q_i}. \quad \square$$

Theorem 3. [33, 87] (Minkowski's Inequality) For $X, Y \in \mathcal{L}^q$ with $1 \leq q \leq \infty$,

$$\|X + Y\|_q \leq \|X\|_q + \|Y\|_q. \quad \square$$

Since $f_i(t) = \mathbb{P}\{T_{sr_i} + T_{r_id} > t\} \leq 1$, it follows that $f_i(T_{sd}) \in \mathcal{L}^q$ and $p_i f_i(T_{sd}) + (1 - p_i) \in \mathcal{L}^q$ for $1 \leq q \leq \infty$. Thus, for any $1 \leq q_i \leq \infty$ with $\sum_{i=1}^n 1/q_i = 1$, we have

$$\mathbb{E}\{D\}_{\bar{p}} \leq \frac{1}{\lambda_{sd}} \prod_{i=1}^n \|p_i f_i(T_{sd}) + (1 - p_i)\|_{q_i} \quad (4.8)$$

$$\leq \frac{1}{\lambda_{sd}} \prod_{i=1}^n [p_i \|f_i(T_{sd})\|_{q_i} + (1 - p_i)], \quad (4.9)$$

where (4.8) is from the generalized Hölder's inequality and (4.9) is from Minkowski's inequality.

In contrast to the original form of $\mathbb{E}\{D\}_{\bar{p}}$ in (4.6) and (4.7), its upper bound in (4.9) is in a much more tractable form. More important, this upper bound leads us to find an optimal solution \bar{p}^* that minimizes the upper bound, which is good enough to show the benefit of exploiting the heterogeneity in mobile nodes' contact dynamics, as will be shown in Section 4.3.

4.2.2 A Special Case: Multicopy Two-hop Relay Protocol

We below consider the multicopy two-hop relay protocol as a special case ($K = n$) to get an intuition behind the delay upper bound in (4.9).

Let $T_{sr_i}^j$ ($j = 1, \dots, K$) be *i.i.d.* exponential random variables with rate λ_{sr_i} , and similarly for $T_{r_id}^j$ ($j = 1, \dots, K$) with rate λ_{r_id} . We define

$$\tilde{D}_i \triangleq \min\{T_{sd}, T_{sr_i}^1 + T_{r_id}^1, \dots, T_{sr_i}^K + T_{r_id}^K\}, \quad (4.10)$$

for $i = 1, \dots, n$. \tilde{D}_i here is defined for general K -copies which will be used in the rest of this chapter. By definition, \tilde{D}_i can be interpreted as the message delivery delay of multicopy two-hop relay policy over a partially homogeneous network \mathfrak{N}_i (as depicted in Figure 4.2) that is composed of a direct source-destination path and K *i.i.d.* two-hop relay paths, each of which has delay equal to the sum of two exponential random variables with rates λ_{sr_i} and λ_{r_id} . In other words, K two-hop relay paths in \mathfrak{N}_i are *i.i.d.* copies of the two-hop relay path via relay node i in the original heterogeneous network, and the direct path in both networks remains the same. Figure 4.2 shows this decomposition procedure from an original heterogeneous network to n partially homogeneous networks \mathfrak{N}_i ($i = 1, \dots, n$)

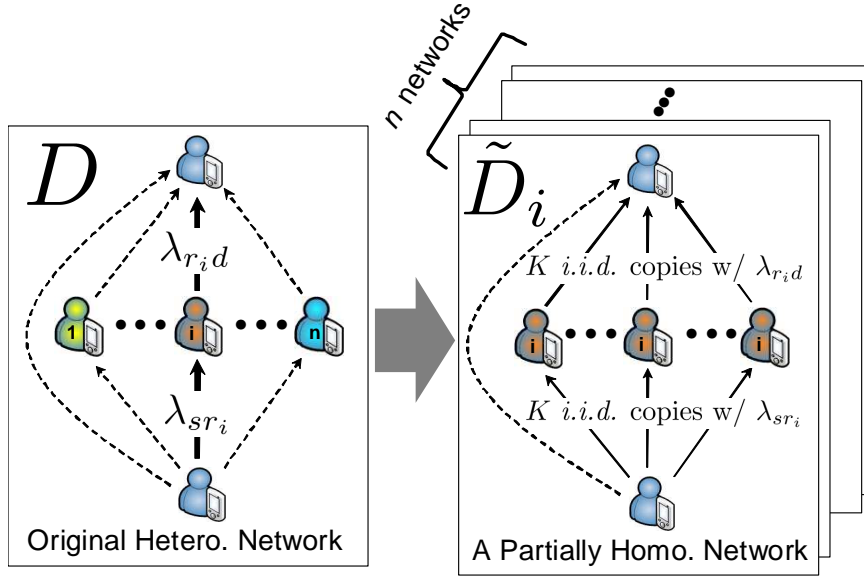


Figure 4.2: Decomposition of a heterogeneous network into n partially homogeneous networks \mathfrak{N}_i ($i = 1, \dots, n$). K two-hop relay paths in \mathfrak{N}_i are *i.i.d.* copies of the two-hop relay path via relay node r_i in the original heterogeneous network.

From $T_{sr_i}^j + T_{r_i d}^j \stackrel{d}{=} T_{sr_i} + T_{r_i d}$ and independence over $j = 1, \dots, K$, for each i , we have

$$\mathbb{E}\{\tilde{D}_i\} = \int_0^\infty f_0(t) [f_i(t)]^K dt. \quad (4.11)$$

We can compute a close-form expression of $\mathbb{E}\{\tilde{D}_i\}$ (See Appendix A.3 for its derivation) as follows: for $\lambda_{sr_i} \neq \lambda_{r_i d}$

$$\mathbb{E}\{\tilde{D}_i\} = \frac{1}{(\lambda_{r_i d} - \lambda_{sr_i})^K} \sum_{j=0}^K \binom{K}{j} \frac{(-\lambda_{sr_i})^j \lambda_{r_i d}^{K-j}}{\lambda_{sd} + j\lambda_{r_i d} + (K-j)\lambda_{sr_i}},$$

and for $\lambda_{sr_i} = \lambda_{r_i d}$

$$\mathbb{E}\{\tilde{D}_i\} = \frac{1}{\lambda_{sr_i}} \sum_{j=0}^K \frac{K!}{(K-j)! (K + \lambda_{sd}/\lambda_{sr_i})^{j+1}}. \quad (4.12)$$

Now, consider $K = n$ and set $q_i = n$ for $i = 1, \dots, n$. Since the forwarding policy simply

becomes $\vec{p} = \vec{1} = [1, \dots, 1]$, (4.9) can be rewritten as

$$\begin{aligned} \mathbb{E}\{D\}_{\vec{1}} &\leq \frac{1}{\lambda_{sd}} \prod_{i=1}^n \|f_i(T_{sd})\|_n = \frac{1}{\lambda_{sd}} \prod_{l=1}^n \left[\int_0^\infty \lambda_{sd} e^{-\lambda_{sd} t} [f_i(t)]^n dt \right]^{1/n} \\ &= \prod_{i=1}^n \left[\int_0^\infty f_0(t) [f_i(t)]^n dt \right]^{1/n} = \prod_{i=1}^n \left[\mathbb{E}\{\tilde{D}_i\} \right]^{1/n}. \end{aligned} \quad (4.13)$$

The delay upper bound in (4.13) is nothing but a geometric mean of $\mathbb{E}\{\tilde{D}_i\}$, the average message delivery delay of multicopy two-hop relay protocol under \mathfrak{N}_i . We observe that this delay upper bound still captures the underlying heterogeneity in mobile nodes' contact dynamics, as each decomposed network \mathfrak{N}_i contains each of n different two-hop relay paths of the original heterogeneous network. In addition, a closed-form solution of this delay upper bound can be immediately obtained from (4.12).

Remark 1. *When the network is homogeneous with $\lambda_{ij} = \lambda$, the upper bound in (4.13) becomes identical to the original expression of $\mathbb{E}\{D\}_{\vec{1}}$ from (4.6), i.e., all the intermediate inequalities that have led to (4.13) hold with equality for this special case of multicopy two-hop relay protocol under the homogeneous network setting. \square*

Remark 2. *Consider two homogeneous networks \mathfrak{N}_U and \mathfrak{N}_L with common contact rates for any node pair given by $\lambda_{\min} = \min_{i,j \in \mathcal{N}} \{\lambda_{ij}\}$ and $\lambda_{\max} = \max_{i,j \in \mathcal{N}} \{\lambda_{ij}\}$, respectively. Also, set the average message delivery delay of multicopy two-hop relay protocol under \mathfrak{N}_U and \mathfrak{N}_L by $\mathbb{E}\{\hat{D}_U\}$ and $\mathbb{E}\{\hat{D}_L\}$, respectively. Then, it is straightforward to see that $\mathbb{E}\{\hat{D}_L\} \leq \mathbb{E}\{D\}_{\vec{1}} \leq \mathbb{E}\{\hat{D}_U\}$. It is also known [39, 96] that the average delay of multicopy two-hop relay protocol under a homogeneous network is asymptotically $\frac{1}{\lambda} \sqrt{\frac{\pi}{2(n+1)}}$ as $n \rightarrow \infty$ where $|\mathcal{N}| = n+2$ and λ is a common contact rate for any node pair. Thus, if we were to focus on the asymptotic average delay of multicopy two-hop relay protocol, it would be $\mathcal{O}\left(\frac{1}{\sqrt{n+1}}\right)$, regardless of whether the underlying network is homogeneous or heterogeneous.[†] This is precisely why we analyze the delay performance under a heterogeneous network setting with a given finite number of mobile nodes. \square*

4.3 Main Results

In this section, we obtain an optimal solution \vec{p}^* which minimizes the delay upper bound derived in the previous section. We also show a closed-form expression of the guaranteed delay bound

[†]Only the constant coefficient $1/\lambda_{\min}$ or $1/\lambda_{\max}$ will change and the order term in n remains the same.

under this optimal solution \vec{p}^* . Finally, we quantify the performance gain of exploiting the heterogeneity in mobile nodes' contact dynamics under heterogeneous network settings using the closed-form expression of the guaranteed delay bound.

4.3.1 A Sub-Optimal Forwarding Policy

We first fix $q_i \geq 1, i = 1, \dots, n$ that satisfy $\sum_{i=1}^n 1/q_i = 1$, and then derive an optimal forwarding policy \vec{p}^* that minimizes the upper bound of $\mathbb{E}\{D\}_{\vec{p}}$ in (4.9). To this end, we consider the following optimization problem, whose solution will be sub-optimal to the original problem (P1).

$$\begin{aligned}
 \text{(P1')} \quad & \text{minimize} \quad \prod_{i=1}^n [p_i \|f_i(T_{sd})\|_{q_i} + (1 - p_i)] \\
 & \text{subject to} \quad \sum_{i=1}^n p_i \leq K.
 \end{aligned}$$

We define a sequence of $a_i(q_i)$ for a given q_i by

$$a_i(q_i) \triangleq \|f_i(T_{sd})\|_{q_i} = \left[\int_0^\infty \lambda_{sd} e^{-\lambda_{sd} t} [f_i(t)]^{q_i} dt \right]^{1/q_i}, \quad (4.14)$$

where $f_i(t) = \mathbb{P}\{T_{sr_i} + T_{r_id} > t\}$. For notational simplicity, we will use a_i instead of $a_i(q_i)$ unless it is necessary to specify the given q_i . Rearrange a_i in an increasing (non-decreasing) order and set $a_{[i]}$ to be the i^{th} smallest one among a_1, \dots, a_n , i.e., $a_{[1]} \leq a_{[2]} \leq \dots \leq a_{[n]}$. Also, let c_1, \dots, c_n be a permutation of $\{1, \dots, n\}$ which satisfies $a_{c_l} = a_{[l]}$ for all $l = 1, \dots, n$. Then, we have the following proposition for the optimal solution \vec{p}^* of (P1').

Proposition 7. *For any arbitrarily fixed $q_i \in [1, \infty]$ such that $\sum_{i=1}^n 1/q_i = 1$, the optimal solution \vec{p}^* of (P1') is always of the following form:*

$$p_i^* = \begin{cases} 1 & \text{if } i \in \{c_1, \dots, c_K\}, \\ 0 & \text{otherwise.} \end{cases} \quad (4.15)$$

Proof. We will find an optimal solution \vec{p}^* of the optimization problem (P1') by obtaining a minimizer which achieves the lowest bound of the objective function in (P1') under the constraint $\sum_{i=1}^n p_i \leq K$. By taking log function to the objective function in (P1'), it can be transformed as

$$\prod_{i=1}^n [p_i \|f_i(T_{sd})\|_{q_i} + (1 - p_i)] = \sum_{i=1}^n \log [p_i \|f_i(T_{sd})\|_{q_i} + (1 - p_i)], \quad (4.16)$$

since log function is a monotone increasing function. From Jensen's inequality and concavity of log, (4.16) is further lower bounded by

$$\sum_{i=1}^n \log [p_i \|f_i(T_{sd})\|_{q_i} + (1 - p_i)] \geq \sum_{i=1}^n p_i \log \|f_i(T_{sd})\|_{q_i}. \quad (4.17)$$

Then, we want to minimize the RHS of (4.17) under the constraint $\sum_{i=1}^n p_i \leq K$, which in turn gives the lowest bound of (4.16). It is equivalent to solving the following simple linear programming problem:

$$\begin{aligned} (\mathbf{P1}'') \quad & \text{minimize} && \sum_{i=1}^n p_i \log \|f_i(T_{sd})\|_{q_i} \\ & \text{subject to} && \sum_{i=1}^n p_i \leq K, \end{aligned}$$

Recall the definition of a_i in (4.14), i.e., $a_i = \|f_i(T_{sd})\|_{q_i}$, and $a_{[l]}$ is the l^{th} smallest one among a_1, \dots, a_n . Also, c_1, \dots, c_n is a permutation over $1, \dots, n$ which satisfies $a_{c_l} = a_{[l]}$ for all $l = 1, \dots, n$. Then, since log function is monotone increasing and the objective function in (P1'') is linear, it is easy to see that an optimal solution of (P1'') is $p_i = 1$ for $i \in \{c_1, \dots, c_K\}$, otherwise $p_i = 0$. Hence, from (4.17) and the optimal solution of (P1''), we have

$$\sum_{i=1}^n \log [p_i a_i + (1 - p_i)] \geq \sum_{i=1}^n p_i \log a_i \geq \sum_{l=1}^K \log a_{[l]}. \quad (4.18)$$

Note that the last lower bound in (4.18) is the lowest bound of (4.16) under the constraint $\sum_{i=1}^n p_i \leq K$, and the equality in (4.18) holds by the optimal solution of (P1''). Thus, the optimal solution of (P1'') is indeed the optimal solution \bar{p}^* of (P1'). This completes the proof. \blacksquare

Remark 3. Proposition 7 implies that, even though we start with a constraint on the average number of message copies $\mathbb{E}\{M\} = \sum_{i=1}^n p_i \leq K$, interestingly enough, the optimal forwarding policy \bar{p}^* under this average constraint actually attains $M = \sum_{i=1}^n Y_i = K$ with probability 1. \square

Proposition 7 says that the optimal forwarding policy \bar{p}^* of (P1') is to choose K relay nodes r_{c_1}, \dots, r_{c_K} and to forward message copies to them. Since the optimal forwarding policy \bar{p}^* in Proposition 7 holds for a given $\{q_i\}$, the choice of K relay nodes under the optimal forwarding policy \bar{p}^* still depends on $\{q_i\}$, which will be specified. In addition, from Proposition 7 and

(4.9), the guaranteed delay bound by the optimal forwarding policy \bar{p}^* becomes

$$\mathbb{E}\{D\}_{\bar{p}^*} \leq \frac{1}{\lambda_{sd}} \prod_{l=1}^K a_{[l]}. \quad (4.19)$$

Since $f_i(\cdot) \leq 1$, from (4.14), $a_i \leq 1$ for all i . Thus, we can interpret $\prod_{l=1}^K a_{[l]}$ in (4.19) as a delay discounting factor by K additional message copies in the heterogeneous network setting, whereby $1/\lambda_{sd}$ is simply the message delivery delay of direct forwarding from source to destination.

We explain how to choose a set of free variables $\{q_i\}$ under constraints $\sum_{i=1}^n 1/q_i = 1$ and $q_i \geq 1$ ($i = 1, \dots, n$). First, observe that if $p_i = 0$, a_i will not contribute to the upper bound of $\mathbb{E}\{D\}_{\bar{p}}$ in (4.9) regardless of the choice of q_i , and thus (4.9) simply becomes (4.19). Also, for any random variable X , $\|X\|_q$ is monotone increasing in q if $X \in \mathcal{L}_q$ [33, 87]. Then, since $f_i(T_{sd}) \in \mathcal{L}_q$ for $1 \leq q \leq \infty$ as mentioned before, $a_i(q_i)$ is monotone increasing in $q_i \geq 1$ for $i = 1, \dots, n$. Also, from $f_i(\cdot) \leq 1$ and the definition of L_∞ norm (i.e., $\|\cdot\|_\infty$), we have $a_i(\infty) = 1$ for $i = 1, \dots, n$. Thus, if we can assign $q_i = \infty$, jointly with $p_i^* = 0$, we can put the smallest possible values to other q_i 's while satisfying $\sum_{i=1}^n 1/q_i = 1$, which in turn gives smaller delay upper bound. Hence, we arrive to the following assignment rule for $\{q_i\}$ that makes the guaranteed delay bound in (4.19) tighter.

We set $q_i = K$ to a_i in (4.14), i.e., $a_i(K)$, for $i = 1, \dots, n$, temporarily. After finding c_1, \dots, c_n as mentioned above, we assign

$$q_i = \begin{cases} K & \text{if } i \in \{c_1, \dots, c_K\}, \\ \infty & \text{otherwise.} \end{cases} \quad (4.20)$$

Then, $\sum_{i=1}^n 1/q_i = \sum_{i=1}^K 1/K = 1$. Since $a_{c_{K+1}}(\infty) = \dots = a_{c_n}(\infty) = 1$ as mentioned above, $a_{c_i}(K)$ ($i = 1, \dots, K$) will fully contribute to the delay upper bound in (4.19). Also, from Proposition 7, the optimal solution \bar{p}^* in (4.15) is still $p_i^* = 1$ for the same $i \in \{c_1, \dots, c_K\}$, otherwise $p_i^* = 0$. Hence, the optimal forwarding policy \bar{p}^* becomes to choose K relay nodes r_{c_1}, \dots, r_{c_K} based on $a_i(K)$ for all i . Also, the assignment rule for $\{q_i\}$ does not change the optimal forwarding policy \bar{p}^* itself, but makes the delay upper bound in (4.19) smaller.

We now derive a closed-form expression of the guaranteed delay bound under the optimal forwarding policy \bar{p}^* . Observe that from the definitions of $\mathbb{E}\{\tilde{D}_i\}$ and $a_i(K)$ in (4.11) and (4.14), respectively, for $i = 1, \dots, n$, we have

$$a_i(K) = \|f_i(T_{sd})\|_K = \lambda_{sd}^{1/K} \left[\mathbb{E}\{\tilde{D}_i\} \right]^{1/K}. \quad (4.21)$$

We denote $\mathbb{E}\{\tilde{D}_{[l]}\}$ to be the l^{th} smallest one among $\mathbb{E}\{\tilde{D}_i\}$ ($i = 1, \dots, n$). Also, let d_1, \dots, d_n be another permutation of $\{1, \dots, n\}$ which satisfies $\mathbb{E}\{\tilde{D}_{d_l}\} = \mathbb{E}\{\tilde{D}_{[l]}\}$ for all l . By noting that $g(x) = x^{1/K}$ is monotone increasing in $x \geq 0$, from (4.21), we have $d_i = c_i$ for all i . It implies that the optimal forwarding policy \bar{p}^* is equivalent to choosing K relay nodes r_{c_1}, \dots, r_{c_K} based on $\mathbb{E}\{\tilde{D}_i\}$ ($i = 1, \dots, n$). Thus, from (4.19) and (4.21), the guaranteed delay bound under the optimal forwarding policy \bar{p}^* becomes

$$\mathbb{E}\{D\}_{\bar{p}^*} \leq \prod_{l=1}^K \left[\mathbb{E}\{\tilde{D}_{[l]}\} \right]^{1/K}. \quad (4.22)$$

Similar to a special case $K = n$ in 4.2.2, as in (4.22), the guaranteed delay bound by the optimal forwarding policy \bar{p}^* under K -copies constraint is nothing but a geometric mean of the K smallest ones among n message delivery delays of multicopy two-hop relay protocol, each of which is obtained under each decomposed network \mathfrak{N}_i (as shown in Figure 4.2) that consists of a direct path and K *i.i.d.* two-hop relay paths with parameters λ_{sr_i} and λ_{r_id} . Then, from the closed-form expression of $\mathbb{E}\{\tilde{D}_i\}$ in (4.12), we immediately have a closed-form expression of the guaranteed delay upper bound in (4.22). Hence, by decomposing an original heterogeneous network into n partially homogeneous networks, we are able to measure the performance gain achieved through exploiting the heterogeneity in mobile nodes' contact dynamics by using the closed-form expression of the derived delay bound.

Remark 4. *Similar to Remark 1, for $K < n$, when the network is homogeneous with $\lambda_{ij} = \lambda$, the delay upper bound by the forwarding policy \bar{p}^* in (4.22) becomes equal to the expression of $\mathbb{E}\{D\}_{\bar{p}^*}$ from (4.6). Since the forwarding policy \bar{p}^* is a form of $[1, \dots, 1, 0, \dots, 0]$ and the expression of $\mathbb{E}\{\tilde{D}_i\}$ in (4.11) is the same for all i , the equality in (4.22) holds. \square*

4.3.2 Performance Gain of Exploiting Heterogeneity

We start our quantitative study on the benefit of exploiting the heterogeneity in contact dynamics under a setting of two social groups as shown in Figure 2.2 (a), a special case of the individual model. We consider 2 social groups G_1 and G_2 forming $\mathcal{N} = \bigcup_{i=1}^2 G_i$, and $|\mathcal{N}| = 22$. Recall that λ'_{lk} is a common contact rate between any member of G_l and another member of G_k for $l, k = 1, 2$. Note that the total number of possible relay nodes for any given source-destination pair is 20. In the heterogeneous network setting, we set $\lambda'_{11} = 2 \times 10^{-4}$, $\lambda'_{22} = 2 \times 10^{-5}$, and $\lambda'_{12} = 10^{-4}$. This setting reflects a scenario that mobile nodes in G_1 are more socially active than those in G_2 and make frequent contacts with other group members as well as same group members. On the other hand, in the corresponding homogeneous network setting, we set

$1/\lambda_{ij} = \bar{\mu}$ for all $i, j \in \mathcal{N}$ and $i \neq j$ where $\bar{\mu}$ is the overall average inter-contact times over all node pairs, given by

$$\bar{\mu} = \left[\sum_{i=1}^2 \frac{1}{\lambda'_{ii}} \binom{|G_i|}{2} + \frac{1}{\lambda'_{12}} \binom{|G_1|}{1} \binom{|G_2|}{1} \right] / \binom{|\mathcal{N}|}{2}.$$

Thus, the overall average inter-contact time over all node pairs is the same for both settings.

Figure 4.3 (a) and (b) depict analytical and simulation results for an average delay obtained using the above optimal forwarding policy p^* of (P1'), a sub-optimal policy (solution) to the original problem (P1), per a given number of message copies under the heterogeneous and corresponding homogeneous network settings where we set the size of each group as $(|G_1|, |G_2|) = (11, 11)$ and $(7, 15)$ for each heterogeneous setting, respectively. We obtain the analytical result of an average delay for a uniformly chosen source-destination pair, i.e., a statistical average of average delays for total 231 source-destination pairs, per each given number of message copies by computing the guaranteed delay bound of the sub-optimal forwarding policy in (4.22). We also implement a custom event-driven simulator using C++ where random contacts of each node pair occur according to a Poisson process with its contact rate, and provide independent simulation results for the actual average delay of the sub-optimal forwarding policy for the uniform source-destination pair per each given number of message copies.

Figure 4.3 shows that very few message copies (*2-copies* or *3-copies*) with the sub-optimal forwarding policy under the heterogeneous network settings are only needed to achieve the same delay performance as the performance limit of any two-hop relay forwarding policies under their homogeneous counterparts. Here, the performance limit is the minimum delay achieved at the expense of unlimited message copies (20 additional message copies) by multicopy two-hop relay protocol[‡]. Figure 4.3 also implies that we can save *more than 80%* of message copies under the heterogeneous network settings, which is significantly helpful in reducing overall resource consumption over the network. Along with this observation, since most of the performance gain (i.e., large reduction of delay) takes place with first few message copies under the heterogeneous network settings, we deduce that few relay nodes with high contact rate in G_1 play a dominant role in actually delivering a message to its destination.

In addition, simulation results in Figure 4.3 exhibit that the delay upper bound of the sub-optimal forwarding policy (i.e., the RHS of (4.22)) is very closed to its actual performance for a small to moderate number of message copies under the heterogeneous network settings, while it is the exact delay under the homogeneous network settings as in Remarks 1 and 4. Also, although an increasing behavior of the delay upper bound exists, it can be explained as

[‡] Although an optimal two-hop forwarding policy under a constraint of K message copies in any homogeneous network setting is to forward K message copies to the first K encountered nodes, its performance still cannot exceed the performance limit.

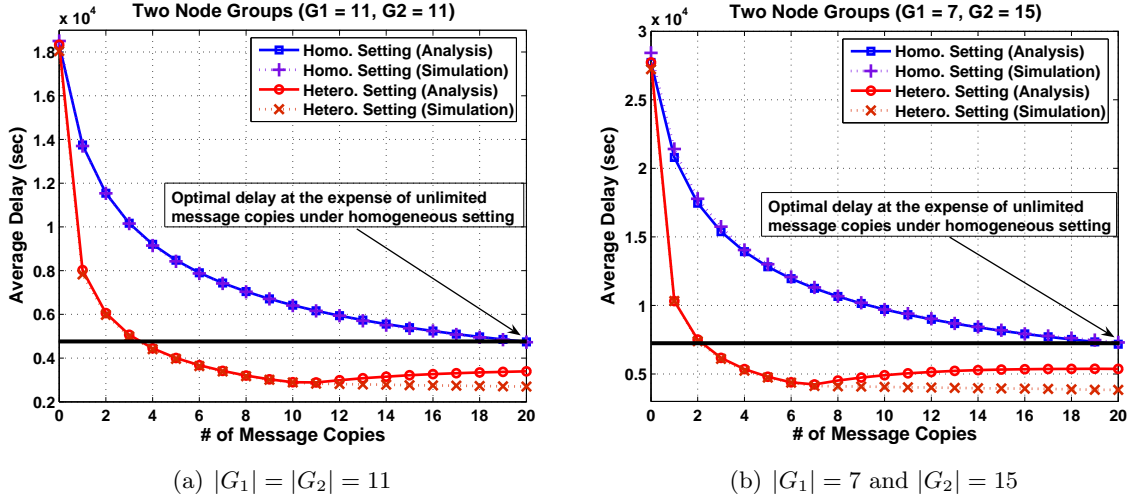


Figure 4.3: Average delay achieved via the sub-optimal two-hop forwarding policy per each given number of message copies under heterogeneous and corresponding homogeneous network settings. The horizontal thick line indicates the optimal delay that any two-hop forwarding policy cannot exceed under the homogeneous settings.

follows. Recall that the RHS of (4.22) can be written in a form of the product of L_q norms as in (4.19), i.e., $\prod_{l=1}^m a_{[l]}(m)$ where $a_i(m) = \|f_i(T_{sd})\|_m$ for $i = 1, \dots, n$. Also, since $a_i(m)$ is monotone increasing in $m \geq 1$ and $a_i(m) \leq 1$ as mentioned in Section 4.3.1, it is possible that $\prod_{l=1}^m a_{[l]}(m) \leq \prod_{l=1}^m a_{[l]}(m+1) \cdot a_{[m+1]}(m+1)$ when delay reduction by adding $a_{[m+1]}(m+1)$ becomes not significant. However, as shown in Figure 4.3, the delay upper bound does not keep increasing and the delay upper bound for a large number of message copies is still useful when compared to its actual performance.

We further continue our investigation over a real Bluetooth contact trace (*Infocom*) [21] which was collected during the IEEE INFOCOM'05 conference. It contains 41 nodes' contact information over 3 days where we here use 22 nodes' information ($|\mathcal{N}| = 22$). In order to adopt this *Infocom* trace under the individual model, we extract the average pairwise inter-contact time of all node pairs and use them under the individual model. Similar to previous test case, for the homogeneous network setting, we set $\bar{\mu} = 18098sec$ as shown in Figure 4.5, where the overall average inter-contact time over all considered node pairs is 18098sec.

Figure 4.4 shows analytical and simulation results for an average delay per a given number of message copies under a heterogeneous network setting based on the *Infocom* trace and its homogeneous counterpart. Both results are similarly obtained as done in the previous test case. In the event-driven simulation, random contacts of each node pair are generated according to a Poisson process with its contact rate extracted from the *Infocom* trace for the heterogeneous

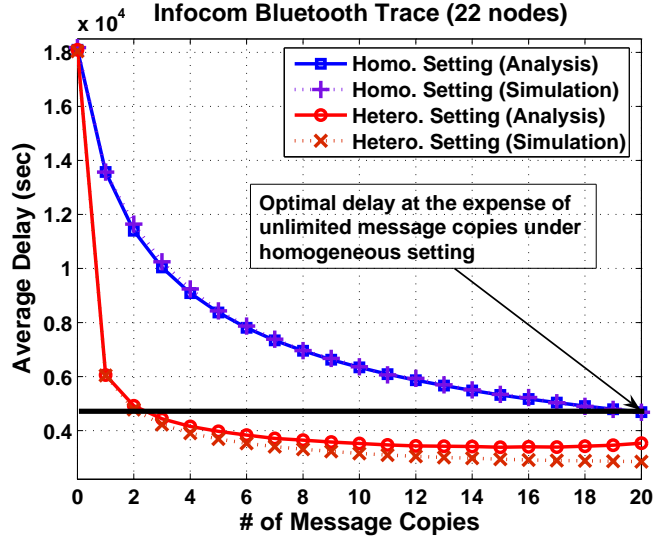


Figure 4.4: Average delay achieved via the sub-optimal two-hop forwarding policy per each given number of message copies under a heterogeneous network setting (*Infocom* trace) and its homogeneous counterpart. The horizontal thick line indicates the optimal delay that any two-hop forwarding policy cannot exceed under the homogeneous setting.

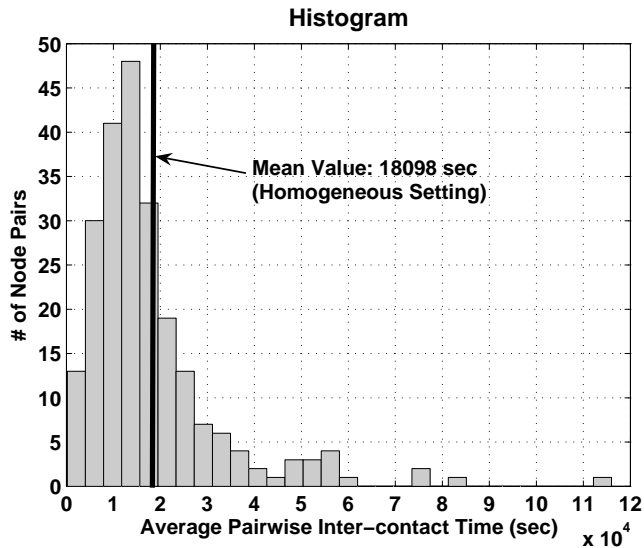


Figure 4.5: Histogram of average *pairwise* inter-contact times over all node pairs in *Infocom* trace.

setting or with rate $1/\bar{\mu}$ for its corresponding homogeneous setting. As shown in Figure 4.4, we again achieve the significant performance improvement (*2-copies* are enough) as similarly observed in the previous case. This performance gain becomes apparent, since the average inter-

contact time is quite heterogeneous over different node pairs as depicted in Figure 4.5. Although we observed similar performance improvement using the sub-optimal forwarding policy for other heterogeneous network settings, we here omit them due to space constraint.

Note that the considerable performance gain is still shown through the delay upper bound of the sub-optimal two-hop forwarding policy. Moreover, it does not include the benefit of changing relay paths or choosing relay nodes on-the-fly upon encounter, as the forwarding policy works based on a predetermined set of relay nodes. In other words, an expected utility of each mobile node as a relay node is changing over time depending on *when* and *who* a source node encounters, and thus it can be taken into account in the design of new forwarding policy so as to minimize the message delivery delay. Therefore, with such a dynamic routing, the maximally achievable performance gain by exploiting the heterogeneity in mobile nodes' contact dynamics will be substantially higher than expected.

Chapter 5

Opportunistic Forwarding in Duty-Cycled WSNs

In Chapters 2–4, we have discussed our study on analyzing and improving forwarding performance under heterogeneous contact dynamics in MONs. We next move on to the second part of this dissertation – the design of smart/distributed duty-cycling for opportunistic forwarding in heterogeneous and dynamic WSNs to achieve faster information delivery and longer network lifetime. In this chapter, we provide preliminaries, for subsequent Chapters 6–8, on network model (Section 5.1), base setup for networking operations including opportunistic forwarding and duty cycling (Section 5.2), and the resulting simple random walk model (Section 5.3).

5.1 Network Model

Consider n sensor nodes placed on a graph (or network) in which each edge corresponds to a reliable communication link between each pair of n nodes, if exists. Let $G = (\mathcal{N}, \mathcal{E})$ be a graph where $\mathcal{N} = \{1, 2, \dots, n\}$ is a set of sensor nodes and \mathcal{E} is a set of edges with $|\mathcal{E}| = m$. If a sensor node $i \in \mathcal{N}$ can reliably communicate with other sensor node $j \in \mathcal{N}$, then an edge between sensor nodes i, j exists, i.e., $(i, j) \in \mathcal{E}$ ($i \neq j$). Throughout the rest of this dissertation, we assume G is an undirected and connected graph. In other words, each communication link is symmetric and there exists at least one routing path from each node to every other nodes. We also define by $N(i)$ a set of neighbors of node $i \in \mathcal{N}$ and by d_i the degree of each node i , i.e., $d_i = |N(i)|$. Note that $\sum_{i \in \mathcal{N}} d_i = 2m$.

5.2 Random Duty Cycling and Opportunistic Forwarding

We explain a typical random duty cycling that each sensor node performs for energy/power conservation, and an opportunistic forwarding proposed in [11, 24] as a packet forwarding method, both of which will be used as a base setup for networking operations in Chapters 6–8. Note that this combination of the opportunistic forwarding and random duty cycling is originally introduced in [11, 24].

We consider a network operating in a synchronous mode, as assumed in [6, 7, 58, 11, 24]. Specifically, time is divided into slots and slot boundaries are synchronized (or can be re-synchronized). By the random duty cycling, we mean that each node independently wakes up (or turns on its RF transceiver) with probability $q > 0$ at each time slot; otherwise, it sleeps (or completely turns off its RF transceiver) for the time slot with probability $1 - q$. In addition, while each sensor node conducts this random duty cycling at each time slot, it forwards a packet, if it has, to one of its neighbors through the following opportunistic forwarding method. Whenever a sensor node having a packet wakes up, it opportunistically transmits the packet to *any* one of its neighbors *if* the neighbor also wakes up at the same slot; otherwise, the node having a packet looks for other next opportunities to forward the packet. When there are multiple neighbors waking up at the same slot, the tie will be randomly broken, i.e., one of the multiple awake neighbors will be chosen uniformly at random, as mentioned in [24]. This can be achieved via the exchange of RTS (request to send) and CTS (clear to send) with random waiting time as will be explained below, while this (practical) issue has been ignored in [24].

The (data) packet transmission/reception between two adjacent nodes can occur, only when they both wake up and each of them is aware that the other node is also ‘on’. Hence, whenever any node having a packet wakes up at a certain time slot, it transmits a RTS packet to notify its existence. If any of its neighbors wakes up and receives the RTS packet at the same slot, it transmits a CTS packet to acknowledge the reception of the RTS packet to the sender. Here, since it is still possible for many nodes to be awake at the same slot as mentioned before, each node waits for a short random amount of time before transmitting a RTS or CTS packet, while performing carrier sense on the channel, to avoid any possible collisions and to ensure successful packet transmission/reception.

Specifically, during the random waiting time, if an awake node having a (data) packet senses that the channel is busy, then it cancels RTS transmission and seeks next opportunities. If it correctly receives an RTS packet from its neighbor, then it rather prepares to receive a data packet from the sender and waits for another short random time to transmit a CTS packet to the sender. On the other hand, if any node receives a CTS packet from another neighbor during its random wait till its own CTS transmission, it goes to sleep. In this way, even if multiple nodes wake up at the same ‘slot’ and have the same purpose (waiting for transmission

or reception of a data packet), we can randomly break the tie. We here suppose that the duration of each time slot is suitably chosen so as to accommodate all these signalings required for the data transmission. We also suppose that traffic load in the network is light as assumed in [6, 7, 58, 11, 24]. Hence, the interference from concurrent data transmissions is not a critical issue, though the above RTS/CTS exchange with random waiting time can reduce the effect of such interference on the system performance. Figure 5.1 depicts an example of the operation of data communication through the opportunistic forwarding with random duty cycling.

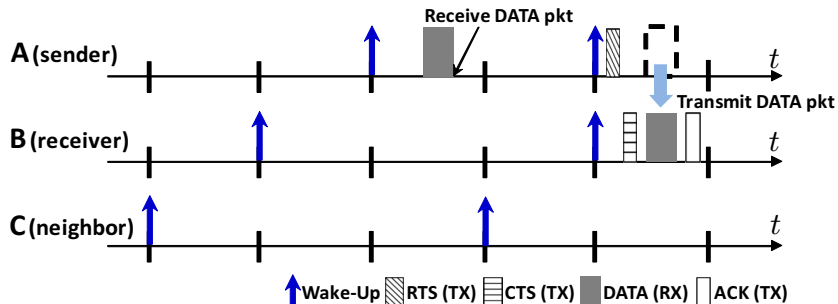


Figure 5.1: The operation of data transmission via the opportunistic forwarding under the random duty cycling. Here, nodes B and C are the neighbors of node A , and a (data) packet is transmitted from node A to node B .

5.3 Simple Random Walk Model For Opportunistic Forwarding

We here explain how the ‘transitions’ of each packet over the network G , governed by the opportunistic forwarding with random duty cycling, can be considered as a SRW, while the packet stays at each node for some random amount of time before it is forwarded to another node.* Suppose that node $i \in \mathcal{N}$ has a packet to transmit. Let $I_i \in N(i)$ be one of the neighbors of i that receives the packet from i or equivalently the first awake node in $N(i)$ that node i can find for the first time, while performing the random duty cycling. Also let W_i be the waiting time (in the number of time slots) for the packet at node i until being forwarded to I_i . As mentioned in [24], for each node $i \in \mathcal{N}$ having a packet,

$$\mathbb{P}\{I_i = k\} = \frac{1}{d_i} \tag{5.1}$$

*While the opportunistic forwarding can also work with a variant of the random duty cycling, called a pseudo-random duty cycling [11, 24], the transition of each packet over network G here is still done in a SRW fashion.

if $k \in N(i)$; otherwise, zero. In other words, the transition of each packet from a node to one of its neighbors over G is done in a SRW fashion.

Observe that at each time slot, node i independently wakes up with probability q and there is at least one awake neighbor with probability $1 - (1 - q)^{d_i}$ at each slot. In other words, node i having a packet can transmit the packet to any of its neighbors with probability $q_i \triangleq q(1 - (1 - q)^{d_i})$ at each time slot. Thus, the waiting time W_i is geometrically distributed with mean

$$\mathbb{E}\{W_i\} = \frac{1}{q_i} = \frac{1}{q(1 - (1 - q)^{d_i})}. \quad (5.2)$$

Therefore, the transition of each packet from node i to one of its neighbors through the opportunistic forwarding follows a SRW, with heterogeneous random sojourn time [11, 24], where the heterogeneity comes from varying degrees d_i , $i \in \mathcal{N}$.

Note that the opportunistic forwarding inherently inherits all the properties of random walks-based algorithms such as simplicity, scalability, load-balancing, and robustness to topology changes. It also operates without any topological or geographical information. In the second part of this dissertation, our goal is to demonstrate that it's always possible to further improve the performance of opportunistic forwarding in *both delay and network lifetime (power) together* under the same setting as random walk-based algorithms, retaining all the aforementioned desirable properties while at the same time overcoming the problem of slow mixing (or diffusion) associated with all simple random walk-based algorithms in WSNs.

Chapter 6

Smart Sleep: Sleep More to Reduce Delay in Duty-Cycled WSNs

In this chapter, we propose a simple yet effective modification of random duty cycling, named *Smart Sleep*, for opportunistic forwarding, which achieves more power-saving as well as faster packet diffusion (or smaller delay) in WSNs. Section 6.1 presents the operation of Smart Sleep and discusses its behavior on a simple topology. In Section 6.2, we introduce a class of p -backtracking random walks along with its properties and analytically explain the fast packet diffusion induced by Smart Sleep under general network settings. We finally present representative simulation results in Section 6.3.

6.1 Smart Sleep: How To Sleep More and Better

In this section, we propose a simple modification on the random duty cycling (explained in Chapter 5), which we call *Smart Sleep*, whose operation is defined as follows. Whenever each node successfully forwards a packet to one of its neighbors, it goes to sleep and stays asleep for a constant amount of time slots $T \geq 0$ after which it resumes the random duty cycling, where the parameter T is to be chosen later. Here, when each node goes into this sleep mode for the time duration T , we say that the node is in a ‘sleep mode’; otherwise, the node is in a ‘normal mode’ in which the node performs the random duty cycling. Note that if $T=0$, then it reduces to the original setting of random duty cycling.

One can see that if T is too long, then many sensor nodes would sleep for a quite long time and hence the packet would get delayed longer. In addition, very large value of T would put more sensors into sleep longer, rendering those sleeping sensors unavailable for forwarding of other packets, if any, and thus affecting the transition behavior of those other packets over the network G . Observe that the power consumption of each sensor is monotonically decreasing as

T increases, thus the advantage of Smart Sleep over the random duty cycling is obvious from the power saving point of view. For packet delay point of view, however, it may seem unclear at first sight whether forcing sensors into more sleep right after forwarding can actually lead to smaller delay in the network. Before going into the details for general set-up, for the rest of this section, we demonstrate using a simple network topology how our Smart Sleep influences the dynamics of packet forwarding/delay.

Consider 1-D ring with a set of nodes \mathcal{N} . This topology is simple, yet able to capture key dynamics, and only used to obtain qualitative understanding. We look at how a packet of interest travels over 1-D ring in which all nodes are initially in a normal mode. Suppose that a packet of interest is generated at node i and its destination is at least three-hop away from node i . This packet will be forwarded to one of two neighbors of i with equal probability as in (5.1), as every node initially performs the random duty cycling. Then, suppose that node i forwards the packet to node j at time (slot) t' as shown in Figure 6.1. From this time on, the packet will stay at i for some random time until forwarding to one of its first awake neighbors. Since node i will be in a sleep mode during $[t', t' + T]$, the packet will be more likely to be forwarded to node k rather than back to i . In what follows, we make this argument precise by computing the probability of forwarding to k .

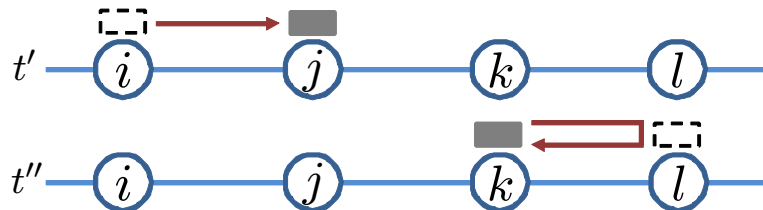


Figure 6.1: A series of four nodes in 1-D ring

From the definition of random duty cycling, nodes j and k both wake up at each slot with probability q^2 . Thus, from time t' onwards, the number of time slots Y until both nodes are awake at the same slot (for possible transmission and/or reception of the packet) is geometrically distributed with mean $1/q^2$. Then, by noting that node i remains asleep until time $t' + T$, the probability that the packet is forwarded to node k (from node j) *no later* than time $t' + T$ is $\mathbb{P}\{Y \leq T\}$. If the packet has not been yet forwarded to node k by time $t' + T$, which happens with probability $\mathbb{P}\{Y > T\}$, then from that time on both of nodes i, k are in normal mode and equally likely to receive the packet as in (5.1). Hence, the probability that the packet is forwarded to node k *after* $t' + T$ is $0.5 \cdot \mathbb{P}\{Y > T\}$. Therefore, the (total) probability that the

packet will be eventually forwarded to node k is

$$\tilde{p} \triangleq \mathbb{P}\{Y \leq T\} + 0.5 \cdot \mathbb{P}\{Y > T\} = 1 - 0.5(1 - q^2)^T > 0.5, \quad (6.1)$$

and the probability that the packet will be forwarded back to node i is $1 - \tilde{p} = 0.5(1 - q^2)^T < 0.5$. Similarly, once the packet is forwarded from node j to node k with probability \tilde{p} , it will be further forwarded to neighbor l (rather than back to node j) with probability \tilde{p} . This operation continues until either the packet reaches its destination or it is not transmitted back to the node that previously forwarded the packet.

Now consider the case of packet being transmitted back to the previous sender. Specifically, the packet, which was forwarded to node l , is now being transmitted back to node k at time (slot) $t'' > t'$ as depicted in the bottom of Figure 6.1. This transition is possible only when node k is awake, i.e., its sleep time T (due to forced sleep mode from previous forwarding to l) must have passed by time t'' . Thus, at t'' , all nodes except node l are in a normal mode. Hence, once the packet is transmitted from node l back to node k which previously forwarded the packet, the transition of the packet over 1-D ring behaves as if the packet is newly generated at node l (in the network where all nodes in a normal mode) and is then forwarded to node k .

From the above observation, one can see that for any node having the packet of interest, its neighbor that previously forwarded the packet is in a sleep mode, while one another neighbor is in a normal mode. Hence, the packet of interest keeps being forwarded to the nodes in the same direction that the packet has followed, with probability $\tilde{p} > 0.5$; otherwise, with probability $1 - \tilde{p}$, the packet is forwarded to the node which previously forwarded the packet in a reverse direction. This is exactly the same as the transition of a correlated random walk (CRW) [9, 19] on 1-D ring. In the CRW on 1-D ring, the walk at a vertex moves to its neighbor in the same direction (right or left) that the walk has taken, with probability larger than 0.5; otherwise, it changes the direction and moves to its another neighbor (or the previously visited vertex). In particular, [19] analytically showed that as the probability of the walk to follow the same direction that the walk has followed gets higher, the ‘diffusion’ of the walk over 1-D ring becomes faster. Observe that \tilde{p} is increasing in T as shown in (6.1). Hence, if the sleep duration T is longer, we can achieve faster diffusion of the packet over the network, which in turn brings out smaller number of packet forwardings required until a packet reaches its destination.

However, we should not push this direction indefinitely. As mentioned before, if there are many other packets from different sources or from a single source, many sensor nodes will be unavailable for delivery of other packets for longer duration as T gets very large, and thus the reduction in the number of packet forwardings in the presence of multiple packets is not certain. More importantly, the CRW* is a discrete-time random walk where the walk spends one time

*In [9, 19], the CRW was studied in the context of mobility modeling for applications of MANETs.

unit in every node. However, in our setup, while the transition of each packet over 1-D ring behaves as if it follows a CRW, the sojourn time at each node is no longer a constant. We next derive the average sojourn time at each node after packet forwarding as a function of T .

When a packet of interest is initially generated at node i and all nodes are in a normal mode, the average waiting (sojourn) time for the packet at node i is simply given by (5.2). However, once the packet is forwarded to one of neighbors of node i , the average sojourn time will be different. Let \tilde{W}_i be the sojourn time of the packet at node i (in the number of time steps) until being further forwarded, given that node i has just received the packet from one of its neighbors. Then, it follows that

$$\begin{aligned}\mathbb{E}\{\tilde{W}_i\} &= \mathbb{E}\{Y|Y \leq T\}\mathbb{P}\{Y \leq T\} + (T + \mathbb{E}\{W_i\})\mathbb{P}\{Y > T\} \\ &= \frac{1}{q^2} - \frac{1}{q^2} \frac{(1-q)}{(2-q)} (1-q^2)^T.\end{aligned}\tag{6.2}$$

The first equality can be obtained by conditioning on whether a neighbor of node i in a normal mode will receive the packet within T slots during which the other neighbor stays in a sleep mode. Due to the symmetry for 1-D ring, the average sojourn time does not depend on i . We refer to Appendix A.4 for the detailed derivation of (6.2). Here, observe that $\mathbb{E}\{\tilde{W}_i\}$ is increasing in T starting from $\mathbb{E}\{\tilde{W}_i\} = \mathbb{E}\{W_i\}$ for the case of $T = 0$. In other words, as the sleep duration T increases, the number of transitions till delivery is generally decreasing in T but at the same time the average sojourn time at each node is now increasing. In addition, in the presence of multiple packets, very large value of T prevents each node from being active *in time* to serve other upcoming packets, rendering the average sojourn time much longer than (6.2). Hence, one has to be careful in choosing T to achieve reduction in actual packet delay. The observation here on a simple 1-D ring topology will be a starting point for our more in-depth discussion in Sections 6.2.4 and 6.3 as to how to suitably choose T in Smart Sleep under general network topologies.

6.2 p -Backtracking Random Walk and Its Connection to Smart Sleep

In the previous section, we have shown that the transition of a packet of interest on 1-D ring caused by Smart Sleep is the same as that of CRW on 1-D ring. In particular, the packet of interest is less likely forwarded back to the node which previously forwarded the packet. In this section, we introduce *p-backtracking random walk* (p -BRW), a class of discrete-time random walks that capture such dynamics – less backtracking to the previous visited node, on general graphs. We then derive several properties of p -BRW and explain how to achieve faster diffusion

of p -BRW over the graph G . We finally discuss how the p -BRW is related to the transition of a packet of interest over G under Smart Sleep.

6.2.1 p -Backtracking Random Walk

The p -BRW is a class of *discrete-time* random walks on G and is defined as follows. A random walk at the current node $i \in \mathcal{N}$ with $d_i > 1$ goes back to the previously visited node with probability p_i (we called *backtracking probability* throughout the rest of this chapter); otherwise, the random walk moves to the next node, chosen uniformly at random among the neighbors of i except the previously visited node. If the current node i has only one neighbor ($d_i = 1$), the walk always returns back to the previously visited node, i.e., $p_i = 1$. At $t=0$, the walk initially chooses one of its neighbors uniformly at random, and then continue to use the previously visited node as a ‘signpost’ to decide the next node that the walk will move to.

Let X_t , $t = 0, 1, 2, \dots$ be the location of p -BRW over $G = (\mathcal{N}, \mathcal{E})$. From the definition of p -BRW, its dynamics can be characterized by

$$\mathbb{P}\{X_{t+1} = k | X_t = j, X_{t-1} = i\} = \begin{cases} p_j & \text{if } k = i, \\ \frac{1-p_j}{d_j-1} & \text{if } (j, k) \in \mathcal{E}, k \neq i, \\ 0 & \text{otherwise,} \end{cases} \quad (6.3)$$

for $d_j > 1$ and $(i, j) \in \mathcal{E}$ ($i \neq j$). If $d_j = 1$, then $\mathbb{P}\{X_{t+1} = i | X_t = j, X_{t-1} = i\} = 1$ for $i \in N(j)$; otherwise, zero. To avoid triviality, we assume that $0 \leq p_j < 1$ for all nodes $j \in \mathcal{N}$ with $d_j > 1$. Figure 6.2 depicts an example of possible transitions of p -BRW from a node to one of its neighbors.

The p -BRW includes the following random walks as special cases. If $p_j = 1/d_j$ in (6.3), then the p -BRW reduces to the SRW where the next node is chosen uniformly at random from the neighbors of the current node, i.e.,

$$\mathbb{P}\{X_{t+1} = k | X_t = j\} = \mathbb{P}\{X_{t+1} = k | X_t = j, X_{t-1} = i\} = \frac{1}{d_j},$$

for $(j, k) \in \mathcal{E}$; otherwise, zero. If $p_j = 0$ for all node j with $d_j > 1$, then the p -BRW reduces to the non-backtracking random walk (NBRW) [3] where the walk at the current node always moves to one of its neighbors except the previously visited node with equal probability if there is any other neighbor.[†] Moreover, if G is 1-D ring and $p_j = p$ ($0 < p < 1$) for all j , then the p -BRW reduces to the CRW [9, 19] in which the walk continues in the same direction with probability $1 - p$; otherwise, it changes the direction with probability p . When G is 2-D grid, however,

[†]In [3] the NBRW is considered only for regular graphs with $d_i = d > 3$ for all $i \in \mathcal{N}$.

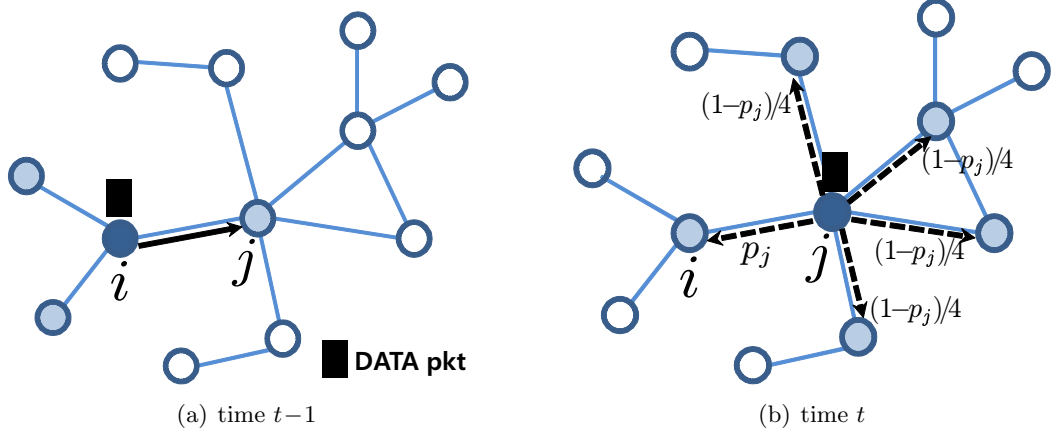


Figure 6.2: Illustration of transitions of p -BRW. (a) A p -BRW is located at node i at time $t-1$ and is going to move to node j . (b) At time t , the p -BRW chooses one of the neighbors of node j according to the transition probability in (6.3) as the next node that it will move to.

the p -BRW is slightly different from the CRW on the same 2-D grid where the walk keeps the same direction (east, north, west, or south) with a certain probability; otherwise, it changes the direction to one of three remaining directions. We note that the CRW can be defined only on a grid structure [9, 19] since the notion of ‘direction’ becomes unclear on a non-grid topology. In contrast, the p -BRW can be defined on any general topology without such restriction, where its backtracking probability p_i at node i describes a *relative* direction to the previously visited node.

6.2.2 Properties of p -BRW

One can see that $\{X_t\}$ with state space \mathcal{N} is not a Markov chain due to its memory of the previous state as shown in (6.3). However, by augmenting the state space, we can construct a Markov chain for the random sequences of nodes visited by the p -BRW as follows. We define by \mathcal{S} a set of directed edges, i.e., $\mathcal{S} \triangleq \{(i, j) : i \in \mathcal{N}, j \in N(i)\}$ and $(i, j) \neq (j, i)$ in general. Note that $|\mathcal{S}| = 2|\mathcal{E}| = 2m$. Let $Z_t \triangleq (X_{t-1}, X_t)$ for $t \geq 0$. Then, $\{Z_t\}_{t \geq 1}$ becomes a Markov chain on the state space \mathcal{S} and its transition probability is given by

$$p_{(i,j)(j,k)} \triangleq \mathbb{P}\{Z_{t+1} = (j, k) \mid Z_t = (i, j)\} = \begin{cases} p_j & \text{if } (j, k) \in \mathcal{S} \text{ and } k = i, \\ \frac{1-p_j}{d_j-1} & \text{if } (j, k) \in \mathcal{S} \text{ and } k \neq i, \\ 0 & \text{otherwise,} \end{cases} \quad (6.4)$$

for each $(i, j) \in \mathcal{S}$ and $d_j > 1$. If $d_j = 1$ for any $j \in \mathcal{N}$, then $p_{(i,j)(j,i)} = 1$ for $i \in N(j)$; otherwise, zero. Note also that $p_{(i,j)(l,k)} = 0$ if $j \neq l$. From the definition of p -BRW, we have

$$\mathbb{P}\{Z_1 = (j, k)\} = \mathbb{P}\{X_0 = j\} \frac{1}{d_j} \quad (6.5)$$

for each $(j, k) \in \mathcal{S}$, though $\mathbb{P}\{X_0 = j\}$, $j \in \mathcal{N}$, will be specified later. Here, without loss of generality, we can assume

$$\mathbb{P}\{Z_0 = (i, j)\} = \mathbb{P}\{X_{-1} = i, X_0 = j\} = \mathbb{P}\{X_0 = j\} \frac{1}{d_j}, \quad (6.6)$$

since for any $(j, k) \in \mathcal{S}$

$$\mathbb{P}\{Z_1 = (j, k)\} = \sum_{(i,j) \in \mathcal{S}} \mathbb{P}\{Z_0 = (i, j)\} p_{(i,j)(j,k)} = \mathbb{P}\{X_0 = j\} \frac{1}{d_j}.$$

where the first equality is from conditioning and the second one follows from (6.4) and (6.6). Therefore, $\{Z_t\}_{t \geq 0}$ is now a well-defined Markov chain on the state space \mathcal{S} with its initial distribution $\mathbb{P}\{Z_0 = (i, j)\}$ given by (6.6).

Let $\pi \triangleq [\pi_{(u,v)}, (u, v) \in \mathcal{S}]$ be the stationary distribution of $\{Z_t\}$ on \mathcal{S} and $\pi_A \triangleq \sum_{(u,v) \in A} \pi_{(u,v)}$ be the probability of $\{Z_t\}$ being in a subset $A \subseteq \mathcal{S}$ in the steady-state. For each $j \in \mathcal{N}$, let $A_j \triangleq \{(i, j) \in \mathcal{S} : i \in N(j)\}$ be the set of directed edges incident to (and directed toward) node j . Note that $\{A_j\}_{j \in \mathcal{N}}$ forms a partition of \mathcal{S} and $|A_j| = d_j$ in the original undirected graph G . Thus, it follows that π_{A_j} is the probability of the p -BRW being at node j in the steady-state, as the walk has to traverse one of those edges in A_j to reach node j . We now have the following result.

Theorem 4. *For any choice of $p_j \in [0, 1)$, $j \in \mathcal{N}$, the stationary distribution of $\{Z_t\}$ is uniform over \mathcal{S} , i.e., $\pi_{(u,v)} = \frac{1}{2m}$ for all $(u, v) \in \mathcal{S}$. Consequently, we also have*

$$\pi_{A_j} = \sum_{(u,v) \in A_j} \pi_{(u,v)} = \frac{d_j}{2m}. \quad (6.7)$$

Proof. Recall that each state in the state space \mathcal{S} is a directed edge. G is also connected, i.e., there is at least a path (a sequence of nodes) from node u to node v for all $u, v \in \mathcal{N}$ ($u \neq v$). Hence, there exists at least a directed path (a sequence of direct edges) connecting each directed edge (u', u) to every other directed edges (v, v') , where $u' \in N(u)$ and $v' \in N(v)$. Then, for $0 < p_j < 1$ at node $j \in \mathcal{N}$ with $d_j > 1$ in (6.4) in addition to $p_j = 1$ for $d_j = 1$, the transition probability $p_{(i,j)(j,k)} > 0$ for any $(i, j), (j, k) \in \mathcal{S}$. Thus, every state in \mathcal{S} is reachable in finite time with positive probability, and the Markov chain $\{Z_t\}$ is irreducible. One can also

see that the case of $p_j = p_{(i,j)(j,i)} = 0$ at node $j \in \mathcal{N}$ with $d_j > 1$ in (6.4), $i \in N(j)$, does not affect the irreducibility of $\{Z_t\}$, because it is not necessary to traverse path $i \rightarrow j \rightarrow i$ to reach (v, v') from (u', u) . Therefore, by noting that the state space \mathcal{S} is finite, i.e., $|\mathcal{S}| = 2m < \infty$, the Markov chain $\{Z_t\}$ is positive recurrent and hence it has a *unique* stationary on \mathcal{S} [74, 2]. Due to this uniqueness, one can easily check that the stationary distribution of $\{Z_t\}$ is $\pi_{(i,j)} = 1/2m$ for each $(i, j) \in \mathcal{S}$ satisfying the following balance equations.

$$\begin{aligned} \pi_{(j,k)} &= \sum_{(i,l) \in \mathcal{S}} \pi_{(i,l)} p_{(i,l)(j,k)} = \pi_{(k,j)} p_{(k,j)(j,k)} + \sum_{i \in N(j) \setminus \{k\}} \pi_{(i,j)} p_{(i,j)(j,k)} \\ &= \pi_{(k,j)} p_j + \sum_{i \in N(j) \setminus \{k\}} \pi_{(i,j)} \frac{1 - p_j}{d_j - 1}, \end{aligned} \quad (6.8)$$

for each $(j, k) \in \mathcal{S}$, and $d_j > 1$. If $d_j = 1$ for any $j \in \mathcal{N}$, then $\pi_{(j,k)} = \pi_{(k,j)} \cdot 1$, where $k \in N(j)$. Also, $\sum_{(j,k) \in \mathcal{S}} \pi_{(j,k)} = 1$.

In addition, since $|A_j| = d_j$, it follows that

$$\pi_{A_j} = \sum_{(u,v) \in A_j} \pi_{(u,v)} = \frac{d_j}{2m}$$

for each $j \in \mathcal{N}$. ■

Theorem 4 says that $\{Z_t\}$ of the p -BRW has the same uniform stationary distribution on \mathcal{S} *regardless of* the amount of backtracking at each node j , or equivalently, the stationary distribution is *invariant* with respect to $\{p_j\}_{j \in \mathcal{N}}$. In particular, the steady-state probability of the p -BRW being at node j , $\pi_{A_j} = d_j/2m$, is proportional to the degree (d_j) of node i , which is the same as that of SRW. This allows us to freely choose $\{p_j\}$ as desired while keeping their stationary distribution the same as if the walk is the SRW on the same graph. This invariance property is a fundamental building block based on which we can obtain other properties of p -BRW and develop methodology as to how to set the backtracking probability p_j for each j , so as to achieve faster diffusion of p -BRW on G and correspondingly smaller delay in our Smart Sleep protocol.

We suppose that the Markov chain $\{Z_t\}$ is a stationary Markov chain, i.e., Z_0 is chosen from the stationary distribution $\boldsymbol{\pi}$ ($\mathbb{P}\{Z_0 = (u, v)\} = \pi_{(u,v)} = 1/2m$). This is equivalent to assuming that the p -BRW on \mathcal{N} starts from its stationary distribution. To see this, observe that $\mathbb{P}\{X_0 = v\} = \pi_{A_v}$ together with (6.6) and (6.7) gives $\mathbb{P}\{Z_0 = (u, v)\} = 1/2m$. Now, we define the following two stopping times (or the first hitting times) of $\{Z_t\}$ to the subset A_j :

$$T_{A_j}^+ \triangleq \min\{t > 0 : Z_t \in A_j\}, \text{ and } T_{A_j} \triangleq \min\{t \geq 0 : Z_t \in A_j\}.$$

Here, one difference between these two is that the former does not count the case of $Z_0 \in A_j$, while the latter includes this case, i.e., $T_{A_j} = 0$ if $Z_0 \in A_j$. We then define the *mean return time* of p -BRW to node $j \in \mathcal{N}$ when starting at node j as

$$\mathbb{E}_{\pi_{A_j}}\{T_{A_j}^+\} \triangleq \mathbb{E}\{T_{A_j}^+ | Z_0 \in A_j\} = \sum_{(u,v) \in A_j} \mathbb{E}\{T_{A_j}^+ | Z_0 = (u,v)\} \pi_{A_j}(u,v), \quad (6.9)$$

where $\pi_{A_j}(u,v) \triangleq \frac{\pi(u,v)}{\pi_{A_j}} = \frac{1}{d_j}$ for $(u,v) \in A_j$, and the equality in (6.9) is from the fact that $\{Z_t\}$ is a stationary chain. This is the average number of (discrete) time steps required for a p -BRW starting at node j to return to j . Similarly, we define the second moment of return time of p -BRW to node j as $\mathbb{E}_{\pi_{A_j}}\{(T_{A_j}^+)^2\} \triangleq \mathbb{E}\{(T_{A_j}^+)^2 | Z_0 \in A_j\}$. In addition, we define the *mean first hitting time* of p -BRW to node $j \in \mathcal{N}$ from a stationary start as

$$\mathbb{E}_{\pi}\{T_{A_j}\} \triangleq \sum_{(u,v) \in \mathcal{S}} \mathbb{E}\{T_{A_j} | Z_0 = (u,v)\} \pi_{(u,v)}. \quad (6.10)$$

Here, by the stationary start we mean that Z_0 is drawn from the stationary distribution of $\{Z_t\}$, or equivalently, the p -BRW starts at node v with its stationary distribution π_{A_v} . Note that $\{Z_t\}$ is already a stationary chain. Thus, by consulting the properties of a stationary Markov chain [2], we have

Proposition 8. *For any choice of $p_j \in [0, 1)$, $j \in \mathcal{N}$, we have*

$$\mathbb{E}_{\pi_{A_j}}\{T_{A_j}^+\} = \frac{1}{\pi_{A_j}} = \frac{2m}{d_j}, \quad \text{and} \quad (6.11)$$

$$\mathbb{E}_{\pi}\{T_{A_j}\} = \frac{1}{2} \frac{\mathbb{E}_{\pi_{A_j}}\{(T_{A_j}^+)^2\}}{\mathbb{E}_{\pi_{A_j}}\{T_{A_j}^+\}} - \frac{1}{2} = \frac{d_j}{4m} \mathbb{E}_{\pi_{A_j}}\{(T_{A_j}^+)^2\} - \frac{1}{2} \quad (6.12)$$

for each A_j , $j \in \mathcal{N}$. □

Proof. For any (finite) stationary Markov chain, the following holds [2, Ch.2.,pp.20–21]:

$$\mathbb{E}_{\pi_A}\{T_A^+\} = \frac{1}{\pi_A}, \quad \text{and} \quad \mathbb{E}_{\pi}\{T_A\} = \frac{1}{2} \frac{\mathbb{E}_{\pi_A}\{(T_A^+)^2\}}{\mathbb{E}_{\pi_A}\{T_A^+\}} - \frac{1}{2}$$

for any subset A of the state space. Hence, from Theorem 4, (6.11)–(6.12) immediately follows. ■

Proposition 8 implies that the mean return time of p -BRW to node $j \in \mathcal{N}$ is *invariant* regardless of the values of backtracking probabilities $\{p_j\}_{j \in \mathcal{N}}$. Moreover, the mean first hitting

time of p -BRW from a stationary start to node j ($\mathbb{E}_\pi\{T_{A_j}\}$), or the average delay of a packet generated from randomly chosen source to destination j under p -BRW, depends only on the first two moments of the return time of p -BRW to node j .

6.2.3 How To Choose Each Backtracking Probability p_i ?

From (6.12), observe that in order to reduce the average delay of a packet, we need to choose each backtracking probability p_i such that the second moment of return time to node j ($\mathbb{E}_{\pi_{A_j}}\{(T_{A_j}^+)^2\}$) gets smaller whenever possible. Unfortunately, however, computing the second or any higher moment of the return to a node in a closed form is extremely difficult even for a SRW on general graphs [2]. Even worse, the sequence of visited nodes under the p -BRW, $\{X_t\}$, itself is not even a Markov chain. Nonetheless, we demonstrate below that it is still possible to ‘shape’ the distribution of the return time toward smaller second moment by resorting to the invariance result in our Theorem 4 and suitably choosing $\{p_j\}$.

For notational convenience, we first denote the return time of p -BRW to node j as R_j , defined by

$$R_j \triangleq \min\{t > 0 : X_t = j | X_0 = j\}, \quad (6.13)$$

where X_t is the location of p -BRW on \mathcal{N} at time $t \geq 0$. Note that from (6.9) and (6.13), we have

$$\mathbb{E}_{\pi_{A_j}}\{T_{A_j}^+\} = \mathbb{E}\{R_j\} = \sum_{t=1}^{\infty} \mathbb{P}\{R_j \geq t\} = \frac{2m}{d_j} \quad (6.14)$$

$$\mathbb{E}_{\pi_{A_j}}\{(T_{A_j}^+)^2\} = \mathbb{E}\{R_j^2\} = \sum_{t=1}^{\infty} 2t \cdot \mathbb{P}\{R_j \geq t\} - \mathbb{E}\{R_j\}, \quad (6.15)$$

where the last equality in (6.14) is from (6.11). While the precise relationship between $\{p_j\}_{j \in \mathcal{N}}$ and $\mathbb{P}\{R_j \geq t\}$ for all t is beyond reach, we can still *locally* control the shape of $\mathbb{P}\{R_j \geq t\}$ for small t , which in turn affects $\mathbb{P}\{R_j \geq t\}$ for large t as well via the invariance property – the total sum $\sum_{t=1}^{\infty} \mathbb{P}\{R_j \geq t\}$ in (6.14) does not depend on the choice of p_j . To be precise, as the backtracking probability p_i gets smaller, the p -BRW at the current node is more unlikely to return to the previously visited node over the next few slots, implying that $\mathbb{P}\{R_j \geq t\}$ for small t will be larger and thus $\mathbb{P}\{R_j \geq t\}$ for large t will be smaller. In view of (6.15), this is always more advantageous toward smaller second moment of the return time $\mathbb{E}\{R_j^2\}$.

Take a 2-D torus (a regular graph with $d=4$) with n nodes for example. From Proposition 8, the mean return time to each node j is $\mathbb{E}\{R_j\} = n$. Let $p_i = p \in [0, 1)$ for all $i \in \mathcal{N}$. Then, from symmetry, $\mathbb{P}\{R_j \geq t\}$ does not depend on j anymore, so we can conveniently drop the subscript j from our notation for the return time R_j . Figure 6.3 shows the second moment

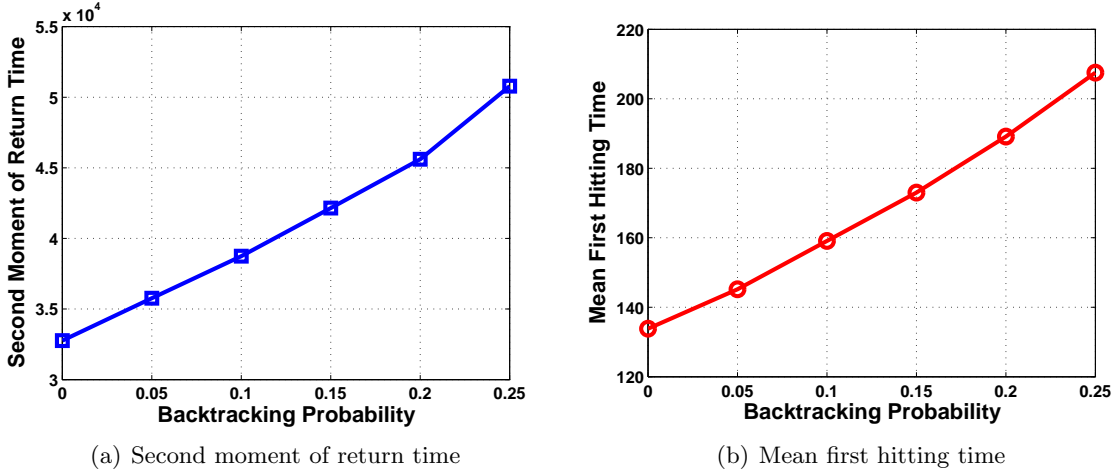


Figure 6.3: Effect of different backtracking probabilities p on the second moment of return time to a given node and the mean first hitting time to that node under a 2-D torus with $n = 11 \times 11$.

of return time $\mathbb{E}\{R^2\}$ and the mean first hitting time to any given node under a 2-D torus with $n = 11 \times 11$, empirically obtained via numerical simulations while varying p . As mentioned before, if $p = 0.25$, the p -BRW reduces to the SRW on a 2-D torus. Thus, we only consider the case of $0 \leq p \leq 0.25$ to see the behavior of p -BRW compared with that of the SRW. As seen from Figure 6.3, the aforementioned argument holds. In other words, the second moment of return time to a given node is *increasing* in the backtracking probability p , and so is the mean first hitting time to that node (from a stationary start).

6.2.4 From p -Backtracking Random Walk To Smart Sleep

We explain how the p -BRW is related to the transition of a packet of interest on G under Smart Sleep protocol. Consider a packet of interest being forwarded from node i to node j . Node i then immediately goes to sleep for T slots while all the other neighbors of j (except node i), i.e., all nodes in $N(j) \setminus \{i\}$, are in a normal mode. Similarly as was done in Section 6.1, it follows that the number of time slots Y_j until successful transmission from j to a node in $N(j) \setminus \{i\}$, is geometrically distributed with mean $1/q'_j$, where $q'_j \triangleq q(1 - (1-q)^{d_j-1})$. Also, if the packet has not been forwarded to any node in $N(j) \setminus \{i\}$ within T slots (during which node i has been in a sleep mode), i.e., $Y_j > T$, then node i resumes its normal random duty cycling and the packet can be forwarded back to node i with probability $1/d_j$. Hence, the probability that the packet backtracks to node i is $\frac{1}{d_j} \mathbb{P}\{Y_j > T\} < \frac{1}{d_j}$ for $T > 0$. Consequently, the packet will be forwarded to a node in $N(j) \setminus \{i\}$ with probability $\frac{1}{d_j-1} (1 - \frac{1}{d_j} \mathbb{P}\{Y_j > T\}) > \frac{1}{d_j}$. These transition probabilities are the same regardless of which node is the one that previously forwarded the packet to node

j , provided that all neighbors of node j except the previous forwarder are in a normal mode. One can also see that this transition behavior is the same as that of p -BRW from a node j to one of its neighbors, where the backtracking probability at node j is $p_j = \frac{1}{d_j} \mathbb{P}\{Y_j > T\}$. Note that p_j becomes smaller for larger T , possibly leading to faster diffusion of the single packet over G .

In a general (non-tree like) graph G , situation is more subtle as there may exist several paths routed to each node, over which the packet can traverse before reaching its destination. Unlike the case of 1-D ring in Section 6.1, when a packet of interest reaches node l , there might be multiple neighbors which are still in their sleep modes. Figure 6.4 shows an example of this case with large sleep duration T , where the packet reaches node l after traversing path $i \rightarrow j \rightarrow k \rightarrow l$, only to realize that in addition to node k , node i is still in its sleep mode (caused by the packet itself earlier). The packet at node l now sees ‘less-than-usual’ transition probabilities to both nodes i and k , whereby p -BRW allows only one such case (different probability of backtracking to its previously visited node while all others are equally likely).

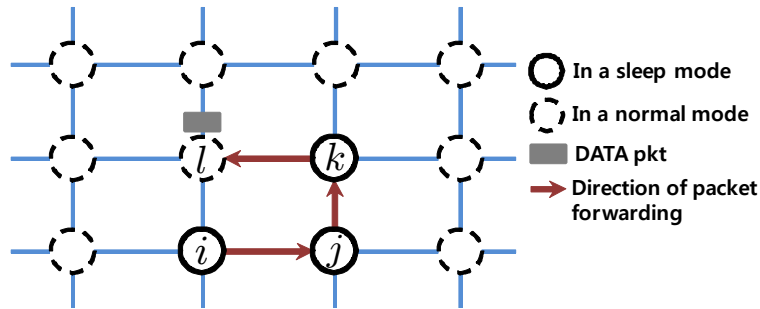


Figure 6.4: A snapshot of a part of 2-D grid topology when a packet of interest reaches node l via path $i \rightarrow j \rightarrow k \rightarrow l$. If T is very large, nodes i, j, k can be still in a sleep mode by the time the packet reaches l .

However, we maintain that this case will be unlikely with reasonably chosen (not too large) value of T . For example, in Figure 6.4, observe that the average sojourn time of the packet at each node is lower bounded by $[q(1 - (1 - q)^4)]^{-1}$, achieved when $T = 0$. Thus, if $T \leq 3[q(1 - (1 - q)^4)]^{-1}$, then the case in Figure 6.4 will not arise. This is even more so, considering that the probability of the packet traversing over the path $i \rightarrow j \rightarrow k \rightarrow l$ (of length 3) is no larger than $1/3^3 \approx 0.038$, and it is even more unlikely with the increase of path-length. Thus, for suitably chosen values of T , the p -BRW can well approximate the transition behavior of the packet over a general graph in Smart Sleep, and all the previous results implying faster diffusion of packet under Smart Sleep still hold.

Necessary condition for the sleep duration T : As mentioned before, too large values of T put many sensors consecutively inactive as relay nodes for the delivery of *other* packets for a long time, which in turn eventually leads to longer packet delay. On the other hand, too small values of T would render Smart Sleep protocol behave just like the usual SRW-based forwarding, thus losing all the benefit of faster diffusion and smaller delay in p -BRW. A moment of thought here thus suggests that the sleep duration T be long enough so that the packet that caused the sleep won't backtrack for a while, but at the same time short enough such that the sensor can resume its normal mode before another packet comes in. To capture this idea precisely, let τ be the interval between two consecutive packet arrivals to sensor i . When there are multiple packets in the network, chances are that these two packets have different IDs. Then, the above argument leads to $T \approx \mathbb{E}\{\tau\}$. See Figure 6.5 for illustration.

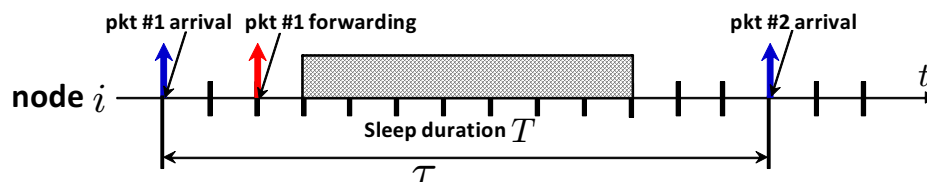


Figure 6.5: A relationship between the sleep duration T and the interval τ between two consecutive packets arriving to sensor i .

To capture the inter-dependency among τ , T , and other network parameters, we define by Λ the total aggregate packet arrival rate into the whole network, and by $D(T)$ the average packet delay under Smart Sleep with parameter $T \geq 0$. (This way, $D(0)$ is the average packet delay via SRW-based forwarding.) Then, by viewing Λ and $D(T)$ as the exogenous arrival rate into the system (network) and the waiting time of each packet in the system, respectively, we see from Little's Law that $\Lambda D(T)$ is the average number of packets in the network in the steady-state, where $\Lambda D(0) < n$ to ensure system stability or from light-traffic load condition.[‡] Consider a randomly tagged sensor node i . From the invariance property in Proposition 8 (see (6.11)), the mean return time of a packet to node i (in the number of packet forwardings) is inversely proportional to the stationary probability of being at node i . If the network of n nodes is roughly regular and if we let $\mathbb{E}\{\tilde{W}\}$ be the average sojourn time of the packet at each node (given that successively arrived different packets do not affect each other), then the actual mean return time to i (in the number of time slots) is $n\mathbb{E}\{\tilde{W}\}$. Since there are $\Lambda D(T)$ number of packets in the network on average, we arrive at

[‡]The performance of SRW-based algorithms [6, 58, 11, 24] is typically measured based on the delivery of a single packet, i.e., $\Lambda D(0) \approx 1$.

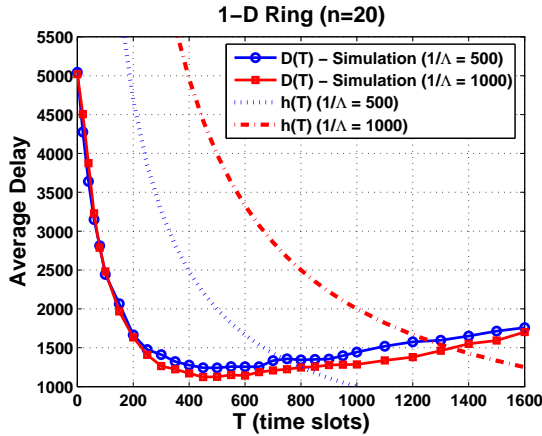
$$T \approx \mathbb{E}\{\tau\} \approx \frac{n\mathbb{E}\{\tilde{W}\}}{\Lambda D(T)} = \frac{\mathbb{E}\{\tilde{W}\}}{\lambda D(T)}, \quad (6.16)$$

where $\lambda := \Lambda/n$ is the exogenous packet arrival rate (as a source) *per each sensor node*. Note that obtaining a closed-form expression of $D(T)$ under general topology and multiple packets would entail rigorous analysis of interacting non-Markovian processes on a general graph, which is clearly beyond the scope of this dissertation. Still, we find that (6.16) is informative, and in particular, we will show later in Section 6.3 that the optimal sleep duration T^* in minimizing packet delay is achieved roughly when $T^* \approx \mathbb{E}\{\tau\}$ via extensive simulation results. This confirms our argument that each sensor can stay asleep as much as possible to prevent the return of the same previous packets while not holding off the delivery of other upcoming packets. We also find (6.16) practically useful in implementing distributed algorithms in which each sensor only needs to independently estimate $\mathbb{E}\{\tau\}$ based on two consecutive incoming packets with different IDs and self-adjust T on the fly, which we leave as a future work.

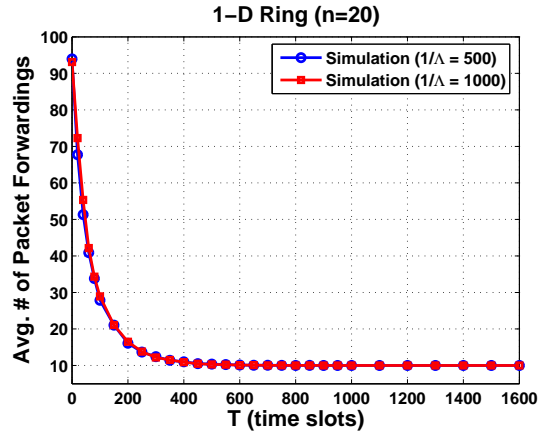
6.3 Simulation Results

In this section, we present representative simulation results to demonstrate and quantify performance improvement of Smart Sleep under a large range of $T > 0$ compared with the SRW-based forwarding ($T = 0$). Our metrics of interest are packet delay, transmission cost (total number of packet forwardings), and the amount of power-saving of each sensor. We conduct simulations over 1-D ring, 2-D grid, and random geometric graph on our custom event-driven simulator using C++. The random geometric graph, denoted as $RGG(n, r)$, is a widely used graph in the literature [6, 7, 11, 24], in which n nodes are uniformly and independently located in a square and two nodes are connected if they are within distance of r .

We use the following common setups for simulations. First, as used in [11, 24], we measure the performance for the farthest source-destination pair under each instance of graph, where the length between two nodes is the number of hops over the shortest path connecting the two nodes. We test under two different arrival rates ($1/\Lambda = 500$ or 1000 slots). Each simulation runs until 50 packets are delivered, and each data point reported here is the average of 300 independent simulations (i.e., average over 15000 packet deliveries). We also measure the average wake-up frequency per each sensor to quantify the amount of power-saving under Smart Sleep. In our scenario, we designate a sensor node as the destination simulating a situation without any powered sink [56, 11, 24], but we note that the main feature of Smart Sleep doesn't change even in the presence of powered sinks. Throughout the simulations, we set the default wake-up probability as $q = 0.1$. This can be easily programmed into each sensor before network deployment or reconfigured if necessary. Note that our focus here is to extend the sleep period

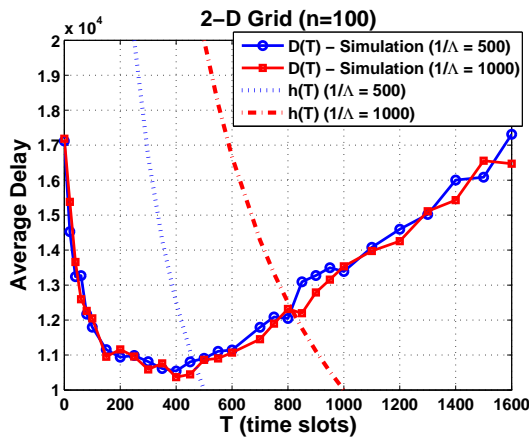


(a) Average Delay $D(T)$

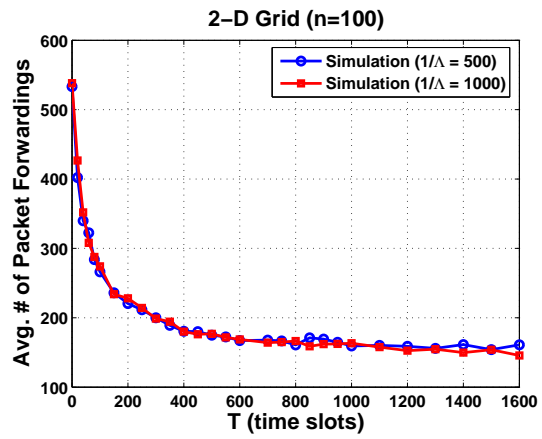


(b) Transmission cost

Figure 6.6: Performance comparison on the packet delivery for the farthest s-d pair while varying T under 1-D ring with $n=20$.



(a) Average Delay $D(T)$



(b) Transmission cost

Figure 6.7: Performance comparison on the packet delivery for the farthest s-d pair while varying T under 2-D grid with $n=100$.

after forwarding for any given q , not to optimally choose q under certain criteria, which is outside the scope of this dissertation.

Figure 6.6 shows the average delay $D(T)$ and transmission cost under a 1-D ring with $n=20$. Clearly, Smart Sleep offers significant improvement (more than 70%) for both metrics for all $T \in [200, 1000]$ compared with SRW-based one ($T=0$), though the average delay starts increasing slowly after around $T=600$ slots. It implies that for $T \lesssim 600$, the reduction in the number of total packet forwardings achieved through faster diffusion of each packet over the

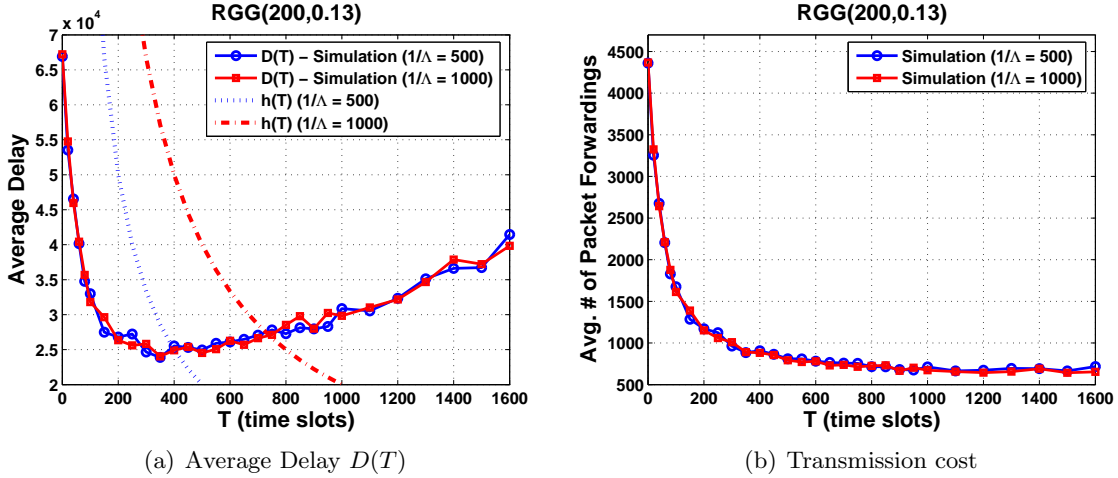


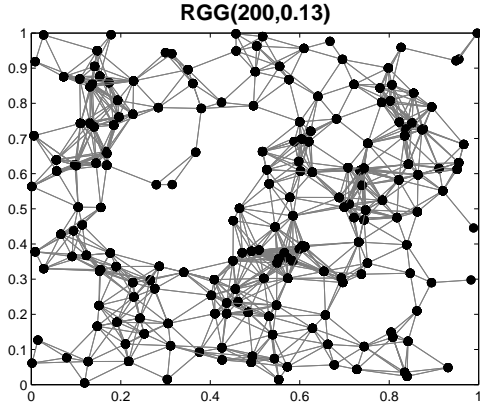
Figure 6.8: Performance comparison on the packet delivery for the farthest s-d pair while varying T under a sample graph of $RGG(200, 0.13)$.

network (the hallmark of p -BRW) weighs more than the slight increase in the average sojourn time of the packet at every node (see (6.2)). Note that the condition for the optimal T^* in (6.16) can be rewritten as

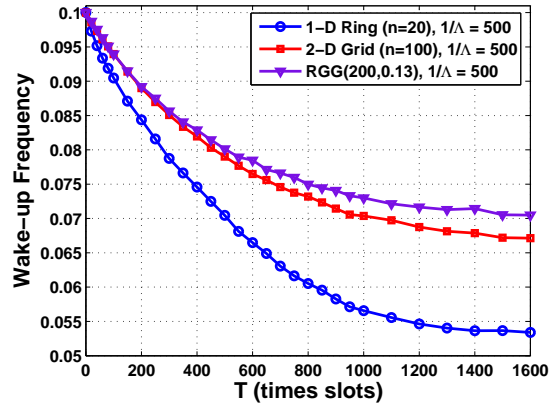
$$D(T) \approx \frac{\mathbb{E}\{\tilde{W}\}}{\lambda} \cdot \frac{1}{T} \triangleq h(T). \quad (6.17)$$

Note that the average sojourn time of a packet at each sensor $\mathbb{E}\{\tilde{W}\}$ is also a function of T . In Figure 6.6(a), we overlay $h(T)$ where the average sojourn time $\mathbb{E}\{\tilde{W}\}$ here for 1-D ring can be computed from (6.2), and observe that the optimal T^* in minimizing the average delay is located roughly around the intersection of $D(T)$ and $h(T)$, confirming the validity of the condition in (6.16).

Figs. 6.7 and 6.8 show the results for a 2-D grid with $n=100$ and for a sample topology of $RGG(200, 0.13)$ displayed in Figure 6.9(a) while T varies, respectively, but now under two different values of Λ . For 2-D grid, the average delay reduces by around 30% and the transmission cost by 60% for $T \in [200, 600]$. For RGG , both performance metrics improve by more than 60% for $T \in [200, 700]$. Similarly as in Figure 6.6(a), we also plot $h(T)$ in all cases. We here use $\mathbb{E}\{\tilde{W}\} = 1/q^2$, corresponding to the case of only one awake neighbor (under duty-cycling with probability q) while all other neighbors are in sleep mode, which is roughly an upper bound of the actual average sojourn time. In all these cases, the plotted $h(T)$ is thus an upper bound of the true values, and the actual intersection point with more accurate value of $\mathbb{E}\{\tilde{W}\}$ would be smaller than what is shown in the figures, suggesting that the optimal sleep duration T^* is again well approximated by the fixed point satisfying (6.16) or (6.17). Lastly, Figure 6.9(b)



(a) A sample topology of RGG



(b) Wake-up frequency

Figure 6.9: (a) A sample topology of $RGG(200, 0.13)$; (b) Measured wake-up frequency for a sensor under various topologies as T varies.

shows the average wake-up frequency per each sensor to quantify the amount of power-saving through Smart Sleep measured during the simulation time for all the above topologies with $1/\Lambda = 500$. We see that the additional power-saving (compared with the SRW-based duty-cycling, i.e., $T = 0$) is around 20% for the estimated optimal values T^* . In other words, the observed 30% to 60% reduction in the average delay is achieved when each sensor turns off 20% more than the usual random duty-cycling. In addition, since the packet transmission itself also consumes power, the actual power-saving will be even greater by noting the reduction in the average number of packet forwardings in all cases. We also point out here that in all the simulations, the range of T values for which we enjoy great improvement both in delay and power is fairly broad, implying that our Smart Sleep protocol allows easy configuration and offers robust and superior performance even under inaccurately estimated T^* .

Chapter 7

Exploiting Heterogeneity for Delay and Power Efficient WSNs – A Delay Perspective

In this chapter, we study another design of autonomous/distributed random duty cycling in WSNs, which is complementary to Smart Sleep presented in Chapter 6. In particular, we propose a distributed wake-up rate control scheme exploiting local heterogeneity structure for opportunistic forwarding, which achieves both smaller delay and longer network lifetime. In this chapter, we focus on the delay aspect, and will address the network lifetime aspect in the next chapter. Section 7.1 explains an asynchronous, heterogeneous random duty cycling which largely extends the homogeneous duty cycling (under synchronous network setting) in Chapter 5. We then provide the modeling and analysis for the delay performance of the opportunistic forwarding with the duty cycling in Section 7.2, and present our proposed wake-up rate control scheme with theoretically proven performance enhancement in Section 7.3. We finally provide numerical evaluations and independent simulation results in Section 7.4.

7.1 Opportunistic Forwarding under An Asynchronous, Heterogeneous Random Duty Cycling

We explain how an opportunistic forwarding performs under an *asynchronous, heterogeneous* random duty cycling. The principle of the opportunistic packet forwarding is the same as the one in [11, 24] (see Chapter 5), while the underlying duty cycling is different, but more beneficial.

In the asynchronous and heterogenous duty cycling, each node i sleeps (i.e., completely turns

off its RF transceiver or is in an ‘off’ state) and independently wakes up (i.e., turns on the RF transceiver or is in an ‘on’ state) according to a Poisson process with rate parameter $\lambda_i > 0$. In other words, the inter-wake-up time (the duration of ‘off’ state) for each sensor node i is drawn from an independent exponential distribution with rate λ_i . Again, this asynchronous random duty cycling is self-configurable and does not need any (global) synchronization overhead and complexity, which is appealing for ad-hoc networking systems. Note also that in contrast to [11, 24], we allow different λ_i for each sensor node i rather than simply using the same $\lambda_i = \lambda$ for all nodes i . Recall the homogeneous duty cycling under synchronous network setting in Chapter 5.

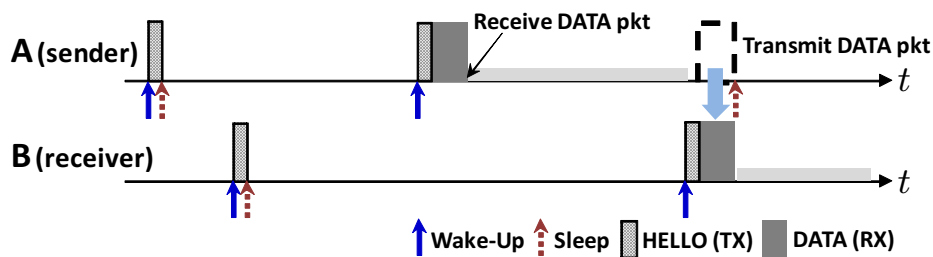


Figure 7.1: The operation of data transmission via an opportunistic forwarding under an asynchronous, heterogeneous random duty cycling

While performing this duty cycling, if any sensor node i has a packet to transmit, it opportunistically forwards the packet to a first awake node among $N(i)$. Here, any packet transmission/reception between two adjacent sensor nodes can occur, only when they are both on and each of them is aware that the other node is also on. To this end, prior to data communication, when each sensor node i has a packet to transmit, it simply performs an idle listening on the channel until to find a first awake node in $N(i)$. When a node without a packet wakes up, it first conducts a carrier sense on the channel, and then broadcasts a small hello message to notify its ‘on’ state to any neighboring node having a packet only if the channel is idle; otherwise, it goes to sleep. Figure 7.1 depicts the operation of data transmission between two nodes via this opportunistic forwarding. From Poisson process assumption for the beginning instants of ‘on’ state and short duration for the small hello message, it is unlikely that two or more sensor nodes wake up at the same time, and therefore ignored in our consideration. In addition, since a carrier sensing range (or interference range) is typically twice larger than a transmission range, any awake two-hop neighbors of a transmitting node can detect the presence of a packet transmission if it happens, and thus there will be no collision between a packet transmission and any hello message transmission.

Throughout the rest of this chapter, we suppose that traffic load in the network is light as assumed in [6, 7, 58, 11, 24]. Hence, an interference from concurrent data transmissions is not an issue, and we measure the delay performance based on the delivery of a single packet. Also, due to the light traffic load and small size of hello message, we assume that time duration required for a packet transmission/reception is relatively negligible compared with the duration of ‘off’ state for each node.

7.2 Performance Modeling and Analysis

In this section, we show that the random trajectory of a packet traveling over a given graph (network) G under the opportunistic forwarding with asynchronous and heterogeneous duty cycling, can be interpreted as a continuous-time random walk (CTRW) on G , or equivalently, a discrete-time random walk (DTRW) on G with heterogeneous sojourn time. Hence, the forwarding algorithm in our class also retains natural properties of random walk-based algorithms such as simplicity, scalability, load-balancing, and robustness to topology changes. We then define our performance metrics and provide analytical formulas to compute the metrics numerically.

7.2.1 Continuous-Time Random Walk on A Graph

We consider a packet of interest which travels over G where its source and destination are not specified here, temporarily. Let $\{X(t) \in \mathcal{N}\}_{t \geq 0}$ be a continuous-time random sequence (or trajectory) of the packet, indicating where the packet is located at time t . One can observe that the sojourn time of $X(t)$ at node i (say W_i), i.e., the waiting time for each node i until to find any first awake node in $N(i)$, is independent of the index of the first awake node among $N(i)$ (say I_i), i.e., the node which receives the packet from node i . We refer to Appendix A.5 for details. Then, from this independence, $\{X(t)\}$ becomes a continuous-time Markov chain (CTMC) with state space \mathcal{N} where each state i corresponds to node i currently holding the packet, and it can be also interpreted as a CTRW on G . Then, the transition rate from state i to state j is given by

$$q_{ij} = \begin{cases} \lambda_j & \text{if } (i, j) \in \mathcal{E} \\ 0 & \text{otherwise} \end{cases} \quad (7.1)$$

for $i \neq j$ and $q_{ii} = -\sum_{k \in N(i)} \lambda_k$. We define by $\mathbf{Q} \triangleq \{q_{ij}\}_{i, j \in \mathcal{N}}$ the transition rate matrix of $\{X(t)\}$. Note that the amount of sojourn time the process spends in state i before jumping into one of its neighboring nodes $j \in N(i)$ is simply the waiting time W_i of the packet at sensor node i .

Equivalently, we can construct an *embedded* discrete-time Markov chain (DTMC) with transition probability p_{ij} given by

$$p_{ij} = \begin{cases} \mathbb{P}\{I_i = j\} = \frac{\lambda_j}{\sum_{k \in N(i)} \lambda_k} & \text{if } (i, j) \in \mathcal{E} \\ 0 & \text{otherwise,} \end{cases} \quad (7.2)$$

where $\sum_{j \neq i} p_{ij} = 1$ and $p_{ii} = 0$. We define by $\{Y_m\}_{m \geq 0}$ the random sequence of nodes visited and by $\mathbf{P} \triangleq \{p_{ij}\}_{i, j \in \mathcal{N}}$ the transition probability matrix of $\{Y_m\}$. Then, we can also interpret the random trajectory of the packet traveling over G as a DTRW on G with heterogeneous sojourn time W_i at state i , where the state transition probability of DTRW is the same as p_{ij} of the embedded DTMC in (7.2). As a special case, if $\lambda_i = \lambda$ for all $i \in \mathcal{N}$, then the resulting DTRW on G becomes a *simple* random walk, i.e., $p_{ij} = 1/d(i)$, if $(i, j) \in \mathcal{E}$, otherwise $p_{ij} = 0$. Note that this is the case (homogeneous duty cycling) considered in [11, 24] (and also explained in Chapter 5) under the synchronous network setting.

7.2.2 Performance Metric and Analysis

Consider the *hitting time* (or first passage time) from state (node) i to state j on G , which is defined as

$$H_{ij} \triangleq \inf\{t > 0 : X(t) = j \mid X(0) = i\} \quad (7.3)$$

for $i, j \in \mathcal{N}$ and $i \neq j$, and $\bar{H}_{ij} \triangleq \mathbb{E}\{H_{ij}\}$. The hitting time represents the delay of unicast where the source node i sends a packet containing its local observation (e.g., temperature) to the destination node j , as similarly used in [11, 24]. Note that the destination node can be a powered sink with Internet connection or a usual sensor node in the scenario [56] where the powered sink is not available due to geographical reasons. To be precise, (7.3) is proper for the latter case. For the former case, the powered sink may not need to perform the duty cycling and its neighboring nodes can be aware of its presence via a neighbor discovery process [89]. Hence, in this case, the delay of unicast becomes the time taken for a packet from the source node to reach any one of neighbors of the destination, and (7.3) can be properly modified as the hitting time to the set of neighbors of the destination.

For any given graph (network) G , the mean hitting time \bar{H}_{ij} can be obtained as ‘mean time to absorption’ for an absorbing chain that can be constructed from the CTMC $\{X(t)\}$. Specifically, suppose that state j is an absorbing state. We can re-label the set of states \mathcal{N} such that transient states $\mathcal{N} \setminus \{j\}$ come first. Then, the transition rate matrix \mathbf{Q} of $\{X(t)\}$ can be rewritten as

$$\mathbf{Q} = \begin{bmatrix} \mathbf{T} & \mathbf{T}^0 \\ \mathbf{0} & 0 \end{bmatrix},$$

where \mathbf{T} is a $(n-1) \times (n-1)$ transition rate matrix, \mathbf{T}^0 is an $(n-1)$ -dimensional column vector, each of whose elements is the transition rate from state i to the absorbing state j , and $\mathbf{0}$ is a

row vector of zeros. Then, \overline{H}_{ij} can be obtained as [15]

$$\overline{H}_{ij} = -\boldsymbol{\alpha} \mathbf{T}^{-1} \mathbf{e}, \quad (7.4)$$

where $\boldsymbol{\alpha}$ is an initial distribution (row) vector in which an element of state i is one and other elements are zeros, and \mathbf{e} is a column vector of ones. Hence, one can easily evaluate \overline{H}_{ij} by numerically computing (7.4).

The performance of the mean hitting time \overline{H}_{ij} depends on how to perform random duty cycling at each sensor node i , or specifically, how to control wake-up rate λ_i of each sensor node i . Note that we do not assume any coordination in network operations and any node can be a source or destination node for the packet delivery. It is also desirable to avoid the extremely large end-to-end delay even for delay-tolerant applications. Hence, in the design of a distributed wake-up rate control, we will focus on improving the worst-case delay performance \overline{H}_{max} , defined as

$$\overline{H}_{max} \triangleq \max_{i,j \in \mathcal{N}, i \neq j} \overline{H}_{ij}, \quad (7.5)$$

i.e., the maximum mean hitting time over all possible source-destination pairs in the network.

7.3 A Distributed Wake-up Rate Control Based on Local Degree Information

In this section, we first examine how to control wake-up rate λ_i of each node i depending on the underlying structure of a given graph (network) G , and then propose a distributed wake-up rate control scheme in which each node i autonomously controls its wake-up rate λ_i based only on its own degree information in order to improve (shorten) the maximum mean hitting time \overline{H}_{max} than the case with homogeneous random duty cycling $\lambda_i = \lambda$ for all i .

For a fair comparison among all possible heterogeneous duty cycling strategies, we set

$$\frac{1}{\lambda} = \frac{1}{n} \sum_{i=1}^n \frac{1}{\lambda_i} \quad (7.6)$$

for all possible wake-up rates $\{\lambda_i, i \in \mathcal{N}\}$, and compare the delay performance under $\{\lambda_i\}$ with that under the homogeneous duty cycling with the same wake-up rate λ given by (7.6) for all nodes in the network. Since sensor node i consumes one unit amount of power whenever it wakes up every $1/\lambda_i$ seconds on average, the above condition implies that the average power consumption rate over the whole network is kept the same under heterogeneous duty cycling with $\{\lambda_i\}$ and under the corresponding homogeneous case with λ in (7.6).

Recall that the embedded DTMC, $\{Y_m\}$, (or a DTRW on G) under any homogeneous duty

cycling becomes a *simple* random walk, as mentioned in Section 7.2. It is well known that the stationary distribution π'_i is proportional to the degree of node i , i.e., $\pi'_i = d(i) / \sum_{k \in \mathcal{N}} d(k)$, where π'_i is the stationary distribution of $\{Y_m\}$. This implies that a packet of interest (a random walk) in the network visits more likely to a sensor node with higher degree. At the same time, if the underlying graph G is a regular graph where $d(i) = d$ for all $i \in \mathcal{N}$, then the stationary distribution is uniform, i.e., $\pi'_i = 1/n$ for all i . Hence, the packet of interest visits every node equally likely and there may not be any benefit by making the wake-up rates λ_i heterogeneous in shortening or minimizing the maximum mean hitting time \bar{H}_{max} . This observation can be made rigorous for a complete graph $G = K_n$ (a special case of regular graphs) as shown in the following.

Theorem 5. *For a complete graph $G = K_n$, and for a given $\lambda > 0$, $\lambda_i = \lambda$ for all $i \in \mathcal{N}$ is optimal in minimizing \bar{H}_{max} over all $\{\lambda_i\}$ satisfying (7.6), i.e., $1/n \sum_{i=1}^n 1/\lambda_i = 1/\lambda$. \square*

Proof. For a complete graph $G = K_n$, and for a given $\lambda > 0$, we first fix $\lambda_i > 0$, $i \in \mathcal{N}$, satisfying

$$\frac{1}{n} \sum_{i=1}^n \frac{1}{\lambda_i} = \frac{1}{\lambda}. \quad (7.7)$$

Then, for $G = K_n$, the transition rate of the CTMC, $\{X(t)\}$, from each state i to *any* other state is

$$q_i \triangleq \sum_{k \in \mathcal{N}(i)} \lambda_k = \sum_{k \in \mathcal{N} \setminus \{i\}} \lambda_k.$$

Also, from (7.2), the transition probability of its embedded DTMC, $\{Y_m\}$, from state i to state j is

$$p_{ij} = \frac{\lambda_j}{\sum_{k \in \mathcal{N}(i)} \lambda_k} = \frac{\lambda_j}{q_i} \quad (7.8)$$

for $j \in \mathcal{N} \setminus \{i\}$, and $p_{ii} = 0$ (no self-loops).

We here use a technique of *uniformization* [74, 15] in which *any* CTMC with finite state space can be thought of as being a stochastic process or a *uniformized* CTMC that spends an exponential amount of time with rate q in *every* state i and then makes transition into state j with new transition probability p_{ij}^* (that is the transition probability of embedded DTMC of the uniformized chain), if the new transition rate q in the uniformized chain is not smaller than the transition rate at *any* state in the original chain.

Let $\{X'(t)\}_{t \geq 0}$ be an uniformized CTMC of the original CTMC $\{X(t)\}$. Here, the new transition rate q of $\{X'(t)\}$ is chosen to be

$$q = \sum_{k \in \mathcal{N}} \lambda_k > q_i = \sum_{k \in \mathcal{N} \setminus \{i\}} \lambda_k$$

for all $i \in \mathcal{N}$. The transition probability p_{ij}^* of its embedded DTMC, denoted as $\{Y'_m\}_{m \geq 0}$, is given by [74, 15]

$$p_{ij}^* = \begin{cases} 1 - \frac{q_i}{q} = 1 - \frac{\sum_{k' \in \mathcal{N} \setminus \{i\}} \lambda_{k'}}{\sum_{k \in \mathcal{N}} \lambda_k} = \frac{\lambda_i}{q} & j = i \\ \frac{q_i}{q} p_{ij} = \frac{\lambda_j}{q} & j \neq i. \end{cases} \quad (7.9)$$

In addition, let $Z_k, k \geq 1$, be *i.i.d.* exponential random variables with rate q to represent the sequence of the exponential sojourn times at every state i . We also define by H'_{ij} hitting time from state i to state j for the embedded DTMC $\{Y'_m\}$, which is given by

$$H'_{ij} \triangleq \min\{m > 0 : Y'_m = j \mid Y'_0 = i\}$$

for $i, j \in \mathcal{N}$ and $i \neq j$. Note that this hitting time is the number of state transitions (or discrete-time steps) that the embedded DTMC $\{Y'_m\}$ starting at state i takes to reach state j .

From the definition of the above uniformized CTMC and the definition of hitting time H_{ij} for the original CTMC $\{X(t)\}$ as in (7.3), we arrive at

$$H_{ij} \stackrel{d}{=} \sum_{k=1}^{H'_{ij}} Z_k$$

for $i, j \in \mathcal{N}$ and $i \neq j$. Note that $\{Z_k\}$ is independent of H'_{ij} , since the amount of time that the process $\{Y'_m\}$ spends in any current state, and the next state visited, are independent. Hence, we obtain

$$\bar{H}_{ij} = \mathbb{E}\{H_{ij}\} = \mathbb{E}\left\{\sum_{k=1}^{H'_{ij}} Z_k\right\} = \mathbb{E}\{H'_{ij}\}\mathbb{E}\{Z_1\}, \quad (7.10)$$

for $i, j \in \mathcal{N}$ and $i \neq j$.

From (7.9), observe that the transition probability of the embedded DTMC $\{Y'_m\}$ from *any* state i to state j is $p_{ij}^* = \lambda_j/q$ for any $i, j \in \mathcal{N}$. Hence, the embedded DTMC $\{Y'_m\}$ can be viewed as a DTRW on a complete graph $G = K_n$ with *self-loops*. Let $p'_i \triangleq \lambda_i/q$ for $i \in \mathcal{N}$. Then, the number of discrete-time steps that the DTRW takes from node i until to reach node j , H'_{ij} , simply follows a geometric distribution with parameter p'_j and thus

$$\mathbb{E}\{H'_{ij}\} = \frac{1}{p'_j} = \frac{q}{\lambda_j}, \quad (7.11)$$

for any $i, j \in \mathcal{N}$ and $i \neq j$. Therefore, from (7.10)–(7.11) and by noting that $\mathbb{E}\{Z_1\} = 1/q$, we finally have

$$\bar{H}_{max} = \max_{i, j \in \mathcal{N}, i \neq j} \bar{H}_{ij} = \max_{i, j \in \mathcal{N}, i \neq j} \mathbb{E}\{H'_{ij}\}\mathbb{E}\{Z_1\} = \max_{j \in \mathcal{N}} \frac{1}{\lambda_j}.$$

Then, it is easy to see that $\lambda_i = \lambda$ for all $i \in \mathcal{N}$ is optimal in minimizing \overline{H}_{max} over all $\{\lambda_i\}$ satisfying (7.7) and its resulting \overline{H}_{max} is $1/\lambda$. ■

Note that the proof of optimality in Theorem 5 is still non-trivial, though it is straightforward to derive \overline{H}_{max} under the *homogeneous* duty cycling for a complete graph K_n .

However, in general, unless one carefully designs a *coordinated* sensor network, sensor network topologies would be rather heterogeneous (i.e., the degree of each node is different) and form non-regular graphs. Since a packet of interest is more likely to visit a sensor node with higher degree as mentioned above, the homogeneous duty cycling may be no longer optimal. Instead, it would be helpful to control the wake-up rate λ_i of each node i such that the packet visits every node more evenly so as to shorten \overline{H}_{max} under non-regular graphs.

In addition, a recent work [46] by Ikeda et al. addresses how to design a ‘better’ (discrete-time) random walk on a graph than a simple random walk, where the transition probability of the random walk is given by

$$\tilde{p}_{ij} = \begin{cases} \frac{d(j)^{-\alpha}}{\sum_{k \in N(i)} d(k)^{-\alpha}} & \text{if } (i, j) \in \mathcal{E} \\ 0 & \text{otherwise,} \end{cases} \quad (7.12)$$

for some constant α . In particular, they prove that if $\alpha = 1/2$ in (7.12), then the maximum mean hitting time, or the maximum average number of transitions taken to visit any given node (state), is $O(n^2)$ for *any* graph. Note that we here use different notation \tilde{p}_{ij} to distinguish it from the transition probability p_{ij} of the *embedded* DTMC, $\{Y_m\}$. This result suggests that a (proper) bias of a transition into a node with *smaller* degree can bring out an improvement of the maximum mean hitting time from $O(n^3)$ (guaranteed under the simple random walk [16, 46]) to $O(n^2)$ for *any* graph. Note that this asymptotic upper bound may be loose depending on underlying graphical structures. Also, (biased) random walks with transition probabilities in the form of (7.12) have been also studied in the physics literature (e.g., see [36]).

Inspired by the Ikeda et al.’s finding in [46], we propose a distributed wake-up rate control scheme in which each node i *autonomously* controls its wake-up rate λ_i based *only* on its own degree information as

$$\lambda_i = \lambda_0 d(i)^{-\beta}, \quad (7.13)$$

where λ_0 is an initial wake-up rate and β is a tunable parameter. Note that the value of λ_0 can be programmed into each sensor system before bootstrapping, and the degree information can be easily obtained through a neighbor discovery process [89] which takes place right after the network is deployed, and remain up-to-date through data communications as time goes on. Then, from (7.2) and (7.13), the transition probability p_{ij} of $\{Y_m\}$ becomes

$$p_{ij} = \begin{cases} \frac{\lambda_j}{\sum_{k \in N(i)} \lambda_k} = \frac{d(j)^{-\beta}}{\sum_{k \in N(i)} d(k)^{-\beta}} & \text{if } (i, j) \in \mathcal{E} \\ 0 & \text{otherwise,} \end{cases} \quad (7.14)$$

where now this transition probability p_{ij} becomes identical to \tilde{p}_{ij} in (7.12). Hence, we arrive to the following asymptotic upper bound of \bar{H}_{max} achievable under our proposed algorithm by extending* the Ikeda et al.'s result [46].

Theorem 6. *For any graph G , if $\beta = 1/2$, then $\bar{H}_{max} \leq \frac{3\sqrt{d_{max}n^2}}{\lambda_0}$, and hence $\bar{H}_{max} = O(\sqrt{d_{max}n^2})$, where $d_{max} \triangleq \max_{i \in \mathcal{N}} d(i)$. \square*

Proof. We first define by H''_{ij} hitting time from state i to state j for the embedded DTMC $\{Y_m\}$, which is given by

$$H''_{ij} \triangleq \min\{m > 0 : Y_m = j \mid Y_0 = i\}$$

for $i, j \in \mathcal{N}$ and $i \neq j$. Also, recall that if $\beta = 1/2$, then $\lambda_i = \lambda_0/\sqrt{d(i)}$ as in (7.13), and the transition probability p_{ij} of $\{Y_m\}$ in (7.14) becomes

$$p_{ij} = \begin{cases} \frac{d(j)^{-1/2}}{\sum_{k \in N(i)} d(k)^{-1/2}} & \text{if } (i, j) \in \mathcal{E} \\ 0 & \text{otherwise.} \end{cases} \quad (7.15)$$

Note that it is shown in [46, Theorem 2] that for *any* graph G , if this is the transition probability of a DTRW on G , then

$$\max_{i, j \in \mathcal{N}, i \neq j} \mathbb{E}\{H''_{ij}\} \leq 3n^2. \quad (7.16)$$

In addition, observe that

$$\max_{k \in \mathcal{N}} \mathbb{E}\{W_k\} = \max_{k \in \mathcal{N}} \frac{1}{\sum_{j \in N(k)} \lambda_j} \leq \max_{k \in \mathcal{N}} \frac{1}{\lambda_k} = \frac{\sqrt{d_{max}}}{\lambda_0}, \quad (7.17)$$

where $d_{max} \triangleq \max_{i \in \mathcal{N}} d(i)$. Since $\mathbb{E}\{W_i\} \leq \max_{k \in \mathcal{N}} \mathbb{E}\{W_k\}$ for all $i \in \mathcal{N}$, it is also easy to see that

$$\bar{H}_{ij} = \mathbb{E}\{H_{ij}\} \leq \mathbb{E}\{H''_{ij}\} \max_{k \in \mathcal{N}} \mathbb{E}\{W_k\}, \quad (7.18)$$

for all $i, j \in \mathcal{N}, i \neq j$. Note that the RHS of (7.18) is the mean (continuous-time) hitting time from state i to state j for a uniform CTMC where the sojourn time in every state is exponentially distributed with mean $\max_{k \in \mathcal{N}} \mathbb{E}\{W_k\}$ and its state transition probability is same as (7.15).

*[46] is based on a discrete-time random walk where the walk spends one time unit in every vertex. In contrast, we are dealing with the embedded DTMC $\{Y_m\}$ whose sojourn time in node i is random and different over i .

From (7.16)–(7.18), we finally have that for any graph G

$$\begin{aligned}
\overline{H}_{max} &= \max_{i,j \in \mathcal{N}, i \neq j} \overline{H}_{ij} \stackrel{(7.18)}{\leq} \max_{i,j \in \mathcal{N}, i \neq j} \mathbb{E}\{H''_{ij}\} \max_{k \in \mathcal{N}} \mathbb{E}\{W_k\} \\
&\stackrel{(7.17)}{\leq} \max_{i,j \in \mathcal{N}, i \neq j} \mathbb{E}\{H''_{ij}\} \frac{\sqrt{d_{max}}}{\lambda_0} \\
&\stackrel{(7.16)}{\leq} 3n^2 \frac{\sqrt{d_{max}}}{\lambda_0}. \tag{7.19}
\end{aligned}$$

Therefore, for *any* graph G , if $\beta = 1/2$, then $\overline{H}_{max} = O(\sqrt{d_{max}}n^2)$. ■

Similarly, we can show that any homogeneous random duty cycling (or a simple random walk with random sojourn time) guarantees $\overline{H}_{max} = O(n^3)$ for any graph, based on the fact that a discrete-time simple random walk (one unit of sojourn time at every node) guarantees $O(n^3)$ maximum mean hitting time for any graph [16, 46]. Since $d_{max} < n$, we have $O(\sqrt{d_{max}}n^2) \leq O(n^{2.5}) < O(n^3)$, i.e., our proposed algorithm improves its guaranteed asymptotic upper bound of \overline{H}_{max} from $O(n^3)$ to $O(\sqrt{d_{max}}n^2)$ for *any* graph.

7.4 Numerical Evaluations and Simulation Results

In this section, we present the exact performance of \overline{H}_{max} via numerical evaluations of (7.4) and provide independent simulation results to show that our proposed algorithm significantly outperforms pure homogeneous random duty cycling under random geometric graphs, which have been widely used in the literature [6, 7, 12, 11, 24] to model diverse wireless sensor or ad-hoc network topologies. The random geometric graph, denoted as $RGG(n, r)$, is a graph where n nodes are uniformly and independently located in the unit square, and two nodes are connected if they are within distance of r . While $RGG(n, r)$ becomes regular asymptotically for sufficiently large r [12], it typically exhibits heterogeneity in its resulting degree sequence for any given finite value of r . Thus, we set out to investigate the performance of our proposed algorithm or how the local degree information can be exploited in controlling the wake-up rate λ_i of each node i to improve \overline{H}_{max} under various sample topologies of $RGG(n, r)$.

Figure 7.2 shows the numerical results of \overline{H}_{max} by computing (7.4) and simulation results, obtained through our custom event-driven simulator using C++, for our proposed algorithm (heterogeneous random duty cycling) and its corresponding homogeneous duty cycling with λ from (7.6), under 50 different sample topologies of $RGG(50, 0.3)$. Here, the connectivity of each of 50 sample graphs is ensured, and $\beta = 1/2$ in (7.13) is set for our algorithm with $\lambda_0 = 0.02$. Since (7.4) is exact for CTMC, the simulation results precisely match with the numerical computations. Figure 7.2 clearly shows that our algorithm outperforms the pure

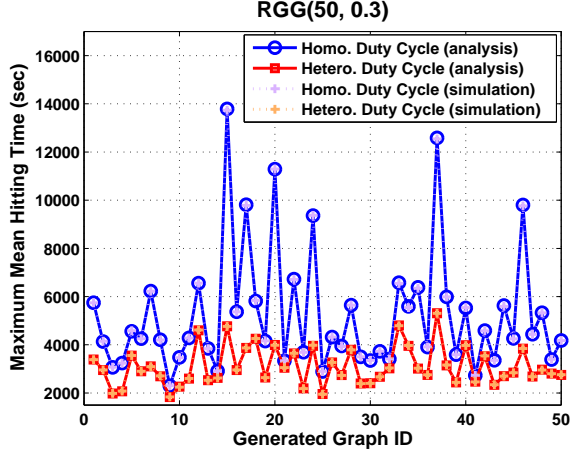


Figure 7.2: \overline{H}_{max} under 50 different sample topologies of $RGG(50, 0.3)$.

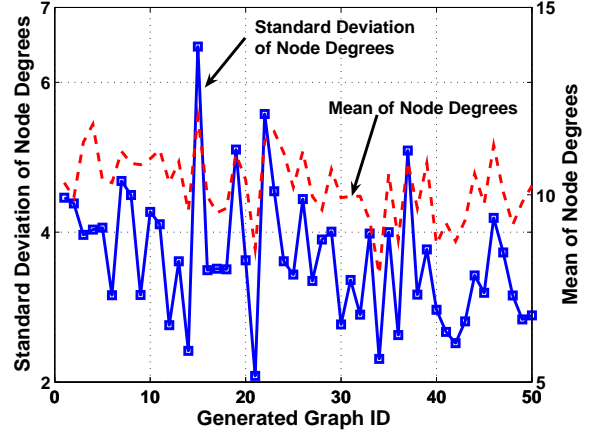


Figure 7.3: Statistics of node degrees of 50 different sample topologies of $RGG(50, 0.3)$ used in Figure 7.2.

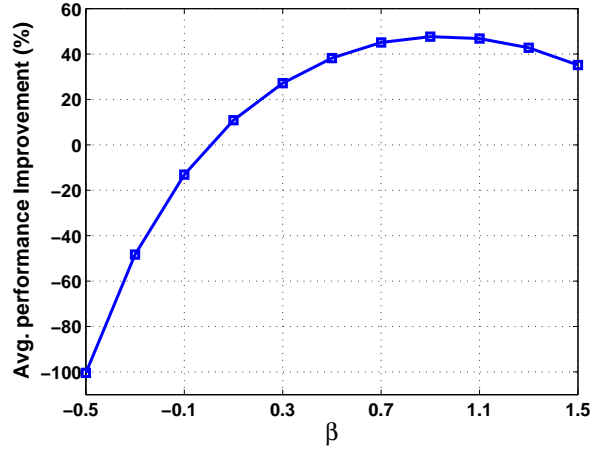


Figure 7.4: Average performance improvement in \overline{H}_{max} over 500 different sample topologies of $RGG(50, 0.3)$ while varying β in (7.13).

homogeneous duty cycling for all 50 different generations of $RGG(50, 0.3)$. Specifically, an average performance improvement over 50 generated graphs is about 35%, while some case (graph id: 15) exhibits 65% performance improvement (reduction in \overline{H}_{max}).

To see any relationship between the heterogeneity of the graph topology and the amount of performance improvement of our proposed algorithm over the simple homogeneous duty-cycling, we plot in Figure 7.3 the average and standard deviation of degree sequence for each of 50 sample topologies of $RGG(50, 0.3)$ used in Figure 7.2. We observe that the pure homogeneous duty

cycling performs poorly under topologies with higher standard deviation of degree sequence (e.g., graph id: 15, 37, 46), while our algorithm not only outperforms the pure homogeneous duty cycling but also tend to ‘stabilize’ the delay performance regardless of such irregularity in the node degrees of the given topology.

So far we have set $\beta = 1/2$ in (7.13) as originally suggested by [46]. While our asymptotic worst-case delay guarantee $\bar{H}_{max} = O(\sqrt{d_{max}}n^2)$ holds under $\beta = 1/2$, for finite sized graphs, it is still possible that our algorithm may perform better under different values of β . Figure 7.4 shows the average performance improvement of our proposed algorithm compared with its corresponding homogeneous duty cycling with λ from (7.6) under various values of β in (7.13). We use the same $\lambda_0 = 0.02$ as before, and each data point in this figure is obtained by averaging the performance improvements over 500 different sample topologies of $RGG(50, 0.3)$. As seen in Figure 7.4, it is possible to achieve close to 50% improvement when β is around 0.9, although $\beta = 1/2$ still results in 38% performance improvement on average, along with asymptotic guarantee for delay reduction for any arbitrary graph as shown in Theorem 6.

Chapter 8

Exploiting Heterogeneity for Delay and Power Efficient WSNs – A Network Lifetime Perspective

In this chapter, we evaluate the network lifetime induced from our proposed distributed wake-up rate control scheme presented in Chapter 7. To this end, we adopt a more realistic metric for the network lifetime – the time instant at which the network (graph) becomes fragmented without a ‘giant cluster’ for the first time. Our approach here is to employ and extend the percolation technique tailored to time-varying graphs, whereby results only on simple degree-dependent site percolation for static graphs are available in literature. Section 8.1 describes the background for percolation theory. We review the existing results on degree-dependent site percolation for static graphs in Section 8.2. By extending such results to time-varying graphs, we show, in Section 8.3, that our proposed wake-up rate control leads to a proper control of node lifetime exploiting the heterogeneity over the node degrees to our advantage and in turn achieves longer network lifetime.

8.1 Background

8.1.1 A Generalized Random Graph Model

For analytical treatment, we consider a generalized random graph model with any given degree distribution (a.k.a. configuration model), which is widely used in statistical physics and computer science (e.g., [20, 67, 66, 85]). In this model, the degree of any randomly chosen node follows the given degree distribution in the limit of large graph size ($n \rightarrow \infty$). Also, nodes in G are inter-connected at random with their degrees so that the degrees of any two adjacent nodes

remain independent. Thus, the nodes in G have degrees that are independently and identically distributed (*i.i.d.*) of one another in the large- n limit. Since our focus is to investigate the behavior of network lifetime in such limit (or large-scale network) as studied in [54, 34, 94], it is enough to measure all relevant quantities from the viewpoint of a *randomly chosen node*. This model is simple yet versatile. First, one can assign any arbitrary degree distribution to properly capture or represent the level of heterogeneity over the node degrees, allowing us to examine the impact of degree-dependent node lifetime upon the network lifetime, which is defined below, under a wide range of scenarios. Also, under this model, we can recover the results for the network lifetime recently obtained in [94] where node lifetimes are assumed to be *i.i.d.* as a special case.

8.1.2 Definitions

We use the following definitions throughout the rest of this chapter. First, a *component* in G is a subset of nodes in G where each node is reachable from others, i.e., there exists at least one path from a node to any other in the component. Each component can be disconnected from other components. If the size of the largest component in G (or the expected number of nodes in the component), say $\mathbb{E}\{C\}$, scales with n ($\mathbb{E}\{C\} \rightarrow \infty$) as $n \rightarrow \infty$, we call it a *giant component* in G . There exists a critical point at which the size of the largest component in G undergoes a sudden change, or *phase transition*, from a constant size, to being proportional to n in the large- n limit [62, 66]. In other words, a giant component forms in G above the critical point of phase transition.

Each sensor node in G is equipped with its own battery, and it only functions for a limited amount of time, or *node lifetime*. Here, the node lifetime can vary over the nodes due to the different battery drain rates. The size of the largest component consisting of *alive* nodes that correctly function in G , say $\mathbb{E}\{C(t)\}$, is now a function of time t . Assuming that there exists a giant component in G at time $t=0$, as will be shown later, there exists a *critical time* T_c before which such giant component remains to form, i.e., $\mathbb{E}\{C(t)\} \rightarrow \infty$ as $n \rightarrow \infty$ for $t < T_c$, while the existence of a giant component is not ensured or the network may be fully partitioned for $t > T_c$. In this chapter, we define the critical time T_c as the *network lifetime* before which a majority of nodes in G remain to work properly, and our main focus is to investigate the network lifetime when the lifetime of each node varies depending on its degree.

8.2 A Critical Point of Site Percolation

To analyze the network lifetime in the presence of degree-dependent node lifetime, we consult the theory of site percolation [20, 66]. When some fraction of nodes (or sites) are removed from

a graph (or network) in a certain way, from the percolation theory one can find a critical point of *percolation transition* or percolation threshold above which a giant component of remaining nodes forms or below which such giant component no longer exists.

Consider a random graph G with a given degree distribution whose mean is finite. If a node is correctly functioning, we say that the node is *occupied* (or alive). Then, each node is occupied with some occupation probability, which is a function of its own degree. In this set-up, it was shown in [20, 66] that there exists a critical point of percolation transition at which a giant component consisting of occupied nodes first forms. Since the percolation threshold will be a basis for our subsequent analysis, we here provide a brief review on it.

Suppose that G is below the critical point of percolation transition in the large- n limit. Let C be the number of occupied nodes in a component to which a *randomly chosen node*, say $i \in \mathcal{N}$, belongs. In order to find the percolation threshold, we first need to know how many occupied neighbors node i has and then how many alive neighbors those occupied neighbors also have, *other than* node i . Let D be a nonnegative integer-valued random variable to denote the degree of randomly chosen node i having the given degree distribution. We also define by q_d the occupation probability that a node is occupied given that it has degree d . Then, the joint probability that node i has degree d and is also occupied, is $f_o(d) \triangleq \mathbb{P}\{D=d\} \cdot q_d$. Hence, the probability that node i is occupied is $\sum_{d=0}^{\infty} f_o(d)$.

In addition, let D_1 be the number of edges of a neighbor of node i other than the edge connecting node i and the neighbor. It is just one less than the total number of edges of the neighbor. Then, by noting that a node with higher degree has higher chance to be connected to node i , one can see that D_1 is proportional to $d \cdot \mathbb{P}\{D=d\}$, and after a correct normalization, we have

$$\mathbb{P}\{D_1 = d\} = \frac{(d+1)\mathbb{P}\{D = d+1\}}{\sum_{d=0}^{\infty} (d+1)\mathbb{P}\{D = d+1\}} = \frac{(d+1)\mathbb{P}\{D = d+1\}}{\mathbb{E}\{D\}}. \quad (8.1)$$

Then, the joint probability that a neighbor of node i has degree $d+1$ and is also occupied, is $g_o(d) \triangleq \mathbb{P}\{D_1 = d\} \cdot q_{d+1}$. Thus, the probability that a neighbor of node i is occupied is $\sum_{d=0}^{\infty} g_o(d)$. Note that $f_o(d) \neq g_o(d)$ in general.

Observe that if node i is *not occupied* with probability $1 - \sum_{d=0}^{\infty} f_o(d)$, then $C = 0$. Also, occupied nodes in a component to which node i belongs, if node i has *degree* d and is *occupied* with probability $f_o(d)$, are composed of node i itself and other occupied nodes in d different components originating from each of the d neighbors of node i . Note that node i is not included in any one of such d components. Let S_1, \dots, S_d be the size of each of such d different components. Since degrees of node i and its neighbors are *i.i.d.*, S_1, \dots, S_d are also *i.i.d.* with common distribution F .^{*} Hence, for each $d \geq 0$, it follows that

^{*}More precisely, in the regime below the percolation threshold we assumed at the beginning, the size of any existing component in G is finite. Since the degrees of any two adjacent nodes are *i.i.d.*, in the large- n limit,

$$C \stackrel{d}{=} 1 + \sum_{k=1}^d S_k \text{ with probability } f_o(d), \quad (8.2)$$

where $\stackrel{d}{=}$ means equal in distribution. Subsequently,

$$\mathbb{E}\{C\} = \sum_{d=0}^{\infty} f_o(d) + \mathbb{E}\{S_1\} \sum_{d=0}^{\infty} d \cdot f_o(d). \quad (8.3)$$

We can compute $\mathbb{E}\{S_1\}$ in terms of $g_o(d)$ (or $\mathbb{P}\{D = d\}$ and q_d) in a similar way. If a *neighbor* of node i is not occupied with probability $1 - \sum_{d=0}^{\infty} g_o(d)$, then $S_1 = 0$. Each component originating from the neighbor of node i , if the neighbor has *degree* $d+1$ and is *occupied* with probability $g_o(d)$, consists of the neighbor itself and other occupied nodes in d different components initiated from each of its d neighbors. Note that one of $d+1$ edges of the neighbor connects itself and node i . Also, these d components do not include the neighbor of i . Thus, if we let \tilde{S}_k ($k = 1, 2, \dots, d$) be *i.i.d.* copy of S_1 , after repeating the same argument above, S_1 must satisfy the following self-consistent relationship

$$S_1 \stackrel{d}{=} 1 + \sum_{k=1}^d \tilde{S}_k \text{ with probability } g_o(d) \quad (8.4)$$

for each $d \geq 0$, and so we have

$$\mathbb{E}\{S_1\} = \sum_{d=0}^{\infty} g_o(d) + \mathbb{E}\{S_1\} \sum_{d=0}^{\infty} d \cdot g_o(d). \quad (8.5)$$

From (8.3) and (8.5), we finally have

$$\mathbb{E}\{C\} = \sum_{d=0}^{\infty} f_o(d) + \frac{\sum_{d=0}^{\infty} g_o(d)}{1 - \sum_{d=0}^{\infty} d \cdot g_o(d)} \sum_{d=0}^{\infty} d \cdot f_o(d). \quad (8.6)$$

One can now observe that if $\sum_{d=0}^{\infty} d \cdot g_o(d) = 1$, then $\mathbb{E}\{C\} \rightarrow \infty$, i.e., a giant component composed of occupied nodes first appears in G or the occupied nodes in G start to be percolated. By recalling $g_o(d) = \mathbb{P}\{D_1 = d\} \cdot q_{d+1}$ and from (8.1), the critical point of percolation transition, $\sum_{d=0}^{\infty} d \cdot g_o(d) = 1$, can be written as

$$\frac{\sum_{d=1}^{\infty} d(d-1)\mathbb{P}\{D = d\}q_d}{\mathbb{E}\{D\}} = 1. \quad (8.7)$$

clustering coefficient – the probability that two neighbors of a node are also neighbors of one another, tends to zero, and thus all finite components do not contain loops and are rather tree-like, which in turn makes the sizes of such components be *i.i.d.* [20, 67, 66].

This is exactly the same as the percolation threshold obtained in [66, pp.609–614] via a different method. See also [20].[†] Since the sum in the LHS of (8.7) monotonically increases as edges are added to the graph G for given q_d , it follows that a giant component consisting of occupied nodes exists, if and only if the LHS of (8.7) is larger than one, i.e.,

$$\frac{\sum_{d=1}^{\infty} d(d-1)\mathbb{P}\{D=d\}q_d}{\mathbb{E}\{D\}} > 1. \quad (8.8)$$

In what follows, we demonstrate how these percolation threshold and condition can be interpreted so as to obtain the network lifetime in the presence of degree-dependent node lifetime.

8.3 From Site Percolation To Network Lifetime

We first show there exists a critical time T_c , or the network lifetime, after which a giant component composed of active nodes starts to disintegrate in a random graph G with a given degree distribution, provided that the existence of such giant component (or network connectivity) is initially ensured at $t = 0$. Then, we analytically examine how the degree-dependent node lifetime impacts the network lifetime through the comparison with the network lifetime driven from its comparable degree-independent node lifetime.

Let $L(d)$ be a random variable denoting the lifetime of any node with degree d (degree-dependent node lifetime). Then, the lifetime of a randomly chosen node i becomes $L(D)$, a function of random variable D . If node i has degree d , then the probability that it is alive or properly functioning at time $t > 0$ is given by

$$\mathbb{P}\{L(D) > t \mid D = d\} = \mathbb{P}\{L(d) > t\}, \quad (8.9)$$

where the equality is from the independence of $L(d)$ and D . In other words, the probability that node i has degree d and is alive at time t , is $\mathbb{P}\{D=d\} \cdot \mathbb{P}\{L(d) > t\}$.

Now, we fix $t \geq 0$ and set $q_d = \mathbb{P}\{L(d) > t\}$, the probability that a node with degree d is alive (or occupied) at time t . We define a function $\mathcal{L}(t)$ as

$$\mathcal{L}(t) \triangleq \frac{\sum_{d=1}^{\infty} d(d-1)\mathbb{P}\{D=d\}\mathbb{P}\{L(d) > t\}}{\mathbb{E}\{D\}}. \quad (8.10)$$

It then follows from (8.8) that, for a given time t , a giant component of active nodes exists if and only if $\mathcal{L}(t) > 1$. Observe that $\mathbb{P}\{L(d) > t\}$ is decreasing in $t \geq 0$ for any given d , $\mathcal{L}(t)$ is also decreasing in t . Hence, from (8.7), (8.8) and (8.10), the critical time T_c , or the network

[†]A set of equations, obtained via a formalism of generating functions, to find the percolation threshold was first given in [20]. The percolation threshold is not clearly stated there, but can be obtained from Equations (1)–(4) therein.

lifetime, can be obtained as

$$T_c = \inf\{t \geq 0 : \mathcal{L}(t) = 1\}. \quad (8.11)$$

It implies that $\mathcal{L}(t) > 1$ for $t < T_c$, or a giant component composed of functional (active) nodes remains to form in G for $t < T_c$, while the existence of such giant component is not guaranteed and network may be fully partitioned for $t > T_c$.

To avoid triviality, we assume that all the nodes are initially functioning (active) and there exists a giant component of active nodes at $t = 0$, i.e., $\mathcal{L}(0) > 1$. Since $\mathbb{P}\{L(d) > 0\} = 1$, from (8.10), the condition $\mathcal{L}(0) > 1$ amounts to $\mathbb{E}\{D^2\}/\mathbb{E}\{D\} > 2$, which is the condition for a critical point of phase transition as mentioned in Section 8.1 for a *static* random graph with given degree distribution [62, 66]. Note that we are here dealing with a dynamic (time-varying) random graph in which each node with degree d will stop functioning and thus be removed from the network after its (degree-dependent) lifetime $L(d)$.

8.3.1 Degree-independent Node Lifetime

We first discuss the network lifetime for the case of degree-independent node lifetime, i.e., the lifetime of every node is *i.i.d.* with common distribution, regardless of its degree, i.e. $L \stackrel{d}{=} L(d)$ for all d . Thus (8.10) becomes

$$\mathcal{L}(t) = \frac{\mathbb{E}\{D^2\} - \mathbb{E}\{D\}}{\mathbb{E}\{D\}} \mathbb{P}\{L > t\}. \quad (8.12)$$

Here, from (8.11)–(8.12), one can easily see that for any given distribution of L , the network tends to live longer (T_c gets larger) as the underlying network topology becomes more heterogeneous in the sense of larger $\mathbb{E}\{D^2\}$ while $\mathbb{E}\{D\}$ is kept the same. When D is Poisson distributed with $\mathbb{E}\{D\} = \mu > 1$ (to ensure the initial connectivity of the network, i.e. $\mathcal{L}(0) > 1$) in the large- n limit, we have the following.

Proposition 9. *If L is exponentially distributed with mean $1/\alpha$, i.e., $\mathbb{P}\{L > t\} = e^{-\alpha t}$, then $T_c = \frac{1}{\alpha} \log(\mu)$. In addition, if L follows a Pareto (or power-law) distribution, i.e., $\mathbb{P}\{L > t\} = \left(\frac{t}{\eta}\right)^{-\rho}$ for $\rho > 1$, then $T_c = \eta(\mu)^{1/\rho}$. \square*

Proof. Since D is Poisson distributed with $\mathbb{E}\{D\} = \mu$, we have $\mathbb{E}\{D^2\} = \mu^2 + \mu$ and thus $\mathcal{L}(t) = \mu \mathbb{P}\{L > t\}$ from (8.12). Then, from (8.11), the results follow. \blacksquare

Remark 5. *The Poisson degree distribution often arises in the modelling of wireless ad-hoc or sensor networks (e.g., [53, 94]). Specifically, n (sensor) nodes are uniformly distributed on a square area of size A and two nodes are connected if they are within distance of r , which*

is called a random geometric graph. Then, as $n \rightarrow \infty$ and $A \rightarrow \infty$ while the node density $\nu = n/A$ is kept constant, the node degree approximately follows a Poisson distribution with mean $\mu = \nu\pi r^2$ [27, 53]. \square

Remark 6. It was shown in [94] that the last time until the network possesses a giant component composed of surviving nodes (i.e., network lifetime T_c in our definition) is $\Theta(\log(\log n))$ and $\Theta((\log n)^{1/\rho})$ for the exponential and Pareto node lifetime, respectively, under a random geometric graph where the node density ν is fixed as in Remark 5, but $\mu = \nu\pi r^2 = \Theta(\log n)$ (or $r^2 = \Theta(\log n)$) in the large- n limit.[‡] In this set-up, we can recover these results from Proposition 9, which clearly demonstrates the effectiveness of our approach based on a random graph model with a given degree distribution. \square

8.3.2 Degree-dependent Node Lifetime

We turn our attention to the network lifetime in the presence of degree-dependent node lifetime. Specifically, we examine how the network lifetime can be prolonged if one can control the lifetime of each node as a function of its degree. To this end, as used in Chapter 7, we consider the following scenario of WSNs with random duty-cycling which is adopted for energy/power conservation: each node wakes up according to a Poisson process with some wake-up rate to communicate with its awake neighbors.[§]

Clearly, the lifetime of each node and the induced network lifetime both depend on the wake-up rate of each node since each node consumes certain amount of its battery power whenever it wakes up and stays on. We consider a class of wake-up rate controls in which the wake-up rate of each node with degree d is given by

$$\lambda(d) = \lambda_0 d^{-\beta}, \tag{8.13}$$

where λ_0 is an initial wake-up rate (constant) and β is our control parameter. This set of wake-up rate controls is exactly the same as in Chapter 7, which addressed how to choose β to improve the delay performance of an opportunistic forwarding, but disregarding the lifetime aspect of the network. In contrast, our focus here is on which values of β lead to longer network lifetime when compared to that under its comparable degree-independent node lifetime as will be specified shortly.

[‡]As the average node degree is on the order of $\log n$ while node density remains fixed, the network lifetime scales with the number of nodes n .

[§]This setting has been also used in [53, 51], while the underlying packet-forwarding algorithm and the target in each work are different from others.

We assume that the lifetime of a node $L(d)$ with degree d is given by

$$L(d) = \frac{B}{a\lambda(d)} = \frac{B}{a\lambda_0}d^\beta, \quad (8.14)$$

where B is an initial battery power and a is a common unit of battery consumption made whenever a node wakes up. This power consumption model and its resulting constant node lifetime were similarly used in [51]. This choice allows tractable analysis for the network lifetimes under various scenarios and their quantitative comparison while still capturing the inversely-proportional relationship between the node lifetime and its wake-up rate. We however note that more sophisticated power consumption models and their resulting random node lifetimes can be still considered in our framework at the cost of more complicated analysis. As a special case, if $\lambda(d) = \lambda$ (the same wake-up rate for every node), then the node lifetime in (8.14) becomes degree-independent, i.e. $L = L(d)$ for all d .

To find the values of β in (8.13)–(8.14) leading to longer network lifetime, we compare each resultant network lifetime with the network lifetime \bar{T}_c obtained under the degree-independent node lifetime. Since a randomly chosen node has a degree D , it follows that

$$\bar{T}_c = \mathbb{E}\{L(D)\} = \frac{B}{a\lambda_0}\mathbb{E}\{D^\beta\}, \quad (8.15)$$

where the expectation is with respect to D . It means that every node will be no longer functional at the same time \bar{T}_c . We use \bar{T}_c for the network lifetime under this degree-independent node lifetime to be distinguished from the network lifetime T_c under the more general degree-dependent case.

Now, we can obtain the desirable value of β in (8.13)–(8.14) such that $T_c \geq \bar{T}_c$ by showing $\mathcal{L}(\bar{T}_c) \geq 1$. Observe that

$$\mathbb{P}\{L(d) > \bar{T}_c\} = 1_{\{L(d) > \bar{T}_c\}} = 1_{\{d > \mathbb{E}\{D^\beta\}^{1/\beta}\}}, \quad (8.16)$$

where $1_{\{\cdot\}}$ is an indicator function. Since $\mathbb{E}\{D^\beta\}^{1/\beta}$ is increasing in $\beta > 0$ [5], from (8.10) and (8.16), if one finds β^* such that

$$\mathcal{L}(\bar{T}_c) = \frac{1}{\mathbb{E}\{D\}}\mathbb{E}\left\{D(D-1)1_{\{D > \mathbb{E}\{D^{\beta^*}\}^{1/\beta^*}\}}\right\} \geq 1, \quad (8.17)$$

then $T_c \geq \bar{T}_c$ for any given $\beta \in (0, \beta^*]$. By using this property, for a random graph G with a Poisson degree distribution with mean $\mu > 1$, we show the following.

Theorem 7. *For any given $\beta \in (0, 1]$, we have $T_c \geq \bar{T}_c$.* □

Proof. We set $\beta^* = 1$. After little algebraic computation, (8.17) becomes

$$\mu \sum_{d=\lfloor \mu \rfloor - 1}^{\infty} \frac{\mu^d}{d!} e^{-\mu} \geq 1, \quad (8.18)$$

which is equivalent to

$$\mathbb{P}\{D \leq \lfloor \mu \rfloor - 2\} \leq 1 - \frac{1}{\mu}, \quad (8.19)$$

where $\lfloor \mu \rfloor$ is the largest integer n with $n \leq \mu$. For $1 < \mu < 3$, this trivially holds. To show that (8.19) holds for $\mu \geq 3$, we recall from [38, Theorem 1] that for $m \geq 2$ and $\mu \geq 2$,

$$\mathbb{P}\{D \leq \lfloor \mu \rfloor - m\} \leq e^{\frac{1}{8\mu}} \left(1 + \frac{1}{\mu}\right) Q\left(\frac{m - 3/2}{\sqrt{\mu}}\right), \quad (8.20)$$

where $Q(x) \triangleq \frac{1}{\sqrt{2\pi}} \int_x^{\infty} e^{-\frac{y^2}{2}} dy$. Since $Q(x) \leq \frac{1}{2} e^{-\frac{x^2}{2}}$ for all $x \geq 0$, from (8.20), we have

$$\mathbb{P}\{D \leq \lfloor \mu \rfloor - 2\} \leq \frac{1}{2} \left(1 + \frac{1}{\mu}\right) \leq 1 - \frac{1}{\mu}, \quad (8.21)$$

where the second inequality holds for $\mu \geq 3$, and this completes the proof. \blacksquare

Note that the range of $\beta \in (0, 1]$ leading to longer network lifetime also results in smaller delay of opportunistic forwarding as shown in Chapter 7. That is, our proposed distributed wake-up rate control scheme achieves both smaller delay and longer network lifetime for opportunistic forwarding in heterogeneous duty-cycled WSNs.

To support our analysis, we also conduct simulations to numerically measure the network lifetime. To this end, whenever any sensor dies out (runs out of battery), we compute a relative giant component size – defined by the ratio of the number of surviving nodes in the largest component to the total number of surviving nodes at each observation time instant as used in [94], and plot this value over time. We use a sample topology of random geometric graph (defined in Remark 5) generated as follows: $n = 400$ nodes are uniformly distributed over a square area $[0, \sqrt{\frac{n}{\nu}}]^2$ with node density $\nu = 2$, and any two nodes are connected if they are within $r = 2$. For the degree-dependent node lifetime, we use $\frac{B}{a} = 100$ and $\lambda_0 = 0.01$ with $\beta = 0.2$ or 0.5 in (8.14). The actual lifetime of each node with its wake-up rate $\lambda(d)$ in (8.13) is now the sum of 100 exponential inter-wake-up durations (from Poisson wake-up), whose mean is $L(d)$. For fair comparison, as was done in (8.15), the empirical average of the mean lifetime over $n = 400$ nodes under degree-dependent case is used as the mean lifetime of every node for the corresponding degree-independent case for each choice of β , while the lifetime of each node (with common wake-up rate) is still the sum of 100 exponential inter-wake-up durations.

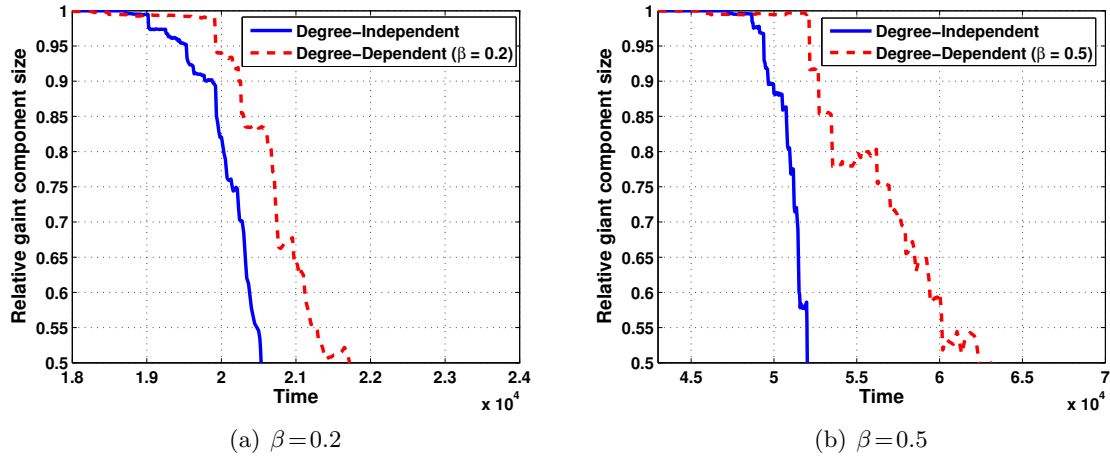


Figure 8.1: The comparison between the network lifetime induced from the degree-dependent node lifetime with different β and its corresponding network lifetime under the degree-independent node lifetime.

All simulation results are obtained by averaging over 10 independent trials. As shown in Figure 8.1, we can observe that the network lifetime driven from the degree-dependent node lifetime is prolonged for both $\beta = 0.2, 0.5$ (a majority of surviving nodes remains connected of one another for a longer period of time), which coincides with our analysis.

Chapter 9

Conclusion

We have studied the design and analysis of opportunistic forwarding in challenged networks. In the first part of this dissertation, we have presented our study on analyzing and improving the forwarding performance under heterogeneous contact dynamics in MONs.

In Chapter 3, we have mainly focused on how the underlying heterogeneity structure in mobile nodes' contact dynamics impacts the performance of forwarding algorithms in MONs. Based upon two representative heterogeneous network models, we have investigated their non-Poisson contact dynamics and stochastically compared their delay performance of direct forwarding and multicopy two-hop relay protocol with those under the homogeneous model. In particular, our findings show that each heterogeneous model predicts an entirely opposite delay performance when compared with that under the homogeneous model. Simulation results including the delay performance of epidemic routing are also provided to support these findings. Our results call for much more careful studies on the forwarding performance under non-Poisson contacts, and perhaps more importantly, under properly chosen heterogeneous models.

In Chapter 4, we have showed the significant performance gain obtained from exploiting the heterogeneity in mobile nodes' contact dynamics using the guaranteed delay bound of the sub-optimal two-hop forwarding policy. Thanks to the close-form expression of the guaranteed delay bound, we are able to show quantitative results for the performance improvement attainable through leveraging the underlying heterogeneity structure in the design of the forwarding policy, which cannot be captured in existing analytical studies based on the homogeneous network model. We expect that our analytical results will also complement the existing empirical studies on the design of forwarding algorithms which exploit the underlying heterogeneity in MONs.

In the second part of this dissertation, we have discussed the design of smart/distributed duty-cycling for opportunistic forwarding in heterogeneous and dynamic WSNs so as to achieve both faster information delivery and longer network lifetime.

In Chapter 6, we have demonstrated that our Smart Sleep protocol, a simple modification

of random duty cycling, can overcome the slow-mixing problem of SRW-based forwarding in randomly duty-cycled WSNs while achieving more power-saving at each sensor. To analytically address the packet dynamics in Smart Sleep, we introduce p -BRW, a variation of random walk with past memory, and establish several properties of p -BRW to explain why Smart Sleep leads to smaller delay of each packet over the network. Numerical simulations confirm our reasonings and reveal that Smart Sleep can be made very robust while yielding superior performance, with high potential for distributed and autonomous implementation under dynamic environments. We expect that our reasoning behind Smart Sleep and p -BRW for faster delivery can be also applicable to many other SRW-based algorithms in general networks beyond WSNs.

In Chapters 7–8, we have proposed a distributed wake-up rate control scheme exploiting local heterogeneity structure for opportunistic forwarding under an asynchronous, heterogeneous duty cycling in WSNs, and examined its resulting performance of (worst-case) delay and network lifetime. In particular, we prove that our proposed scheme leads to performance improvement from $O(n^3)$ to $O(\sqrt{d_{max}}n^2)$ in its guaranteed worst-case delay for any arbitrary graph. While our scheme already achieves significant reduction in delay performance for any network topology, we also show that it is still possible to extract even further performance improvement by carefully calibrating a tunable parameter in our scheme. Next, we studied the resulting network lifetime via our analytical framework developed based upon the percolation theory on a random graph model with an arbitrarily given degree distribution. We show that our proposed wake-up rate control (thus leading to a proper control of node lifetime taking advantage of the heterogeneity over the node degrees) indeed achieves longer network life, saving huge cost and effort for network maintenance. We expect that our framework can be easily extended to address the temporal characteristics of networks beyond WSNs with general degree distributions.

REFERENCES

- [1] I. F. Akyildiz, W. Su, Y. Sankarasubramaniam, and E. Cayirci, “A survey on sensor networks,” *IEEE Communications Magazine*, vol. 40, no. 8, pp. 102–114, 2002.
- [2] D. Aldous and J. Fill, *Reversible Markov Chains and Random Walks on Graphs*. monograph in preparation.
- [3] N. Alon, I. Benjamini, E. Lubetzky, and S. Sodin, “Non-backtracking random walks mix faster,” *Communications in Contemporary Mathematics*, vol. 9, no. 4, pp. 585–603, 2007.
- [4] E. Altman, T. Basar, and F. De Pellegrini, “Optimal monotone forwarding policies in delay tolerant mobile ad-hoc networks,” in *InterPerf*, Athens, Greece, Oct. 2008.
- [5] R. B. Ash and C. A. Doléans-Dade, *Probability and measure theory*, 2nd ed. Academic Press, 2000.
- [6] C. Avin and C. Brito, “Efficient and robust query processing in dynamic environments using random walk techniques,” in *ACM/IEEE IPSN*, Berkeley, CA, April 2004.
- [7] C. Avin and B. Krishnamachari, “The power of choice in random walks: an empirical study,” in *ACM MSWiM*, Torremolinos, Spain, Oct. 2006.
- [8] A. Balasubramanian, B. N. Levine, and A. Venkataramani, “DTN Routing as a Resource Allocation Problem,” in *ACM Sigcomm*, Kyoto, Japan, Aug. 2007.
- [9] S. Bandyopadhyay, E. J. Coyle, and T. Falck, “Stochastic properties of mobility models in mobile ad hoc networks,” *IEEE Trans. on Mobile Computing*, vol. 6, no. 11, pp. 1218–1229.
- [10] N. Banerjee, M. D. Corner, D. Towsley, and B. N. Levine, “Relays, base stations, and meshes: enhancing mobile networks with infrastructure,” in *ACM MobiCom*, San Francisco, CA, Sep. 2008.
- [11] P. Basu and C.-K. Chau, “Opportunistic forwarding in wireless networks with duty cycling,” in *CHANTS*, San Francisco, CA, Sep. 2008.
- [12] S. Boyd, A. Ghosh, B. Prabhakar, and D. Shah, “Mixing times for random walks on geometric random graphs,” in *SIAM Workshop on Analytic Algorithmics and Combinatorics*, Vancouver, Jan. 2005.
- [13] S. Boyd and L. Vandenberghe, *Convex optimization*. Cambridge University Press, 2004.
- [14] D. Braginsky and D. Estrin, “Rumor routing algorithm for sensor networks,” in *First ACM International Workshop on Wireless Sensor Networks and Applications (WSNA)*, Atlanta, GA, Sep. 2002.
- [15] P. Brémaud, *Markov chains: gibbs fields, monte carlo simulation, and queues*. Springer-Verlag, 1999.

- [16] G. Brightwell and P. Winkler, “Maximum hitting time for random walks on graphs,” *Random Structures and Algorithms*, vol. 1, no. 3, pp. 263–276, 1990.
- [17] S. Burleigh, A. Hooke, L. Torgerson, K. Fall, V. Cerf, B. Durst, K. Scott, and H. Weiss, “Delay-tolerant networking: an approach to interplanetary internet,” *IEEE Communications Magazine*, vol. 14, no. 6, pp. 128–136, June 2003.
- [18] H. Cai and D. Y. Eun, “Crossing over the bounded domain: from exponential to power-law inter-meeting time in MANET,” in *ACM MobiCom*, Montreal, Canada, Sept. 2007.
- [19] —, “Toward stochastic anatomy of inter-meeting time distribution under general mobility models,” in *ACM MobiHoc*, Hong Kong SAR, China, May 2008.
- [20] D. S. Callaway, M. E. J. Newman, S. H. Strogatz, and D. J. Watts, “Network robustness and fragility: percolation on random graphs,” *Physical Review Letters*, vol. 85, no. 25, pp. 5468–5471, Dec. 2000.
- [21] A. Chaintreau, P. Hui, J. Crowcroft, C. Diot, R. Gass, and J. Scott, “Impact of human mobility on the design of opportunistic forwarding algorithms,” in *IEEE INFOCOM*, Barcelona, Spain, April 2006.
- [22] A. Chaintreau, J.-Y. Le Boudec, and N. Ristanovic, “The age of gossip: spatial mean field regime,” in *ACM SIGMETRICS/Performance*, Seattle, WA, June 2009.
- [23] J.-H. Chang and L. Tassiulas, “Maximum lifetime routing in wireless sensor networks,” *IEEE/ACM Trans. on Networking*, vol. 12, no. 4, pp. 609–619, 2004.
- [24] C.-K. Chau and P. Basu, “Exact analysis of latency of stateless opportunistic forwarding,” in *IEEE INFOCOM*, Rio de Janeiro, Brazil, April 2009.
- [25] V. Conan, J. Leguay, and T. Friedman, “Characterizing pairwise inter-contact patterns in delay tolerant networks,” in *Autonomics*, Rome, Italy, Oct. 2007.
- [26] —, “Fixed point opportunistic routing in delay tolerant networks,” *IEEE JSAC*, vol. 26, no. 5, pp. 773–782, June 2008.
- [27] J. Dall and M. Christensen, “Random geometric graphs,” *Physical Review E*, vol. 66, no. 1, pp. 016 121(1)–016 121(9), July 2002.
- [28] E. M. Daly and M. Haahr, “Social network analysis for routing in disconnected delay-tolerant manets,” in *ACM MobiHoc*, Sep. 2007.
- [29] I. Dietrich and F. Dressler, “On the lifetime of wireless sensor networks,” *ACM Trans. on Sensor Networks*, vol. 5, no. 1, pp. 1–39, Feb. 2009.
- [30] S. Durocher, E. Kranakis, D. Krizanc, and L. Narayanan, “Balancing traffic load using one-turn rectilinear routing,” in *International Conference on Theory and Applications of Models of Computation (TAMC)*, Xi’an, China, April 2008.

- [31] A. Feldmann and W. Whitt, “Fitting mixtures of exponentials to long-tail distributions to analyze network performance models,” in *IEEE INFOCOM*, Washington, DC, April 1997.
- [32] W. Fischer and K. Meier-Hellstern, “The markov-modulated poisson process (mmp) cookbook,” vol. 18, no. 2, pp. 149–171, 1993.
- [33] G. B. Folland, *Real analysis: modern techniques and their applications*. John Wiley & Son, 1984.
- [34] M. Franceschetti and R. Meester, “Critical node lifetimes in random networks via the Chen-Stein method,” *IEEE Trans. on Information Theory*, vol. 52, no. 6, pp. 2831–2837, June 2006.
- [35] G. Froc, I. Mabrouki, and X. Lagrange, “Design and performance of wireless data gathering networks based on unicast random walk routing,” *IEEE/ACM Trans. on Networking*, vol. 17, no. 4, pp. 1214–1227, 2008.
- [36] A. Fronczak and P. Fronczak, “Biased random walks in complex networks: the role of local navigation rules,” *Physical Review E*, vol. 80, no. 1, pp. 1–6, July 2009.
- [37] W. Gao, G. Li, B. Zhao, and G. Cao, “Multicasting in delay tolerant networks: a social network perspective,” in *ACM MobiHoc*, New Orleans, Louisiana, May 2009.
- [38] P. W. Glynn, “Upper bounds on Poisson tail probabilities,” *Operations Research Letters*, vol. 6, no. 1, pp. 9–14, March 1987.
- [39] R. Groenevelt, G. Koole, and P. Nain, “Message delay in mobile ad hoc networks,” in *Performance*, Juan-les-Pins, France, Oct. 2005.
- [40] M. Grossglauser and D. N. C. Tse, “Mobility increases the capacity of ad hoc wireless networks,” *IEEE/ACM Trans. on Networking*, vol. 10, no. 4, pp. 477–486, Aug. 2002.
- [41] A. A. Hanbali, A. A. Kherani, and P. Nain, “Simple models for the performance evaluation of a class of two-hop relay protocols,” in *IFIP Networking*, May 2007.
- [42] O. Helgason and G. Karlsson, “On the effect of cooperation in wireless content distribution,” in *IEEE/IFIP WONS*, Garmisch-Partenkirchen, Germany, Jan. 2008.
- [43] W. Hsu, K. Merchant, C. Hsu, and A. Helmy, “Weighted waypoint mobility model and its impact on ad hoc networks,” *Mobile Computer Communications Review*, Jan. 2005.
- [44] P. Hui, J. Crowcroft, and E. Yoneki, “BUBBLE Rap: social-based forwarding in delay tolerant networks,” in *ACM MobiHoc*, Hong Kong SAR, China, May 2008.
- [45] M. Ibrahim, A. A. Hanbali, and P. Nain, “Delay and resource analysis in manets in presence of throwboxes,” *Performance Evaluation*, vol. 64, no. 9-12, pp. 933–947, 2007.
- [46] S. Ikeda, I. Kubo, and M. Yamashita, “The hitting and cover times of random walks on finite graphs using local degree information,” *Theoretical Computer Science*, vol. 410, no. 1, pp. 94–100, January 2009.

- [47] Y.-K. Ip, W.-C. Lau, and O.-C. Yue, “Performance modeling of epidemic routing with heterogeneous node types,” in *ICC*, Beijing, China, May 2008.
- [48] A. Jindal and K. Psounis, “Performance analysis of epidemic routing under contention,” in *ACM IWCMC*, Vancouver, Canada, July 2006.
- [49] P. Kamat, Y. Zhang, W. Trappe, and C. Ozturk, “Enhancing source-location privacy in sensor network routing,” in *ICDCS*, Columbus, OH, June 2005.
- [50] T. Karagiannis, J.-Y. Le Boudec, and M. Vojnovic, “Power law and exponential decay of inter contact times between mobile devices,” in *ACM MobiCom*, Montreal, Canada, Sep. 2007.
- [51] J. Kim, X. Lin, N. B. Shroff, and P. Sinha, “On maximizing the lifetime of delay-sensitive wireless sensor networks with anycast,” in *IEEE INFOCOM*, Phoenix, AZ, April 2008.
- [52] Z. Kong, S. A. Aly, and E. Soljanin, “Decentralized coding algorithms for distributed storage in wireless sensor networks,” *IEEE JSAC*, vol. 28, no. 2, pp. 261–267, 2010.
- [53] Z. Kong and E. M. Yeh, “Distributed energy management algorithm for large-scale wireless sensor networks,” in *ACM MobiHoc*, Montreal, Quebec, Canada, Sep. 2007.
- [54] S. S. Kunnuyur and S. S. Venkatesh, “Threshold functions, node isolation, and emergent lacunae in sensor networks,” *IEEE Trans. on Information Theory*, vol. 52, no. 12, pp. 5352–5372, Dec. 2006.
- [55] F. Li and Y. Wang, “Circular sailing routing for wireless networks,” in *IEEE INFOCOM*, Phoenix, AZ, April 2008.
- [56] Y. Lin, B. Liang, and B. Li, “Data persistence in large-scale sensor networks with decentralized fountain codes,” in *IEEE INFOCOM*, Anchorage, Alaska, May 2007.
- [57] I. Mabrouki, G. Froc, and X. Lagrange, “On the data delivery delay taken by random walks in wireless sensor networks,” in *International Conference on Quantitative Evaluation of SysTems (QEST)*, Saint-Malo, France, Sep. 2008.
- [58] I. Mabrouki, X. Lagrange, and G. Froc, “Random walk based routing protocol for wireless sensor networks,” in *InterPerf*, Nantes, France, Oct. 2007.
- [59] R. Madan, S. Cui, S. Lal, and A. Goldsmith, “Cross-layer design for lifetime maximization in interference-limited wireless sensor networks,” *IEEE Trans. on Wireless Communications*, vol. 5, no. 11, pp. 3142–3152, 2006.
- [60] A. W. Marshall and I. Olkin, *Inequalities: theory of majorization and its applications*. Academic Press, 1979.
- [61] A. Mei and J. Stefa, “Routing in outer space: fair traffic load in multi-hop wireless networks,” in *ACM MobiHoc*, Hong Kong SAR, China, May 2008.

- [62] M. Molloy and B. Reed, “A critical point for random graphs with a given degree sequence,” *Random Structures and Algorithms*, vol. 6, no. 2, pp. 161–180, 1995.
- [63] M. Musolesi and C. Mascolo, “A community based mobility model for ad hoc network research,” in *REALMAN*, Florence, Italy, May 2006.
- [64] G. Neglia and X. Zhang, “Optimal delay-power tradeoff in sparse delay tolerant networks: a preliminary study,” in *CHANTS*, Pisa, Italy, Sep. 2006.
- [65] M. Neuts, *Structured stochastic matrices of M/G/1 type and their applications*. New York: Marcel Dekker, 1989.
- [66] M. E. J. Newman, *Networks: an introduction*. Oxford University Press, 2010.
- [67] M. E. J. Newman, S. H. Strogatz, and D. J. Watts, “Random graphs with arbitrary degree distributions and their applications,” *Physical Review E*, vol. 64, no. 2, pp. 026 118(1)–026 118(17), Aug. 2001.
- [68] C. Ozturk, Y. Zhang, and W. Trappe, “Source-location privacy in energy-constrained sensor network routing,” in *ACM SASN*, Washington, DC, Oct. 2004.
- [69] C. Park, K. Lahiri, and A. Raghunathan, “Battery discharge characteristics of wireless sensor nodes: an experimental analysis,” in *IEEE SECON*, Santa Clara, CA, Sep. 2005.
- [70] M. Piorkowski, N. Sarafijanovic-Djukic, and M. Grossglauser, “A parsimonious model of mobile partitioned networks with clustering,” in *COMSNETS*, Jan.
- [71] J. Polastre, R. Szewczyk, and D. Culler, “Telos: enabling ultra-low power wireless research,” in *ACM/IEEE IPSN/SPOTS*, Los Angeles, CA, April 2005.
- [72] L. Popa, A. Rostamizadeh, R. M. Karp, C. Papadimitriou, and I. Stoica, “Balancing traffic load in wireless networks with curveball routing,” in *ACM MobiHoc*, Montreal, Quebec, Canada, Sep. 2007.
- [73] V. Raghunathan, C. Schurgers, S. Park, and M. B. Srivastava, “Energy-aware wireless microsensor networks,” *IEEE Signal Processing Magazine*, vol. 19, no. 2, pp. 40–50, 2002.
- [74] S. M. Ross, *Stochastic processes*, 2nd ed. John Wiley & Son, 1996.
- [75] N. Sarafijanovic-Djukic, M. Piorkowski, and M. Grossglauser, “Island hopping: efficient mobility-assisted forwarding in partitioned networks,” in *IEEE SECON*, Reston, VA, Sep. 2006.
- [76] M. Shaked and J. G. Shanthikumar, *Stochastic orders and their applications*. Academic Press, 1994.
- [77] S. Shakkottai, “Asymptotics of query strategies over a sensor network,” in *IEEE INFOCOM*, Hong Kong SAR, China, March 2004.

- [78] G. Sharma, R. Mazumdar, and N. B. Shroff, “Delay and capacity trade-offs in mobile ad hoc networks: a global perspective,” in *IEEE INFOCOM*, Barcelona, Catalunya, SPAIN, Aug. 2006.
- [79] V. Shnayder, M. Hempstead, B. Chen, G. W. Allen, and M. Welsh, “Simulating the power consumption of large-scale sensor network applications,” in *ACM SenSys*, Baltimore, MD, Nov. 2004.
- [80] T. Small and Z. J. Haas, “Resource and performance tradeoffs in delay-tolerant wireless networks,” in *WDTN*, Philadelphia, PA, Aug. 2005.
- [81] T. Spyropoulos, K. Psounis, and C. S. Raghavendra, “Spray and wait: an efficient routing scheme for intermittently connected mobile networks,” in *WDTN*, Philadelphia, PA, Aug. 2005.
- [82] —, “Spray and Focus: Efficient Mobility-Assisted Routing for Heterogeneous and Correlated Mobility,” in *ICMAN*, White Plains, NY, Mar. 2007.
- [83] —, “Efficient routing in intermittently connected mobile networks: the multiple-copy case,” *IEEE/ACM Trans. on Networking*, vol. 16, no. 1, pp. 77–90, Feb. 2008.
- [84] T. Spyropoulos, T. Turletti, and K. Obraczka, “Routing in delay-tolerant networks comprising heterogeneous node populations,” *IEEE Trans. on Mobile Computing*, vol. 8, no. 8, pp. 1132–1147, Aug. 2009.
- [85] A. O. Stauffer and V. C. Barbosa, “Probabilistic heuristics for disseminating information in networks,” *IEEE/ACM Trans. on Networking*, vol. 15, no. 2, pp. 425–435, April 2007.
- [86] G. Strang, *Linear algebra and its applications*, 3rd ed. Harcourt Brace Jovanovich, 1988.
- [87] J. C. Taylor, *An introduction to measure and probability*. Springer, 1997.
- [88] A. Vahdat and D. Becker, “Epidemic routing for partially-connected ad hoc networks,” Duke University Technical Report CS-200006, Tech. Rep., April 2000.
- [89] S. Vasudevan, D. Towsley, D. Goeckel, and R. Khalili, “Neighbor discovery in wireless networks and the coupon collector’s problem,” in *ACM MobiCom*, Beijing, China, Sep. 2009.
- [90] D. Vukobratović, Č. Stefanović, V. Crnojević, F. Chiti, and R. Fantacci, “Rateless packet approach for data gathering in wireless sensor networks,” *IEEE JSAC*, vol. 28, no. 7, pp. 1169–1179, 2010.
- [91] D. Vukobratović, M. S. Č. Stefanović, and V. Stanković, “Raptor packets: a packet-centric approach to distributed raptor code design,” in *IEEE ISIT*, Seoul, South Korea, June 2009.
- [92] W. Wang, V. Srinivasan, and K.-C. Chua, “Using mobile relays to prolong the lifetime of wireless sensor networks,” in *ACM MobiCom*, Cologne, Germany, Aug. 2005.

- [93] Y. Wang, M. C. Vuran, and S. Goddard, “Stochastic analysis of energy consumption in wireless sensor networks,” in *IEEE SECON*, Boston, MA, June 2010.
- [94] F. Xing and W. Wang, “On the critical phase transition time of wireless multi-hop networks with random failures,” in *ACM MobiCom*, San Francisco, CA, Sep. 2008.
- [95] Y. Zeng, J. Cao, S. Zhang, S. Guo, and L. Xie, “Random-walk based approach to detect clone attacks in wireless sensor networks,” *IEEE JSAC*, vol. 28, no. 5, pp. 677–691, 2010.
- [96] X. Zhang, G. Neglia, J. Kurose, and D. Towsley, “Performance modeling of epidemic routing,” *Computer Networks*, vol. 51, no. 10, pp. 2867–2891, 2007.

APPENDIX

Appendix A

A.1 Proof of Proposition 1

We here prove that the inter-contact time of any node pair which is uniformly chosen in \mathcal{I} has a hyper-exponential distribution under the spatial model. By the definition of the spatial model, the distribution of inter-contact time of a node pair is identical to the others, it is enough to show the inter-contact time distribution of a given node pair $i \in \mathcal{I}$.

Let T_{AB} be inter-contact time between randomly chosen nodes A and B . Without loss of generality, we assume that a contact between nodes A and B occurs at time 0. Let $A(t), B(t) \in \Omega$ be the sites that nodes A and B belong to at time t , respectively. By the definition of the spatial model, we know $\{A(t)\}_{t \geq 0}$ and $\{B(t)\}_{t \geq 0}$ are continuous time Markov chains with state space Ω . We hereafter use state i , instead of state S_i , for simplicity ($\Omega = \{1, 2, \dots, M\}$). Since each of the Markov chains is irreducible and its state space is finite, it is ergodic and thus there exists a unique stationary distribution $\vec{\pi} = [\pi_i, i \in \Omega]$ such that $\vec{\pi}\mathbf{Q} = \vec{0}$ [74, 15]. We assume that the system is in the steady-state with its stationary distribution $\vec{\pi}$. Recall that the transition rate matrix \mathbf{Q} of the Markov chains is given by

$$\mathbf{Q} = \begin{bmatrix} -q_1 & q_{12} & \cdots & q_{1M} \\ q_{21} & -q_2 & \cdots & q_{2M} \\ \vdots & \vdots & \ddots & \vdots \\ q_{M1} & q_{M2} & \cdots & -q_M \end{bmatrix},$$

where $q_i = \sum_{k \neq i} q_{ik}$. We also define a matrix \mathbf{B} by $\mathbf{B} = \text{diag}\{\beta_1, \beta_2, \dots, \beta_M\}$. From the definition of the spatial model, we know that a contact process based on \mathbf{B} between nodes A and B is modulated by $\{A(t)\}$ and $\{B(t)\}$. In other words, a contact between nodes A and B happens according to a Poisson process with rate β_i , only when two nodes reside in the same state $i \in \Omega$. One can expect the similarity as a point process between the contact process under the spatial model and an arrival process governed by the Markov Modulated Poisson

Process (MMPP) [32] widely used in teletraffic engineering. In the MMPP, packet arrivals occur according to a Poisson process with a different rate which is modulated by an irreducible continuous time Markov chain.

Let $C(t) \triangleq (A(t), B(t)) \in \Omega^2$ to represent a pair of states that nodes A and B belong at time t . Then, $\{C(t)\}_{t \geq 0}$ is a continuous time Markov chain with state space Ω^2 and its transition rate matrix $\mathbf{Q}' = \{q'_{\vec{u}, \vec{v}}\}_{\vec{u}, \vec{v} \in \Omega^2}$ is also written as

$$\mathbf{Q}' = \begin{bmatrix} -q'_1 & q_{12} & q_{13} & \cdots & 0 \\ q_{21} & -q'_2 & q_{23} & \cdots & 0 \\ q_{31} & q_{32} & -q'_3 & \cdots & 0 \\ \vdots & \vdots & \vdots & \ddots & \vdots \\ 0 & 0 & 0 & \cdots & -q'_{M^2} \end{bmatrix}.$$

Here, the entries of the rate matrix \mathbf{Q}' are ordered lexicographically, i.e., $(1, 1), (1, 2), \dots, (1, M), (2, 1), (2, 2), \dots, (M, M)$, and $q'_l = \sum_{k \neq i} q_{ik} + \sum_{k \neq j} q_{jk}$ for each $l = M(i-1) + j$, where $i, j \in \Omega$. Also, the stationary distribution $\vec{\pi}'$ of $\{C(t)\}$ is now given by $\vec{\pi}' = [\pi_1^2 \pi_1 \pi_2 \cdots \pi_1 \pi_M \pi_2 \pi_1 \cdots \pi_M^2]$.

For notational convenience, we define another $M^2 \times M^2$ matrix \mathbf{B}' from the $M \times M$ matrix \mathbf{B} , as the rate matrix \mathbf{Q}' is a $M^2 \times M^2$ matrix. The \mathbf{B}' is a diagonal matrix with $\mathbf{B}'_{jj} = \beta_i$ if $j = M(i-1) + i$, otherwise zero, where $j \in \{1, 2, \dots, M^2\}$ and $i \in \{1, 2, \dots, M\}$. Thus, the contact process based on \mathbf{B}' between nodes A and B is modulated by $\{C(t)\}$. That is, when the Markov chain $\{C(t)\}$ is in state (i, i) , contacts occur according to the Poisson process of β_i . Therefore, it has exactly the same structure of MMPP with $(\mathbf{Q}', \mathbf{B}')$.

Consider the epochs of successive contacts in the MMPP with $(\mathbf{Q}', \mathbf{B}')$ to obtain the pairwise inter-contact time distribution between nodes A and B , i.e., $\mathbb{P}\{T_{AB} > t\}$. As mentioned above, the contact process between nodes A and B starts at an ‘‘arbitrary contact epoch’’, i.e., $t = 0$ is a contact epoch. It is called *interval-stationary* process in the MMPP [32]. We denote J_n , $n \geq 0$, to be the state of the Markov chain $\{C(t)\}$ associated with the n^{th} contact (J_0 is the state at $t = 0$). We also denote X_n , $n \geq 1$, to be the inter-contact time between the $(n-1)^{\text{st}}$ and the n^{th} contacts with $X_0 = 0$. Then, the sequence $\{(J_n, X_n), n \geq 0\}$ is a Markov renewal sequence with transition probability matrix [32, 65]

$$\mathbf{F}(\mathbf{t}) = \int_0^t e^{(\mathbf{Q}' - \mathbf{B}')u} du \mathbf{B}' = [\mathbf{I} - e^{(\mathbf{Q}' - \mathbf{B}')t}] (\mathbf{B}' - \mathbf{Q}')^{-1} \mathbf{B}' = [\mathbf{I} - e^{(\mathbf{Q}' - \mathbf{B}')t}] \mathbf{F}(\infty), \quad (\text{A.1})$$

where the element $F_{ij}(t)$ of $\mathbf{F}(\mathbf{t})$ is the conditional probability $\{J_n = j, X_n \leq t \mid J_{n-1} = i\}$ for any $n \geq 1$, and \mathbf{I} is a $M^2 \times M^2$ identity matrix.

The matrix $\mathbf{F}(\infty) = (\mathbf{B}' - \mathbf{Q}')^{-1}\mathbf{B}'$ is stochastic and its stationary vector \vec{p} is given by [32, 65]

$$\vec{p} = \vec{p} (\mathbf{B}' - \mathbf{Q}')^{-1}\mathbf{B}' = \frac{1}{\vec{\pi}'\vec{\beta}'}\vec{\pi}'\mathbf{B}',$$

where $\vec{\beta}'_{M^2 \times 1} \triangleq [\beta'_1 \beta'_2 \cdots \beta'_{M^2}]^T$. Here, $\beta'_j = \beta_i$ if $j = M(i-1) + i$, otherwise zero, where $j \in \{1, \dots, M^2\}$ and $i \in \{1, \dots, M\}$. Thus, an element of \vec{p} is $\frac{\pi_i^2 \beta_i}{\sum_{k=1}^M \pi_k^2 \beta_k}$ if it corresponds to that of state (i, i) , otherwise 0. Here, since the contact process between nodes A and B governed by the MMPP with $(\mathbf{Q}', \mathbf{B}')$ is interval-stationary, the initial probability vector $\{J_0\}$ of the MMPP with $(\mathbf{Q}', \mathbf{B}')$ is chosen to be \vec{p} . Thus, since $\mathbb{P}\{T_{AB} > t\} = \mathbb{P}\{X_n > t\}$ for any $n \geq 1$, from (A.1) with \vec{p} , we have

$$\mathbb{P}\{T_{AB} > t\} = \vec{p} e^{(\mathbf{Q}' - \mathbf{B}')t} (\mathbf{B}' - \mathbf{Q}')^{-1}\mathbf{B}'\vec{e} = \vec{p} e^{(\mathbf{Q}' - \mathbf{B}')t}\vec{e}, \quad (\text{A.2})$$

where $\vec{e}_{M^2 \times 1} = [1 \ 1 \ \cdots \ 1]^T$. The second equality is from the fact that the matrix $(\mathbf{B}' - \mathbf{Q}')^{-1}\mathbf{B}'$ is stochastic. Note that (A.2) is the marginal distribution of an inter-contact time between two successive contact epochs.

Recall that $q_{ij} = q_{ji}$ in the rate matrix \mathbf{Q} of each of $\{A(t)\}$ and $\{B(t)\}$, where $i, j \in \Omega$. Hence, it is easy to see that the matrix $\mathbf{Q}' - \mathbf{B}'$ is symmetric, and thus its eigenvalues and eigenvectors are real. By the spectral theorem [86], the matrix $\mathbf{Q}' - \mathbf{B}'$ can be diagonalized by an orthogonal matrix. In other words, $\mathbf{Q}' - \mathbf{B}' = \mathbf{M}\mathbf{U}\mathbf{M}^{-1}$, where \mathbf{M} is a $M^2 \times M^2$ orthogonal matrix containing orthonormal eigenvectors of $\mathbf{Q}' - \mathbf{B}'$, and \mathbf{U} is a $M^2 \times M^2$ diagonal matrix in which each diagonal element is its an eigenvalue. Thus, (A.2) becomes

$$\mathbb{P}\{T_{AB} > t\} = \vec{p} e^{(\mathbf{Q}' - \mathbf{B}')t}\vec{e} = \vec{p} \mathbf{M} e^{\mathbf{U}t} \mathbf{M}^{-1}\vec{e}. \quad (\text{A.3})$$

Here, since all the eigenvalues of $\mathbf{Q}' - \mathbf{B}'$ are real and $e^{(\mathbf{Q}' - \mathbf{B}')t} \rightarrow \mathbf{0}$ as $t \rightarrow \infty$ in (A.1), all the eigenvalues (in \mathbf{U}) should be negative [86]. Therefore, (A.3) becomes a weighted sum of exponentials (i.e., hyper-exponential). This completes the proof. \blacksquare

A.2 Proof of Corollary 1

We here show that if $\mathbb{E}\{T_I^{\text{HO}}\} = \mathbb{E}\{T_I^{\text{IN}}\} = \sum_{i \in \mathcal{I}} \frac{1}{\lambda_i} \frac{1}{|\mathcal{I}|}$, then $\mathbb{E}\{D_{\text{IN}}^{[2]}\} \leq \mathbb{E}\{D_{\text{HO}}^{[2]}\}$. First, observe that from the independence of T_{ij}^{HO} over different node (i, j) pairs, for any source and destination

pair, we have

$$\begin{aligned}
\mathbb{E}\{D_{\text{HO}}^{[2]}\} &= \int_0^\infty \mathbb{P}\{\min\{T_{sr_1}^{\text{HO}} + T_{r_1d}^{\text{HO}}, \dots, T_{sr_n}^{\text{HO}} + T_{r_nd}^{\text{HO}}\} > t\} dt \\
&= \int_0^\infty \prod_{i=1}^n \mathbb{P}\{T_{sr_i}^{\text{HO}} + T_{r_id}^{\text{HO}} > t\} dt = \int_0^\infty (1 + t/\tau)^n e^{-nt/\tau} dt \\
&= \tau \sum_{i=0}^n \frac{n!}{(n-i)!n^{i+1}} = \tau f(n),
\end{aligned} \tag{A.4}$$

where $\tau = \mathbb{E}\{T_I^{\text{HO}}\}$ and $f(n) \triangleq \sum_{i=0}^n \frac{n!}{(n-i)!n^{i+1}}$. Also, from Theorem 1, we know that if $\tau = \frac{1}{2n} \sum_{i=1}^n [1/\lambda_{sr_i} + 1/\lambda_{r_id}]$, then

$$\mathbb{E}\{D_{\text{IN}(s,d)}^{[2]}\} \leq \mathbb{E}\{D_{\text{HO}}^{[2]}\} = \frac{1}{2n} \sum_{i=1}^n \left[\frac{1}{\lambda_{sr_i}} + \frac{1}{\lambda_{r_id}} \right] f(n), \tag{A.5}$$

where the equality is from (A.4).

As mentioned earlier, the average delay for a uniform source and destination pair is the arithmetic mean of the average delays for all $|\mathcal{N}|(|\mathcal{N}|-1)/2$ source and destination (s, d) pairs. We hereafter use (i, j) , instead of (s, d) , to clearly distinguish each source and destination pair, where $i, j \in \mathcal{N} \triangleq \{1, 2, \dots, n+2\}$. Then, the average delay for a uniform source and destination pair is given by

$$\begin{aligned}
\mathbb{E}\{D_{\text{IN}}^{[2]}\} &= \frac{2}{(n+2)(n+1)} \sum_{i=1}^{n+2} \sum_{j>i}^{n+2} \mathbb{E}\{D_{\text{IN}(i,j)}^{[2]}\} = \frac{1}{(n+2)(n+1)} \sum_{i=1}^{n+2} \sum_{j \neq i}^{n+2} \mathbb{E}\{D_{\text{IN}(i,j)}^{[2]}\} \\
&\leq \frac{1}{(n+2)(n+1)} \sum_{i=1}^{n+2} \sum_{j \neq i}^{n+2} \frac{1}{2n} \sum_{k \neq i,j}^{n+2} \left(\frac{1}{\lambda_{ik}} + \frac{1}{\lambda_{kj}} \right) f(n) \\
&= \frac{f(n)}{(n+2)(n+1)2n} \sum_{i=1}^{n+2} \sum_{j \neq i}^{n+2} \sum_{k \neq i,j}^{n+2} \left(\frac{1}{\lambda_{ik}} + \frac{1}{\lambda_{kj}} \right),
\end{aligned} \tag{A.6}$$

where the first equality is from the symmetry of the contact process of each node pair ($\lambda_{ij} = \lambda_{ji}$) under the individual model, and the inequality is from (A.5). Further, the summation terms in (A.6) can be simplified as follows. Observe that

$$\sum_{i=1}^{n+2} \sum_{j \neq i}^{n+2} \sum_{k \neq i,j}^{n+2} \frac{1}{\lambda_{ik}} = \sum_{i=1}^{n+2} \left(\sum_{k \neq i}^{n+2} \frac{n+1}{\lambda_{ik}} - \sum_{j \neq i}^{n+2} \frac{1}{\lambda_{ij}} \right) = \sum_{i=1}^{n+2} \sum_{j \neq i}^{n+2} \frac{n}{\lambda_{ij}},$$

and

$$\begin{aligned}
\sum_{i=1}^{n+2} \sum_{j \neq i}^{n+2} \sum_{k \neq i,j}^{n+2} \frac{1}{\lambda_{kj}} &= \sum_{i=1}^{n+2} \sum_{j=1}^{n+2} \sum_{k \neq i,j}^{n+2} \frac{1}{\lambda_{kj}} - \sum_{j=1}^{n+2} \sum_{k \neq j}^{n+2} \frac{1}{\lambda_{kj}} \\
&= \sum_{j=1}^{n+2} \left(\sum_{k \neq j}^{n+2} \frac{n+2}{\lambda_{kj}} - \sum_{h \neq j}^{n+2} \frac{1}{\lambda_{hj}} \right) - \sum_{j=1}^{n+2} \sum_{k \neq j}^{n+2} \frac{1}{\lambda_{kj}} \\
&= \sum_{j=1}^{n+2} \sum_{k \neq j}^{n+2} \frac{n}{\lambda_{kj}} = \sum_{j=1}^{n+2} \sum_{k \neq j}^{n+2} \frac{n}{\lambda_{jk}}.
\end{aligned}$$

Thus, (A.6) can be rewritten as

$$\begin{aligned}
\mathbb{E}\{D_{\text{IN}}^{[2]}\} &\leq \frac{f(n)}{(n+2)(n+1)} \sum_{i=1}^{n+2} \sum_{j \neq i}^{n+2} \frac{1}{\lambda_{ij}} = \left(\frac{2}{(n+2)(n+1)} \sum_{i=1}^{n+2} \sum_{j>i}^{n+2} \frac{1}{\lambda_{ij}} \right) f(n) \\
&= \left(\sum_{i \in \mathcal{I}} \frac{1}{\lambda_i} \frac{1}{|\mathcal{I}|} \right) f(n) = \mathbb{E}\{T_I^{\text{IN}}\} f(n),
\end{aligned} \tag{A.7}$$

where the equalities are from the definition of the individual model. Then, from the assumption that $\mathbb{E}\{T_I^{\text{HO}}\} = \mathbb{E}\{T_I^{\text{IN}}\} = \sum_{i \in \mathcal{I}} \frac{1}{\lambda_i} \frac{1}{|\mathcal{I}|}$ and from (A.4) and (A.7), we have

$$\mathbb{E}\{D_{\text{IN}}^{[2]}\} \leq \mathbb{E}\{T_I^{\text{IN}}\} f(n) = \tau f(n) = \mathbb{E}\{D_{\text{HO}}^{[2]}\}.$$

This completes the proof. ■

A.3 The closed-form expression of $\mathbb{E}\{\tilde{D}_i\}$

Here, we derive the closed-form expression of $\mathbb{E}\{\tilde{D}_i\}$ as in (4.12). Recall that $f_0(t)$ is the complementary cumulative distribution function (ccdf) of an exponential random variable with rate λ_{sd} and $f_i(t)$ is the ccdf of the sum of two exponential random variables with rates λ_{sr_i} and λ_{r_id} . Then, observe that by using binomial theorem, for $\lambda_{sr_i} \neq \lambda_{r_id}$,

$$\begin{aligned}
[f_i(t)]^K &= \left[\frac{\lambda_{sr_i}}{\lambda_{sr_i} - \lambda_{r_id}} e^{-\lambda_{r_id} t} + \frac{\lambda_{r_id}}{\lambda_{r_id} - \lambda_{sr_i}} e^{-\lambda_{sr_i} t} \right]^K \\
&= \frac{1}{(\lambda_{r_id} - \lambda_{sr_i})^K} \sum_{j=0}^K \binom{K}{j} (-\lambda_{sr_i})^j e^{-j\lambda_{r_id} t} \lambda_{r_id}^{K-j} e^{-(K-j)\lambda_{sr_i} t},
\end{aligned}$$

and for $\lambda_{sr_i} = \lambda_{r_id}$,

$$[f_i(t)]^K = (1 + \lambda_{sr_i}t)^K e^{-K\lambda_{sr_i}t} = \sum_{j=0}^K \binom{K}{j} (\lambda_{sr_i}t)^j e^{-K\lambda_{sr_i}t}.$$

Thus, we have for $\lambda_{sr_i} \neq \lambda_{r_id}$,

$$\begin{aligned} \mathbb{E}\{\tilde{D}_i\} &= \int_0^\infty f_0(t)[f_i(t)]^K dt \\ &= \frac{1}{(\lambda_{r_id} - \lambda_{sr_i})^K} \sum_{j=0}^K \binom{K}{j} \frac{(-\lambda_{sr_i})^j \lambda_{r_id}^{K-j}}{\lambda_{sd} + j\lambda_{r_id} + (K-j)\lambda_{sr_i}}, \end{aligned}$$

and for $\lambda_{sr_i} = \lambda_{r_id}$,

$$\mathbb{E}\{\tilde{D}_i\} = \frac{1}{\lambda_{sr_i}} \sum_{j=0}^K \frac{K!}{(K-j)!(K + \lambda_{sd}/\lambda_{sr_i})^{j+1}}.$$

A.4 Derivation of the average waiting time $\mathbb{E}\{\tilde{W}_i\}$

We here derive the average waiting time $\mathbb{E}\{\tilde{W}_i\}$ in (6.2). First, observe that

$$\begin{aligned} \mathbb{E}\{\tilde{W}_i\} &= \mathbb{E}\{\tilde{W}_i|Y \leq T\}\mathbb{P}\{Y \leq T\} + \mathbb{E}\{\tilde{W}_i|Y > T\}\mathbb{P}\{Y > T\} \\ &= \mathbb{E}\{Y|Y \leq T\}\mathbb{P}\{Y \leq T\} + (T + \mathbb{E}\{W_i\})\mathbb{P}\{Y > T\}. \end{aligned} \quad (\text{A.8})$$

The first equality is obtained by conditioning on whether a neighbor of node i in a normal mode will receive the packet within T slots during which the other neighbor remains asleep. Here, if the neighbor in a normal mode receives the packet from node i within T , the average waiting time becomes $\mathbb{E}\{\tilde{W}_i|Y \leq T\} = \mathbb{E}\{Y|Y \leq T\}$. Otherwise, other neighbor which was in a sleep mode will in a normal mode after T , and both neighbors have an equal chance to receive the packet from node i . Hence, from memoryless property of geometric distributions, the average waiting time is $\mathbb{E}\{\tilde{W}_i|Y > T\} = T + \mathbb{E}\{W_i\}$. Then, after a little computation, we have

$$\begin{aligned} \mathbb{E}\{Y|Y \leq T\}\mathbb{P}\{Y \leq T\} &= \sum_{y=1}^{\infty} y \cdot \mathbb{P}\{Y = y, Y \leq T\} \\ &= \sum_{y=1}^T y \cdot \mathbb{P}\{Y = y\} = \frac{1 - (1 - q^2)^T}{q^2} - T(1 - q^2)^T. \end{aligned} \quad (\text{A.9})$$

By noting that $\mathbb{E}\{W_i\} = [q(1 - (1 - q)^2)]^{-1}$, we also have

$$(T + \mathbb{E}\{W_i\})\mathbb{P}\{Y > T\} = \left[T + \frac{1}{q(1 - (1 - q)^2)} \right] (1 - q^2)^T. \quad (\text{A.10})$$

Thus, from (A.8)–(A.10), we finally have

$$\mathbb{E}\{\tilde{W}_i\} = \frac{1}{q^2} - \frac{1}{q^2} \frac{(1 - q)}{(2 - q)} (1 - q^2)^T. \quad (\text{A.11})$$

A.5 Independence of W_i and I_i

Suppose that a sensor node $i \in \mathcal{N}$ has a packet of interest at any given time instant. Recall that W_i is a random variable to represent the sojourn time at node i or the waiting time for node i until to find any first awake node in $N(i)$. Let X_i be inter-wake-up time (or the duration of ‘off’ state) for each node $i \in \mathcal{N}$, which follows an independent exponential distribution with rate λ_i . The waiting time W_i for node i to find any first awake node in $N(i)$ is equivalent to looking at the residual (or remaining) time of X_j for each neighboring node $j \in N(i)$ until to wake up, and then to taking the least or minimum residual time. Since the residual time of X_j from any given time instant is still the same as the original X_j for each node j due to the memoryless property of exponential distributions, we have

$$W_i = \min_{j \in N(i)} X_j. \quad (\text{A.12})$$

Note that W_i becomes another exponential distribution with rate $\sum_{j \in N(i)} \lambda_j$. In addition, recall that I_i is a random variable to denote the first awake node in $N(i)$. It is easy to see that the probability distribution of I_i is given by

$$\mathbb{P}\{I_i = j\} = \mathbb{P}\left\{ X_j < \min_{k \in N(i) \setminus \{j\}} X_k \right\} = \frac{\lambda_j}{\sum_{k \in N(i)} \lambda_k}, \quad (\text{A.13})$$

for $j \in N(i)$, or $(i, j) \in \mathcal{E}$. Then, as an immediate consequence of Competition Theorem in [15, pp. 328], we have

Lemma 1. *For each $i \in \mathcal{N}$, two random variables W_i and I_i are mutually independent.* \square

Lemma 1 says that for any node $i \in \mathcal{N}$ having a packet, the process that node i waits any first awake node I_i in $N(i)$ to forward the packet is now equivalent to first randomly choosing

any neighbor I_i with probability $\mathbb{P}\{I_i = j\}$ where $j \in N(i)$, as in (A.13), and then waiting the sojourn time W_i until the randomly chosen node I_i wakes up.